AMC PAMPHLET AMCP 706-242

ENGINEERING DESIGN HANDBOOK

DESIGN FOR CONTROL OF PROJECTILE FLIGHT CHARACTERISTICS

HEADQUARTERS, U.S. ARMY MATERIEL COMMAND SEPTEMBER 1966

HEADQUARTERS
UNITED STATES ARMY MATERIEL COMMAND
WASHINGTON, D. C. 20315

AMC PAMPHLET
NUMBER 706-242*

26 September 1966

AMCP 706-242, Design for Control of Projectile Flight Characteristics, forming part of the Army Materiel Command Engineering Design Handbook Series, is published for the information and guidance of all concerned.

(AMCRD)

FOR THE COMMANDER:

SELWYN D. SMITH, JR.
Major General, USA
Chief of Staff

OFFICIAL:

STANLEY J. [illegible]KI
Colonel, [illegible]
Chief, Administrative Office

DISTRIBUTION:

Special

*This pamphlet supersedes ORDP 20-246, May 1957, redesignated AMCP 706-246.

PREFACE

The Engineering Design Handbook of the Army Materiel Command is a coordinated series of handbooks containing basic information and fundamental data useful in the design and development of Army materiel and systems. The Handbooks are authoritative reference books of practical information and quantitative facts helpful in the design and development of materiel that will meet the needs of the Armed Forces.

This handbook, one of a series on ammunition, presents a general survey of the principal factors affecting the flight of projectiles, and describes the methods commonly used for predicting and influencing the flight performance.

The coefficients which characterize the aerodynamic forces and moments on a moving body are identified, methods for determining the coefficients applicable to a projectile having a given shape and center of gravity location are described, and the coefficients of a number of projectiles and projectile shapes are given.

The use of aerodynamic coefficients in predicting stability, range and accuracy is described. The effects of variations in projectile shape and center of gravity location on range, accuracy and lethality are discussed. Some material on prototype testing and the effects of round-to-round variations in production lots is presented.

It is no longer possible, if it ever was, to cram into a few hundred pages all of the information required to intelligently design every type of conventional projectile. The author must choose between constructing a digest of available information, or directing the designer to the sources pertinent to his problem, together with enough background material to make it possible for him to use the data in the original reports. The second approach has been chosen in this handbook; the material presented is intended to place the designer in a position to use new information as it is produced by the various research facilities.

This text was prepared by E. L. Kessler, assisted by D. Vineberg, both of the staff of The Budd Company. Much of the material and many helpful comments were supplied by the U.S. Army Ballistic Research Laboratories and by the Picatinny and Frankford Arsenals. Final editing and arranging were by the Engineering Handbook Office of Duke University, prime contractor to the Army Research Office-Durham.

Elements of the U.S. Army Materiel Command having need for handbooks may submit requisitions or official requests directly to the Publications and Reproduction Agency, Letterkenny Army Depot, Chambersburg, Pennsylvania 17201. Contractors should submit such requisitions or requests to their contracting officers.

Comments and suggestions on this handbook are welcome and should be addressed to Army Research Office-Durham, Box CM, Duke Station, Durham, North Carolina 27706.

2 Blank

TABLE OF CONTENTS

Paragraph		Page
	PREFACE	i
	LIST OF ILLUSTRATIONS	viii
	LIST OF TABLES	ix
	LIST OF APPENDIXES	x
	LIST OF SYMBOLS	xi
	CHAPTER 1 INTRODUCTION	
1-1.	General	1-1
1-2.	Measures of Performance	1-1
1-3.	Logistical Considerations	1-1
	CHAPTER 2 TRADE-OFFS	
2-1.	General	2-1
2-2.	Increased Range vs Warhead Volume	2-1
2-2.1	Utility of Standard Projectile Assumed Equal to Zero for Standard Range	2-1
2-2.2	Utility of Standard Projectile Assumed Equal to Unity for Standard Range	2-2
2-2.3	Comparison of Results for Utility Equal to Zero and Utility Equal to Unity	2-3
2-3.	Tabulation of Possible Trade-offs	2-3
	CHAPTER 3 AERODYNAMIC COEFFICIENTS	
3-1.	General	3-1
3-2.	Body Aerodynamics	3-1
3-2.1	Coordinate System	3-1
3-2.2	Yaw	3-2
3-2.3	Center of Pressure	3-2
3-3.	Aerodynamic Forces and Moments	3-3
3-3.1	General	3-3
3-3.2	Lift and Drag	3-3

3

TABLE OF CONTENTS (cont'd)

Paragraph		Page
3-3.3	Magnus Force	3-2
3-3.4	Static Moment	3-3
3-3.5	Damping Moment	3-3
3-3.6	Magnus Moment	3-3
3-3.7	Roll Damping Moment	3-3
3-4.	Force and Moment Coefficients	3-3
3-4.1	Aerodynamic Force Coefficients	3-3
3-4.2	Moment Coefficients and Moments	3-4
3-4.2.1	Moment Coefficients	3-4
3-4.2.2	M_p, Moment About Horizontal Axis	3-4
3-4.2.3	M_y, Moment About Vertical Axis	3-4
3-4.2.4	M_x, Moment About Longitudinal Axis	3-4
3-4.2.5	Relationship Between Ballistic and Aerodynamic Systems of Coefficients	3-4
3-4.3	Complex Yaw	3-5
3-4.4	Magnus Moment Sign Convention	3-5
3-5.	Methods of Measuring the Coefficients	3-5
3-5.1	General	3-5
3-5.2	Methods of Measurement	3-5
3-5.3	Factors To Be Considered in Selection of Method	3-6
3-5.3.1	Free Flight (Ballistic Range)	3-6
3-5.3.2	Wind Tunnel	3-6
3-5.4	Data Resulting from Ballistic Range Tests	3-6
3-5.5	Data Resulting from Wind Tunnel Tests	3-7
3-5.6	Test Facilities	3-7
3-6.	Methods of Estimating the Coefficients	3-8

CHAPTER 4

TRAJECTORY CALCULATIONS

4-1.	General	4-1
4-2.	Differential Coefficients or Sensitivity Factors	4-1
4-3.	Digital Computer Programs for Trajectory Calculations	4-1
4-3.1	Simple Particle Trajectory	4-1
4-3.2	Six-Degree-of-Freedom Particle Trajectory	4-2
4-3.3	Example of Simple Particle Trajectory Calculation (FORTRAN Program)	4-2
4-4.	Desk Computer Method for Trajectory Calculation	4-3
4-5.	Method of Calculating Direction of Tangent to Trajectory	4-3
4-6.	Effect of Projectile Mass on Trajectory	4-6
4-6.1	Horizontal Trajectory	4-6
4-6.1.1	Velocity	4-6
4-6.1.2	Time of Flight	4-6
4-6.1.3	Terminal Velocity	4-7
4-6.2	Curved Trajectory, Antiaircraft Fire	4-7
4-7.	Effect of Drag on Trajectory	4-7
4-7.1	General	4-7
4-7.2	Axial Drag	4-8
4-7.3	Effect of Mach Number	4-8
4-7.3.1	Subsonic Region, $0 < M < 0.8 \pm$	4-8
4-7.3.2	Transonic Region, $.08 \pm < M < 1.1 \pm$	4-8
4-7.3.3	Supersonic Region, $1 \pm < M < 5$	4-8
4-7.3.4	Hypersonic Region, $M > 5$	4-8

TABLE OF CONTENTS (cont'd)

Paragraph		Page
4-7.4	Effect of Reynolds Number on Drag Coefficient	4-8
4-7.5	Subsonic Drag	4-8
4-7.5.1	Surface Roughness and Irregularities	4-9
4-7.5.2	Blunt Nose	4-9
4-7.5.3	Boattailing	4-9
4-7.5.4	Fin-Stabilized Projectiles	4-9
4-7.6	Transonic Drag	4-9
4-7.6.1	Spin-Stabilized Projectile	4-9
4-7.6.2	Fin-Stabilized Projectile	4-10
4-7.7	Supersonic Drag	4-10
4-7.7.1	Decrease of C_{D_0} with Mach Number	4-10
4-7.7.2	Effect of Nose Shape on C_{D_0}	4-10
4-7.7.3	Effect of Boattailing on C_{D_0}	4-10
4-7.8	Dual Flow	4-10
4-7.8.1	Spike-Nosed Projectiles	4-10
4-7.8.2	Undercut Projectiles	4-12
4-7.8.3	Hemispherical or Sharply Conical Base Projectiles	4-12
4-7.9	Drag Variation with Yaw	4-12
4-7.10	Muzzle Blast	4-12
4-7.10.1	Yawing Velocity Due to Transverse Vibration of Muzzle	4-12
4-7.10.2	Transverse Pressure Gradients	4-12
4-7.10.3	Fin-Stabilized Projectiles in Reversed Flow	4-13
4-7.10.4	Obturation	4-13
4-7.11	Crosswind	4-13
4-7.11.1	Wind Sensitivity	4-13
4-7.11.2	Lateral Deflection	4-13
4-7.12	Values of C_{D_0} vs Mach Number	4-13

CHAPTER 5

CHOICE OF METHOD OF STABILIZATION

5-1.	Stability	5-1
5-1.1	General	5-1
5-1.2	Static and Gyroscopic Stability	5-1
5-1.3	Factors To Be Considered in Choice of Fin-Stabilization	5-1
5-1.3.1	Against	5-1
5-1.3.2	For	5-1
5-2.	Spin-Stabilized Projectiles	5-2
5-2.1	Gyroscopic Stability	5-2
5-2.1.1	Gyroscopic Stability Factor	5-2
5-2.1.2	Conditions on Value of s_g for Stability	5-2
5-2.2	Yaw of Repose	5-3
5-2.2.1	General	5-3
5-2.2.2	Formula for Angle of Repose	5-3
5-2.2.3	Trailing	5-3
5-2.2.4	Projectile Asymmetries	5-3
5-2.2.5	Method of Computation of Projectile Spin	5-4
5-2.3	Zoning	5-4
5-2.4	Dynamic Stability of Spin-Stabilized Projectiles	5-5
5-2.4.1	Magnitude of Modal Vectors	5-5
5-2.4.2	Dynamic Stability Factor, s_d	5-5

TABLE OF CONTENTS (cont'd)

Paragraph		Page
5-2.4.2.1	Stability for $\lambda_{max} \leq \lambda$	5-5
5-2.4.2.2	Stability for $\lambda = 0$	5-6
5-2.4.3	Further Discussion of Magnitude of Modal Vectors and Stability	5-9
5-2.5	Aerodynamic Jump of Spin-Stabilized Projectiles	5-9
5-2.5.1	General	5-9
5-2.5.2	Aerodynamic Jump Defined	5-9
5-2.5.3	Magnitude of Aerodynamic Jump	5-9
5-2.5.4	Orientation of Aerodynamic Jump	5-11
5-2.5.5	Distribution of Aerodynamic Jump	5-11
5-2.5.6	Relationship Between Aerodynamic Jump and Q.E.	5-11
5-2.5.6.1	Vertical Component	5-11
5-2.5.6.2	Horizontal Component	5-12
5-3.	Fin-Stabilized Projectiles	5-12
5-3.1	General	5-12
5-3.2	C.P.-C.G. Separation	5-12
5-3.3	Fin Type	5-12
5-3.3.1	Fixed Fins	5-13
5-3.3.2	Folding Fins	5-13
5-3.4	Obturation	5-13
5-3.5	Arrow (Subcaliber) Projectiles	5-13
5-3.5.1	General	5-13
5-3.5.2	Sabot	5-13
5-3.5.3	Aeroelasticity	5-14
5-3.6	Dynamic Stability of Fin-Stabilized Projectiles	5-14
5-3.6.1	General	5-14
5-3.6.2	Zero Spin	5-14
5-3.6.3	Equilibrium Roll Rate	5-14
5-3.6.3.1	Equilibrium Spin	5-14
5-3.6.3.2	Torque	5-15
5-3.6.3.3	Computation of Equilibrium Roll Rate	5-15
5-3.6.3.4	Sample Calculation	5-15
5-3.6.4	Computation of Dynamic Stability	5-15
5-3.6.4.1	General	5-15
5-3.6.4.2	Sample Calculation	5-16
5-3.6.4.3	Magnus Moment Coefficients	5-16
5-3.7	Resonance Instability	5-16
5-3.7.1	Variation of Magnitude of Yaw with Asymmetry	5-16
5-3.7.2	Resonance Roll Rate, p_r	5-17
5-3.7.2.1	Computation	5-17
5-3.7.2.2	Sample Calculation	5-17
5-3.7.2.3	Ratio of p_c/p_r to Avoid Resonance Instability	5-17
5-3.8	Roll Lock-in	5-17
5-3.9	Aerodynamic Jump of Fin-Stabilized Projectiles	5-18
5-3.10	Fin Effectiveness at Supersonic Speeds	5-18

CHAPTER 6

ROCKET-ASSISTED PROJECTILES

6-1.	General	6-1
6-2.	Momentum Limited Situation	6-1
6-2.1	Variation of Muzzle Energy, Chamber Pressure and Propellant with Weight of Projectile	6-1

TABLE OF CONTENTS (cont'd)

Paragraph		Page
6-2.2	Variation of Setback Acceleration	6-2
6-2.3	Effect of Rocket Additions on Projectile Design Parameters	6-2
6-2.4	Effect of Rocket Additions on Accuracy	6-2

CHAPTER 7

LIQUID-FILLED PROJECTILES

7-1.	General	7-1
7-2.	Effect of Sloshing of Liquid Filler	7-1
7-3.	Computation of Design Parameters	7-1
7-3.1	Gyroscopic Stability Factor	7-1
7-3.2	Dynamic Stability Factor	7-2
7-3.3	Spin Rate	7-2
7-4.	Rigid Body Theory	7-2

CHAPTER 8

RANGE TESTING OF PROTOTYPE PROJECTILES

8-1.	General	8-1
8-2.	Pre-Fire Data	8-1
8-3.	Testing	8-2
8-3.1	Static Testing	8-2
8-3.2	Flight Testing	8-2
8-3.2.1	Vertical Target Accuracy	8-2
8-3.2.1.1	Measurement of Accuracy	8-2
8-3.2.1.2	Temperature Range	8-2
8-3.2.1.3	Data Recorded	8-2
8-3.2.2	Range (Distance) Accuracy	8-3
8-3.2.2.1	Measurement of Accuracy	8-3
8-3.2.2.2	Data Recorded	8-3
8-3.2.2.3	Instrumentation	8-3

CHAPTER 9

MANUFACTURING TOLERANCES

9-1.	Dimensional Changes	9-1
9-1.1	Problem	9-1
9-1.2	Analysis	9-1

TABLE OF CONTENTS (cont'd)

9-2. Predicted Probable Range Error 9-1
9-3. Dynamic Stability of 175-mm Projectile, M437 9-2

GLOSSARY G-1
APPENDIXES A-1
REFERENCES R-1
BIBLIOGRAPHY B-1

LIST OF ILLUSTRATIONS

Figure No. *Page*

3-1 Coordinate System 3-1
4-1 Diagram of Gravity Force on Projectile 4-3
4-2 Flow Patterns on Varying Length, Constant Caliber .33 Diameter Spike Noses at Supersonic Velocities 4-11
5-1 Abbreviated Graph of $1/s_g$ vs s_d 5-6
5-2 Graph of $1/s_g$ vs s_d 5-10

LIST OF TABLES

Table No.		Page
3-1	Estimated Accuracy of Aerodynamic Coefficients Obtained by Ballistic Range and Wind Tunnel Tests	3-7
3-2	Coefficients of Typical Projectiles Measured in Free Flight and Estimated	3-8
3-3	Partial List of Ballistic Test Ranges in North America	3-9
3-4	Partial List of Wind Tunnels in North America	3-9
3-5	List of Reports Containing Methods of Estimating Coefficients	3-10
4-1	Typical Output of FORTRAN Simple Particle Trajectory Program	4-4
4-2	Sample Trajectory Calculated on Desk Computer (5-inch Sample Projectile)	4-5
5-1	Sample Trajectory for Spin-Stabilized 5-inch Project at Q.E. = 3°	5-7
5-2	Sample Trajectory for Spin-Stabilized 5-inch Projectile at Q.E. = 70°	5-8
9-1	Probable Variability of Rocket-Assisted Projectile Characteristics and Sensitivity Factors Which Affect Range	9-2
9-2	Sample Trajectory for 175-mm Spin-Stabilized Projectile, M437, at Q.E. = 45°	9-3
9-3	Aerodynamic Data Sheet for 175-mm Projectile, M437	9-4
9-4	Dynamic Stability Estimate of 175-mm Projectile, M437	9-5

LIST OF APPENDIXES

Appendix No.		*Page*
I	Sample Spin-Stabilized Projectile	A-1
II	Calculation of C.G. and Radius of Gyration	A-2
III	Gyroscopic Stability Estimates	
	A. Spin-Stabilized Projectile With Boattail	A-3
	B. Spin-Stabilized Projectile Without Boattail (Flat Base)	A-5
IV	Comparison of Estimates of Ballistic Parameters By Various Methods	A-6
V	Dynamic Stability Estimate	A-8
VI	Static Stability Estimate of a 5-inch Fin-Stabilized Projectile	A-9
VII	Projectile Geometry	A-10
VIII	Aerodynamic Data Sheets	
	A. 30-mm HEI Projectile, T306E10	A-11
	B. 20-mm HEI Projectile, T282E1	A-12
	C. Drag vs Truncation: Conical Heads	A-13
	D. 2.75-inch Rocket, T131	A-14
	E. 90-mm HE Projectile, M71	A-15
	F. 105-mm HE Projectile, M1 (Modified)	A-16
	G. 4.9-caliber Projectile at Transonic Speeds	A-17
	H. 90-mm HE Projectile, T91	A-18
	I. Effects of Head Shape Variation	A-19
	J. 120-mm HE Projectile, M73	A-20
	K. Cone Cylinder	A-21
	L. Effect of Boattailing on C_{D_0}	A-22
	M. Effect of Boattailing on C_{D_0} at $M = 2.44$	A-22
	N. 90-mm Model of 175-mm Projectile, T203	A-25
	O. 7.2-inch Spinner Rocket, T99	A-27
	P. 5-caliber A-N Spinner Rocket	A-28
	Q. 7-caliber A-N Spinner Rocket	A-29
	R. 7-caliber A-N Spinner Rocket and 9-caliber A-N Spinner Rocket	A-30
	S. 10-caliber Cone Cylinder	A-32
	T. 105-mm HEAT Projectile, T171 (Modified)	A-33
	U. 60-mm Mortar Projectile, T24	A-34
	V. 105-mm Mortar Projectile, T53	A-35
	W. 57-mm HEAT Projectile, T188E18	A-36
	X. 90-mm HEAT Projectile, T108	A-37
	Y. 90-mm HEAT Projectile, T108	A-38
	Z. 10-caliber Arrow Projectile	A-39
IX	Trajectory Program in FORTRAN Language	A-40

10

LIST OF SYMBOLS

A	A constant describing the kind and degree of asymmetry of a projectile, radians
A	Bore area, ft²
a	Setback acceleration, ft/sec² Constant in Q function
b	Fin span, tip-to-tip, ft Constant in Q function
c	Fin chord, ft Constant in Q function
c.g.	Center of gravity
c.p.	Center of pressure
C_D	Drag coefficient
cal	Caliber
C_{D_0}	Drag coefficient at zero yaw
$C_{D_\delta^2}$	Yaw-drag coefficient, per rad²
C_{L_α}	Lift coefficient, per radian
C_{N_α}	Normal force coefficient, per radian ($C_{N_\alpha} = C_{L_\alpha} + C_D$ for small yaw)
$C_{N_{p_\alpha}}$	Mangus force coefficient, per rad/sec, per radian
C_{M_α}	Static moment coefficient, per radian
$C_{M_{p_\alpha}}$	Magnus moment coefficient, per rad/sec, per radian
$C_{M_q} + C_{M_{\dot\alpha}}$	Damping moment coefficient, per rad/sec
C_{l_p}	Rolling damping moment coefficient, per rad/sec
C_{l_δ}	Roll moment coefficient due to fin cant (at zero spin), per radian
D	Drag, lb
d	Maximum body diameter, ft
e	Base of natural logarithms
fps	Feet per second
g	Acceleration of gravity, ft/sec²
h	Altitude above sea level, ft
I_x	Axial moment of inertia, slug-ft²
I_y	Transverse moment of inertia, slug-ft²
i	$\sqrt{-1}$; in complex notation indicates rotation by 90°
K_j	Modal vector, radians
k_x	Axial radius of gyration, calibers
k_t	Transverse radius of gyration, calibers
L	Lift, lb Bore travel, ft
$\ln$	Natural logarithm
M	Mach number
m	Mass, slugs
N	Normal force, lb
n	Twist of rifling, cal/turn
N_p	Magnus force, lb
P_c	Chamber pressure, lb/ft²
p	Roll rate, rad/sec
p_e	Equilibrium roll rate, rad/sec
Q	$= \sqrt{c + C_{D_0} M^2} = a + bM$

(11)

LIST OF SYMBOLS (cont'd)

q	Dynamic pressure, lb/ft² ($q = \frac{1}{2}\rho V^2$)
	Angular velocity of a nonrolling missile-fixed coordinate system about a horizontal axis, rad/sec (in damping moment expression)
rad	Radians
S	Frontal area ft²
s	Travel of projectile, calibers
s_d	Dynamic stability factor
s_{d_0}	Dynamic stability factor for $\lambda_{max} \leq 0$
s_g	Gyroscopic stability factor
T	Temperature, °F Time of flight, sec
t	Time, sec
U	Utility
V	Velocity or airspeed, fps
V_b	Volume of projectile (including boundary layer over the boattail, if present), ft³
W	Weight, lb
X	Range
x	Distance along trajectory, ft
α	Vertical component of yaw, rad
β	Horizontal component of yaw, rad
δ	Yaw angle, rad
μ	Static moment factor, lb-ft/radian Coefficient of viscosity
ν	Spin (nondimensional) $\nu = pd/V$
θ	Acute angle between a horizontal plane and the tangent to the trajectory at the c.g. of the projectile
ϕ	Angle of roll Angle of orientation of a modal vector, radians
ρ	Density, slug/ft³

Subscripts

1	Pertains to nutation vector
2	Pertains to precession vector
3	Pertains to asymmetry vector
max	Maximum value
std	Standard value
i	Dummy index: to be replaced by a sequence of specific indices when the subscripted quantity is used in a computation
j	Same definition as subscript i
J	Aerodynamic jump
λ_1	Damping exponent, per caliber of travel
r	Repose Resonant
α	Derivative with respect to angle of attack
a	Acoustic (V_a = speed of sound)
B	Body
b	Base
e	Effective Equilibrium
f	Fin
o	Initial conditions Zero-yaw value
p	Derivative with respect to spin
T	Terminal Tail Trim

Superscripts

$\dot{}$	Derivative with respect to time
$'$	Derivative with respect to calibers traveled, e.g., $\phi'_1 = \dot{\phi}_1 d/V$

CHAPTER 1

INTRODUCTION

1—1. GENERAL This handbook is concerned with the design of projectiles fired from guns. The projectiles considered are of greater size and weight than can normally be fired from a hand-held weapon, and they are not equipped with guidance systems. It will be assumed that they are bodies of revolution, sometimes equipped with fins, and fly in the general direction of the longitudinal axis.

1—2. MEASURES OF PERFORMANCE

The principal measures of the performance of a projectile are:

a. Range
b. Lethality
c. Accuracy
d. Time of flight.

The values taken on by these measures when a round, or group of rounds, is fired are determined by atmospheric conditions, muzzle velocity, gun orientation, target or burst elevation relative to gun, and by flight characteristics designed and built into the projectile.

The primary flight characteristics which directly influence the trajectory are:

a. Drag
b. Aerodynamic jump

but both drag, which chiefly affects range and time of flight, and jump, which chiefly affects accuracy, are themselves determined by a number of projectile characteristics which we will call secondary flight characteristics, namely:

a. Zero-yaw drag coefficient
b. Yaw-drag coefficient
c. Sectional density
d. Lift coefficient
e. Stability
f. Asymmetry effects
g. Wind sensitivity
h. Muzzle blast sensitivity

The lift and drag coefficients are functions of projectile shape and airspeed. Stability is primarily a function of shape, airspeed, air density, and spin rate, and of the manner in which the mass of the projectile is distributed. Muzzle blast sensitivity depends on essentially the same parameters as stability. Wind sensitivity depends on the lift and drag coefficients, on stability, and, in the case of rocket-assisted projectiles, on the ratio of thrust to drag. Practically all projectile bodies (and fins) are designed with rotational symmetry; their asymmetry arises in the manufacturing process. Fuzes, however, are usually asymmetric internally; the center of gravity of the fuze does not lie in the projectile axis.

All of the above secondary flight characteristics, and therefore the primary flight characteristics, are controllable by the designer to within a narrow range; round to round variations arise owing to manufacturing tolerances and to changes in muzzle velocity, air density and wind patterns. Stringent manufacturing tolerances may be imposed by the designer if the accuracy improvement obtained can justify the increased cost of manufacture.

1—3. LOGISTICAL CONSIDERATIONS

This above statement leads into the area of logistics. The designer must constantly bear in

mind the elements of cost, storability, and transportability. He should avoid, where possible, the use of materials likely to be in short supply during wartime. He will often be limited by the facilities for loading the projectile into the gun, and by the design of the gun chamber. Most of these considerations are beyond the scope of this particular handbook, but are covered in other design handbooks of this series.

It is not difficult to design a projectile having long range, a relatively short time of flight, and a small round-to-round dispersion. However, the projectile might, and probably would, have such a small destructive value, or lethality, that it would be useless as a weapon. THE PRIME FUNCTION OF THE PROJECTILE DESIGNER IS TO FIND THAT COMPROMISE AMONG RANGE, ACCURACY AND LETHALITY WHICH WILL BEST SUPPORT THE MISSION OF THE WEAPON SYSTEM UNDER CONSIDERATION.

For example, modification of an existing projectile by increasing the length of its ogive, while preserving the overall length of the projectile, should decrease its drag coefficient and, therefore, increase its range. However, the stability of the round will be altered, with some effect on accuracy; the volume of the projectile will be decreased, with resulting decrease in lethality (or other measure of usefulness, as in the case of smoke or illuminating projectiles). These trade-offs are discussed in detail in the body of this handbook.

In most of the discussions in this handbook it will be tacitly assumed that the designer is given the projectile diameter and the characteristics of the gun from which it is to be fired, i.e., upper limits on chamber pressure, muzzle energy and muzzle momentum have been established by the gun designer. Occasionally, but not often, the projectile designer may be able to specify the twist of the rifling. If the designer is equipped to make correct design decisions for any one caliber, he will be able to cope with the problem of choosing an optimum caliber for a given mission, should that problem arise.

CHAPTER 2

TRADE-OFFS

2—1. GENERAL

If the solution of a trade-off problem is expressed in numbers, an intelligent compromise between conflicting goals can only be reached when the cost of falling short of each goal can be expressed in numbers. Furthermore, these penalty numbers must be in the same system, i.e., they must be capable of being added or multiplied together to give a significant number.

One useful concept, borrowed from economics, is that of "utility", expressed as a number which lies between zero, standing for useless, and unity, standing for maximum usefulness attainable in the given situation. If the utility of each element of a situation can be computed, the utility of the overall situation can be found by multiplying, or, in some cases, adding, the utilities of the elements. (The sum may be divided by the number of components if the convention that utility cannot exceed unity is to be retained.)

In order to construct the curves which express the utilities of the various elements of projectile performance, the designer must obtain, from the agency responsible for defining the military requirement, statements about the relative values of warheads of different volumes for the purposes, and at the ranges, pertinent to the mission of the projectile. Similar statements must be obtained about the usefulness of increased range, decreased time of flight, and improved accuracy. While the statements obtained may be mainly qualitative, such as "we can stand a little reduction in warhead volume, but a 50% reduction would be unacceptable," or "anything more than twice the present range is considered to be beyond the mission of this projectile," they can be translated into numerical utility curves. The designer should discuss the utility curves with the customer before proceeding with the design; some clarification of design objectives is likely to result. Examples of trade-off are given below.

2—2. INCREASED RANGE VS WARHEAD VOLUME

2—2.1 Utility of Standard Projectile Assumed Equal to Zero for Standard Range

As an example, suppose that the problem is the design of a rocket-assisted projectile to be fire from an existing gun. Range is increased by the addition of rocket fuel; however, the overall length of the projectile is limited by stability or handling considerations, so that as the amount of rocket fuel is increased, the volume of the warhead, and therefore its lethality, is decreased. The designer can compute the trade-off curve of range vs warhead volume, and fit this curve with a simple algebraic expression. For example, the curve might be as shown below.

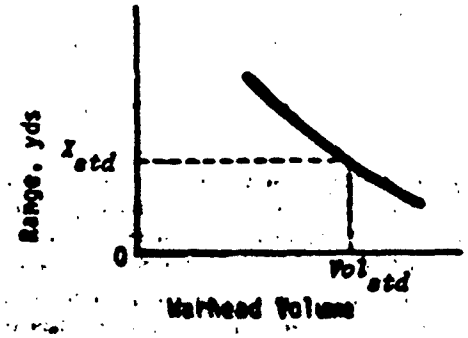

Here X_{std} and Vol_{std} represent the range and warhead volume, respectively, of the standard projectile fired from the given gun. The design problem is to increase the range above X_{std} without sacrificing "too much" warhead volume. The equation for the curve shown would be:

$$\frac{X - X_{std}}{X_{std}} = \frac{Vol_{std}}{Vol} - 1, \text{ or}$$

replacing the fractions by symbols:

$$Z = \frac{1}{R} - 1 = \frac{1 - R}{R}$$

where $$Z = \frac{X - X_{std}}{X_{std}}$$

and $$R = \frac{Vol}{Vol_{std}}$$

This equation might fit the curve well only over the range $\frac{1}{2} < R \leq 1$, but it will turn out that in this example we are not interested in solutions outside of this range.

Suppose that an examination of the user's preferences has established the two utility curves shown below:

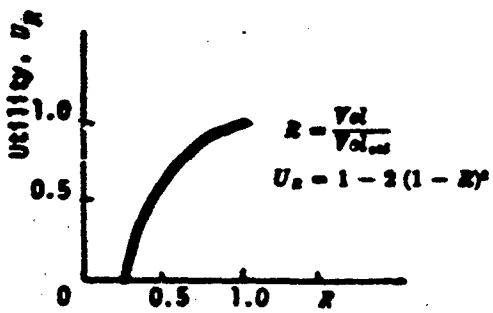

This curve shows that the utility of the warhead declines at first slowly with decreasing volume, then precipitously, and that volumes less than 0.3 the standard volume are worthless, i.e., $U_R = 0$.

The following curve shows that any range lying between the standard range and twice standard range is of interest, and that the rate of increase of range usefulness approaches zero as the range approaches the upper limit.

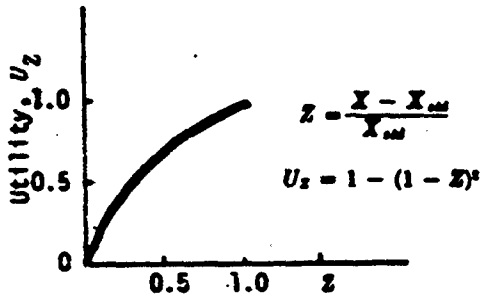

Since we know the relation between Z and R, we can express U_Z in terms of R,

$$U_Z = 1 - \left(\frac{1}{R} - 2\right)^2 = \frac{U_R}{R^2} - 1$$

On the assumption that the utility of the compromise solution is proportional to the product of the utilities of range and warhead volume, we have

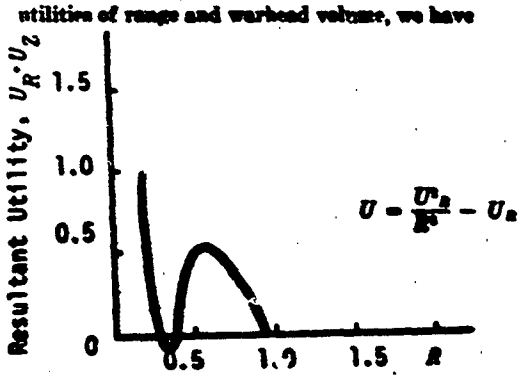

There is no interest below $R = 0.5$ and the best compromise lies at $R = 0.64$, where $U = 0.60$, and $X = 1.56\ X_{std}$. The solution may be reached by either graphical or analytical methods. Note that the resultant utility of the standard projectile is zero by this criterion.

2—2.2 Utility of Standard Projectile Assumed Equal to Unity for Standard Range

If it should be thought more realistic to give the standard projectile a resultant utility of one, then we might decide to add utilities to find the resultant. In this case

16

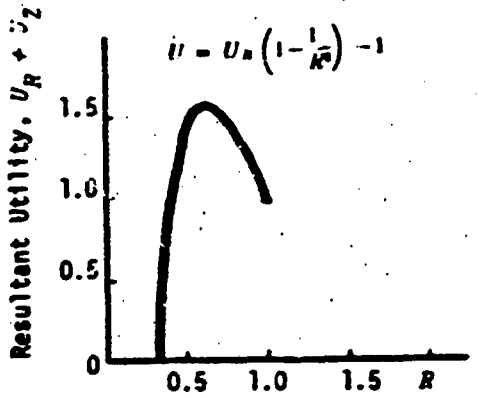

and the best compromise lies at $R = 0.60$, where $U = 1.58$, and $X = 1.67\ X_{std}$. The resultant utility of the standard projectile being 1.0 by this criterion, we have an estimate of the increase in usefulness gained by going to the rocket-assisted projectile, viz., 58%.

2—2.3 Comparison of Results for Utility Equal to Zero and Utility Equal to Unity

In our examples it does not make much difference which criterion we use, however, this will not always be the case. In general, it can be said that the use of the additive criterion places the optimum at the point where the sum of the slopes of the utility curves is zero. In the multiplicative method each slope is multiplied by the product of the other utilities before being summed to zero. After locating the area of optimum solutions, the final solution will be pinpointed only by considerations of accuracy, time-of-flight, and logistics.

2—3. TABULATION OF POSSIBLE TRADE-OFFS

Design changes which increase accuracy sometimes decrease range; range and accuracy might both be improved by increasing the cost of manufacturing the round. The trade-off method outlined above can be useful in these and similar situations.

Many different trade-off situations are mentioned in the discussions in this handbook. For example:

a. Computing time for accuracy of simulation in trajectory calculations.
b. Warhead volume for short time-of-flight by use of a subcaliber projectile.
c. Range or time-of-flight for accuracy where improved stability may be obtained by employing a high drag configuration.
d. Warhead volume for range or time-of-flight by boattailing, or by lengthening the ogive. Unfortunately, increasing range usually diminishes the usefulness of even an undiminished warhead by increasing the dispersion (in meters) at the target.
e. Drag for manufacturing cost in the choice of fin profile.
f. Range or time-of-flight for reduced storage and handling space in the case of a spike-nosed round.
g. Simplicity for warhead volume by using folding fins.

(17) 18 Blank

CHAPTER 3

AERODYNAMIC COEFFICIENTS

3—1. GENERAL

A large part of this handbook is concerned with the interactions between a projectile and the air through which it flies. Frequent use is made of the fact that many aspects of this interaction are independent of which of the two, projectile or air, is actually moving; their relative velocity is the significant quantity. The basic characteristics of the flow of a fluid, such as air, around a body are described in *Foundations of Aerodynamics* by Kuethe and Schetzer, and in *Physical Principles of Mechanics and Acoustics* by Pohl, which present many interesting drawings and photographs of the flow of fluids, using dye or reflecting particles to make the motion visible. The Bibliography at the end of this handbook lists these and other books on aerodynamic theory.

3—2. BODY AERODYNAMICS

A projectile flying through the air creates vortexes, turbulence and, if its speed is sufficiently great, shock waves in the air. Both the air and the projectile are heated. The energy content of these motions is supplied by the kinetic energy of the projectile, and this transfer of energy implies a force, or force system, between the air and the projectile. This force system may be analyzed into components which produce changes in the linear and angular velocities associated with each of the three orthogonal axes which may be chosen as a coordinate system for the description of the motion of the projectile.

3—2.1 Coordinate System

The coordinate system employed in this handbook, Figure 3-1, for describing the forces and moments acting on a projectile has its origin at the center of gravity (c.g.) of the projectile, its X-axis pointing in the direction of the tangent to the trajectory (note that this direction changes as the projectile moves along the trajectory) and its Y- and Z-axes in a plane normal to the X-axis. The Y-axis is horizontal; the Z-axis is normal to the other two.

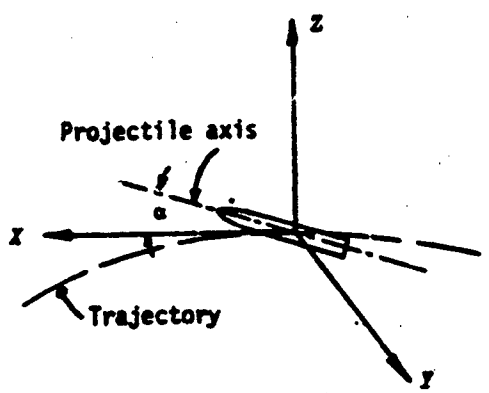

Figure 3—1. Coordinate System

Many different coordinate systems are employed by writers on projectile aerodynamics, the choice of a system being influenced by ease of development of the mathematics involved. However, nearly all of these systems agree in having the origin at the center of gravity of the projectile since the motion of a body can always be resolved into

(15)

translation of, and rotation about, its center of gravity.

3—2.2 Yaw

The aerodynamic forces are functions of the attitude of the projectile with respect to the direction of motion of the c.g. relative to the surrounding air. If there is no wind, this direction of relative motion is along the tangent to the trajectory. (Since wind velocities are small compared with projectile velocities, wind effects are usually introduced as corrections.) Yaw is defined as the angle between the tangent to the trajectory and the direction of the longitudinal axis of the projectile. This angle varies continuously throughout the flight, rapidly at first, but, in a well behaved projectile, less rapidly as time goes on; spin-stabilized projectiles should quiet down to a nearly constant yaw, called the yaw of repose, while the yaw of fin-stabilized projectiles should damp to very small values. In mathematical analyses, the position of the projectile axis is usually projected onto the Y, Z-plane, giving a horizontal and a "vertical" component of yaw. These components are related to the yaw by the cosine and sine of the yaw orientation angle, and are usually handled mathematically by the use of complex numbers.

3—2.3 Center of Pressure

The aerodynamic forces on a projectile are determined by the pressure distribution which exists over the whole exterior surface, but in order to simplify the measurement and mathematical manipulation of these forces, we deal only with a specified set of the resultants of the distributed forces. These resultants have a magnitude and direction, and also a point of application on the body, i.e., a point through which the resultant acts. This point, called the center of pressure (c.p.) of the force in question, is assumed to lie in the longitudinal axis of the projectile, but its position on that axis depends on the shape of the projectile, its air-speed (Mach number), axial spin rate, and, unfortunately, sometimes on the magnitude of the yaw.

In this handbook, the center of pressure of the lift forces is assumed to be independent of yaw angle; this is made possible by considering only "linear" projectile behavior in which the yaw seldom exceeds 10°. One purpose of good design is to keep the yaw well below this figure; not greater than 5°. However, the center of pressure of the magnus forces can move an appreciable distance when the yaw angle changes as much as 10°, and some attempt to describe the effects of this c.p. movement will be made.

3—3. AERODYNAMICS FORCES AND MOMENTS

3—3.1 General

The (resultant) forces and moments which are significant for projectile design are:

a. Normal force
b. Lift
c. Drag
d. Magnus force
e. Static moment
f. Damping moment
g. Magnus moment
h. Roll damping moment

3—3.2 Lift and Drag

The resultant of the pressure forces on a symmetrical nonspinning projectile lies in the plane containing the tangent to the trajectory and the longitudinal axis of the projectile, called the "yaw plane"; the point on the projectile axis through which this resultant passes is called the center of pressure of the lift or normal force, since the resultant may be resolved either into lift and drag components, or into normal force and axial drag. Lift is parallel to the Y, Z-plane, drag is parallel to the X-axis; normal force is perpendicular to, and axial drag is in line with, the axis of the projectile. Each possible pair of components lies, of course, in the yaw plane.

3—3.3. Magnus Force

When a projectile is spinning about its longitudinal axis, the pressure distribution over its surface is altered so that the resultant force no longer lies in the plane of yaw. The aerodynamicist takes care of this situation by introducing a force component normal to the yaw plane, together with its

associated moment. This force, called the "magnus force", is also perpendicular to the longitudinal axis of the projectile, and passes through its own center of pressure. Vector subtraction of the magnus force from the total force on the projectile leaves a force in the yaw plane, which can be resolved into lift and drag.

3—3.4 Static Moment

The static moment is the product of the normal force and the distance between its c.p. and the c.g. of the projectile, which is considered positive when the c.p. is forward of the c.g. as it practically always is for spin-stabilized projectiles. The axis of this moment is a transverse axis through the c.g., normal to the yaw plane. Fin-stabilized projectiles have the c.p. aft of the c.g., so that the static moment opposes an increase in yaw (in normal flight), and can be called a "restoring moment".

3—3.5 Damping Moment

When the yaw of the projectile is changing, the swinging of the projectile about its c.g. changes the pressure distribution so as to produce a couple about an axis through the c.g. normal to the plane of the yawing velocity (which is not necessarily the plane of yaw). This couple, called the "damping moment", usually opposes the yawing velocity.

3—3.6 Magnus Moment

The magnus force produces a moment about an axis through the c.g. parallel to the normal force. This magnus moment changes the yawing velocity in a way which depends on the location of the center of pressure of the magnus force, and on its direction. The magnus force and moment are a result of spinning the projectile, and are absent on a non-rotating projectile; however, even fin-stabilized projectiles may have spin.

3—3.7 Roll Damping Moment

The roll damping moment is a couple about the longitudinal axis of the projectile; this moment on a spinning body is related to the friction between projectile and air. Fins produce large roll damping moments owing to the angle of attack induced by spin.

3—4. FORCE AND MOMENT COEFFICIENTS

It has been found that the aerodynamic forces and the static moment are proportional to the dimensions of the projectile, to the dynamic pressure of the air, and to the yaw of the projectile. The three moments arising from rotations are also proportional to their appropriate angular velocities. The factors of proportionality are known as "aerodynamic coefficients". They are not constant for a given projectile, but are themselves functions of Mach number, Reynolds number, spin rate, and yaw. A brief discussion of the force and moment coefficients follows. For a more complete discussion of the aerodynamic forces and moments see Murphy, *The Free Flight Motion of Symmetric Missiles*, Ref. 12a.

3—4.1 Aerodynamic Force Coefficients

The most significant of the aerodynamic force coefficients are defined as follows; where

$$q = \tfrac{1}{2}\rho V^2$$

is the dynamic pressure, $S = \frac{\pi}{4} d^2$ is the frontal area of the projectile, and α is the yaw in radians:

$$C_N = \frac{N}{qS}$$

$$C_L = \frac{L}{qS}$$

$$C_D = \frac{D}{qS}$$

$$C_{N_p} = \frac{N_p}{qS\left(\frac{pd}{V}\right)}$$

ρ = air density, slug/ft³
V = speed of projectile relative to air, ft/sec
p = roll rate, rad/sec
d = maximum body diameter of projectile, ft
N = normal force, lb
L = lift, lb
D = drag, lb
N_p = magnus force

All of these coefficients are expected to be functions of the yaw angle, α. For small angles ($\alpha <$ 0.17 radian), all, except C_D, can be assumed to vary linearly with yaw; this leads to the use of the slope of the curve of coefficient versus yaw angle as a more convenient description of the characteristics of the projectile. Using the subscript α, to denote a derivative with respect to α, we can write:

$$N = \frac{dC_N}{d\alpha} qS\alpha = C_{N_\alpha} qS\alpha$$

$$L = \frac{dC_L}{d\alpha} qS\alpha = C_{L_\alpha} qS\alpha$$

$$N_p = \frac{dC_{N_p}}{d\alpha} qS\left(\frac{pd}{V}\right)\beta = C_{N_{p\alpha}} qS\left(\frac{pd}{V}\right)\beta \text{ *}$$

Drag varies with the square of the yaw, so we write

$$D = (C_{D_0} + C_{D_{\alpha^2}}\alpha^2)\, qS$$

where C_{D_0} is the drag coefficient at zero yaw and $C_{D_{\alpha^2}}$ is the rate of change of C_D with α^2.

3—4.2 Moment Coefficients and Moments

The moments produced by the aerodynamic forces are referred to the center of gravity of the projectile, unless otherwise stated. The moment coefficients, in the terminology of this handbook, are derivatives with respect to yaw, or with respect to appropriate angular velocities.

3—4.2.1 Moment Coefficients

These coefficients are defined as follows:

$$\frac{dC_M}{d\alpha} = C_{M_\alpha} \quad = \text{static moment coefficient}$$

$$\frac{1}{\frac{1}{2}\rho V^2 Sd}\left(\frac{\partial M_z}{\partial\left(\frac{qd}{V}\right)} + \frac{\partial M_z}{\partial\left(\frac{\dot{\alpha}d}{V}\right)}\right) = C_{M_q} - C_{M_{\dot{\alpha}}} =$$

damping moment coefficient

$$\frac{dC_{M_p}}{d\alpha} = C_{M_{p\alpha}} \quad = \text{magnus moment coefficient}$$

3—4.2.2 M_y, Moment About Horizontal Axis

The total moment about a horizontal axis through the c.g. is given by

$$M_y = \frac{dC_M}{d\alpha} qSD\alpha + \frac{\partial M_y}{\partial\left(\frac{qd}{V}\right)}\left(\frac{qd}{V}\right) + \frac{\partial M_y}{\partial\left(\frac{\dot{\alpha}d}{V}\right)}\left(\frac{\dot{\alpha}d}{V}\right) + \frac{dC_{M_p}}{d\alpha}\left(\frac{pd}{V}\right) qSd\beta$$

where q in the second term is the angular velocity about the horizontal axis when $\dot{\alpha}$, the yawing velocity about that axis, is zero; i.e., the total angular velocity about the horizontal axis is $q + \dot{\alpha}$. q arises from the curvature of the trajectory. Therefore, in coefficient form

$$M_y = \tfrac{1}{2}\rho V^2 Sd\left[C_{M_\alpha}\alpha + C_{M_q}\left(\frac{qd}{V}\right) + C_{M_{\dot{\alpha}}}\left(\frac{\dot{\alpha}d}{V}\right) + C_{M_{p\alpha}}\left(\frac{pd}{V}\right)\beta\right]$$

The first term of the expansion is the static moment, the next two are the damping moments, and the last term is the magnus moment. (Note the each term inside the brackets must be multiplied by

$$\tfrac{1}{2}\rho V^2 Sd$$

to obtain the moment.)

3—4.2.3 M_z, Moment About Vertical Axis

M_z, the aerodynamic moment about the "vertical" axis through the c.g., is obtained by a similar expansion, interchanging α and β, substituting $\dot{\beta}$ for $\dot{\alpha}$, and r for q, where $r + \dot{\beta}$ is the angular velocity about the z-axis.

3—4.2.4 M_x, Moment About Longitudinal Axis

The aerodynamic moment about the longitudinal axis of the projectile is, in the absence of a spin-inducing torque such as might be provided by canted fins, simply

$$M_x = C_{l_p} qSd\left(\frac{pd}{V}\right)$$

and C_{l_p} is called the roll damping moment coefficient. The dimensionless ratio pd/V which appears above is often designated by s, the spin in radians per caliber.

3—4.2.5 Relationship Between Ballistic and Aerodynamic Systems of Coefficients

The earlier work in this area uses a system of coefficients within which ρV^2 takes the place of the dynamic pressure, and d^2 takes the place of the frontal area. This system is, of course, dimensionally correct. It was the system used in AMCP 706-244, Engineering Design Handbook, Ammunition Series, *Section 3, Design for Control of Flight Characteristics*, and is discarded here in the interest of unifying the notation of aerodynamicists and ballisticians, since the latter are forced to use

*Since the magnus force is in the Z direction is proportional to the yaw in the Y direction. See paragraph 3—4.3.

a large amount of wind tunnel data obtained by aerodynamicists.

The ballistic notation will be around for a long time, so it is necessary to know that coefficients in the ballistic system (which are usually denoted by the capital letter K with a subscript) can be converted into the corresponding aerodynamic coefficient slopes (or directly into those coefficients which are not functions of yaw) by multiplying the ballistic system coefficient by $8/\pi$, e.g., $C_{N_\alpha} = \frac{8}{\pi} K_N$. For example,

$$N = C_{N_\alpha}\left(\tfrac{1}{2}\rho V^2 \tfrac{\pi}{4} d^2\right)\alpha = K_N\left(\rho V^2 d^2\right)\sin\alpha$$

When $\sin\alpha \doteq \alpha$, $C_{N_\alpha} = \frac{8}{\pi} K_N$ by cancellation. It should be noted that for C_{l_p}, $C_{M_q} + C_{M_{\dot\alpha}}$, and $C_{M_{p\alpha}}$ the multiplier is $-\frac{8}{\pi}$. (Some authors use $-\frac{16}{\pi}$ as a multiplier, since they use $2V$ as the denominator of their spin terms, e.g., $pd/2V$ instead of pd/V.)

3—4.3 Complex Yaw

In the foregoing discussion, for the sake of simplicity, the symbol α was used for yaw angle. In the notation of Ref. 12a, α is the component of the yaw angle in the "vertical" direction; the component in the horizontal direction is β, and the total yaw angle, δ, is given by

$$\delta = \beta + i\alpha$$

where the orientation of the yaw is $\tan^{-1}\frac{\alpha}{\beta}$.

The aerodynamic coefficient slopes, or "aerodynamic derivatives", can be defined in terms of α because of the rotational symmetry of a projectile; their values can be derived from measurements made on a model which is given a yaw in one plane, identified as the α-plane. (See McShane, Kelley and Reno, *Exterior Ballistics*, Ref. 7.)

3—4.4 Magnus Moment Sign Convention

If the projectile is viewed from the front, β is positive to the right and α is positive upward. A projectile with righthand spin (counter-clockwise when looking from the front) experiences a magnus force downward when β is positive. If the center of pressure of this magnus force is aft of the c.g. of the projectile, then the magnus moment is positive since it adds to the static moment produced by positive α and C_{M_α}. In the study of the effect of c.g. position on the aerodynamic properties of the A-N spinner (Ref. 49), it will be seen that $C_{M_{p\alpha}}$ increases as the c.g. moves forward.

3—5. METHODS OF MEASURING THE COEFFICIENTS

3—5.1 General

In order to be able to predict the performance of a proposed design, a good bit must be known about the probable pattern of the air flow over the projectile in flight. This air flow is mathematically described by the aerodynamic coefficients, so these must be measured or estimated. Estimation, by methods referred to below, is adequate in the preliminary design stages; however, if the coefficients are not well established before prototype rounds are manufactured, the designer runs a great risk of a totally unacceptable performance when the first test firings are made. Furthermore, the process of maximizing one desirable characteristic, such as lethality, which involves reducing other performance characteristics, such as stability, to their minimum acceptable values can not be intelligently carried out if the principal aerodynamic coefficients are not known to a close approximation.

3—5.2 Methods of Measurement

Two methods are in common use for the measurement of coefficients, both of which yield values which are adequate to permit confident design compromises. That is, they yield not only sufficiently accurate values of the coefficients of the design being tested, but also good estimates of the changes in those coefficients which would result from small changes in the design. The two methods are:

a. Ballistic range testing
b. Wind tunnel testing

The method chosen in a particular case may depend on the technical considerations listed be-

low; if not, it depends on factors of time and cost. Major considerations are the availability of the range or the tunnel, and the speed with which the necessary data reduction can be performed at the available facility because costs are usually not widely different.

Estimated accuracy of aerodynamic coefficients obtained by ballistic range and wind tunnel tests is shown in Table 3—1.

3—5.3 Factors to be Considered in Selection of Method

The conditions and objectives of the test should be thoroughly discussed with personnel of the facility chosen before any work is started on test models or prototypes. However, to assist the designer in the preliminary discussion, significant differences between the two methods of testing are described below.

3—5.3.1 Free Flight (Ballistic Range)

a. Good control of Mach number, velocity, temperature, and pressures.
b. Little control of model attitude.
c. Model must be statically or gyroscopically stable.
d. No strut to interfere with base flow.
e. One test covers a range of Mach numbers.
f. Data obtained from shadowgraphs, photographs, and yaw cards, with the possibility of telemetering some data.
g. Data reduction is complicated.
h. Models usually full scale.
i. Reynolds number can be varied by varying model size.

3—5.3.2 Wind Tunnel

a. Excellent control of Mach number, velocity, temperature, and pressures.
b. Excellent control of model attitude.
c. Can obtain data on both stable and unstable configurations.
d. Model support may interfere with base flow.
e. Only one Mach number per test.
f. Data obtained from force and moment balances, pressure taps, schlieren photographs or shadowgraphs.
g. Data reduction is simple.
h. Models usually reduced in size.
i. Reynolds number can be varied by varying tunnel pressure (it may not be possible to test at free-flight Reynolds number).

3—5.4 Data Resulting from Ballistic Range Tests

For a test of this type a projectile is manufactured in accordance with the preliminary design drawings; if length or diameter is too great, a geometrically scaled model with a proper mass distribution may be made. The projectile is fired along a nearly flat trajectory in a suitably instrumented building. For a description of such a range, its instrumentation and method of operation, see Ballistic Research Laboratories Report 1044 (Ref. 13). (The U.S. Army Ballistic Research Laboratories at Aberdeen Proving Ground, Maryland, will be hereinafter referred to by the initials BRL.) The designer should be familiar with the capabilities of BRL, as this installation can be of major assistance to him in any design problem.

As the projectile flies along the instrumented range, a number of parameters of its motion are very carefully measured at successive stations along the range. They are

a. Velocity
b. Roll rate
c. Yaw angle
d. Yaw orientation
e. Swerving motion

From the position versus time (velocity) data, the deceleration of the projectile can be inferred. Knowing the mass and diameter of the projectile, and having observed the current values of barometric pressure, temperature, and humidity; we are able to compute the drag and drag coefficient, C_D. Repeat firings at the same velocity can give the variation of C_D with yaw angle (squared), and sets of firings at different muzzle velocities will give the variation of C_D with Mach number. If the projectile is rocket-assisted, test firings with rocket ignition will give net thrust.

All of the coefficients listed above can be determined in a ballistic range, except that C_{M_q} and $C_{M_{\dot{\alpha}}}$ are always determined as a sum. The yawing frequencies and the damping are deter-

24

TABLE 3—1
ESTIMATED ACCURACY OF AERODYNAMIC COEFFICIENTS OBTAINED BY BALLISTIC RANGE AND WIND TUNNEL TESTS

Coefficient		Estimated Maximum Error* in Percent	
		Ballistic Range	Wind Tunnel
C_D	Drag	± 0.5	± 2.
C_{L_α}	Lift	± 5.	± 1.
C_{M_α}	Static moment	± 2.	± 1.
$C_{M_q} + C_{M_{\dot\alpha}}$	Damping moment	±10.	±10.
$C_{M_{p\alpha}}$	Magnus moment	±15.	±10.
C_{l_p}	Roll damping moment	± 1.	± 1.
c.p.-c.g.	Separation	± .10 cal	± 0.10 cal
$C_{N_{p\alpha}}$	Magnus force	±25	±10

*Maximum error equals 3 std. deviations

mined early in the process of the reduction of the data, and indeed the dynamic stability of the projectile at various Mach numbers can be directly observed. Dynamic instability may be catastrophically apparent; observation of the projectile in a free flight condition is one of the major advantages of testing in a ballistic range. If it is desired to assess the effects of varying initial roll rate, this may be accomplished if suitable gun tubes are available. Usually, however, the designer does not have roll rate at his disposal because even if the projectile is not designed to fit an existing gun, rotating band strength or tube wear usually puts a limit on the allowable spin rate.

Coefficients of typical projectiles, determined in a ballistic range, with estimates of their accuracy, are given in Table 3-2, and in the Aerodynamic Data Sheets, Appendixes VIII-A through VIII-Z. A list of the ballistic ranges in North America which are usually used for projectile testing appears in Table 3-3.

3—5.5 Data Resulting from Wind Tunnel Tests

A test of this type is usually made on scaled models having the exterior configuration of the projectile's preliminary design. The interior of the model is hollow and contains suitable provisions for mounting the model on a sting or strut which in turn is supported by a structure attached to a stationary portion of the wind tunnel. If the model is to spin, the internal provisions include bearings and often a drive motor. Internal strain gage balances are generally used to measure the aerodynamic forces and moments.

All of the aerodynamic coefficients previously discussed can be determined in wind tunnel tests. C_{M_q} and $C_{M_{\dot\alpha}}$ can be determined separately if desired. Very accurate determinations can be made if the need for such accuracy justifies the cost.

Coefficients of a typical projectile, determined in a tunnel, with estimates of their accuracy, are given in Appendix VIII-Y.

3—5.6 Test Facilities

A partial list of ballistic ranges and wind tunnels in North America which are suitable for artillery projectile model testing appears in Table 3-3 and Table 3-4, respectively.

TABLE 3—2
COEFFICIENTS OF TYPICAL PROJECTILES MEASURED IN FREE FLIGHT AND ESTIMATED

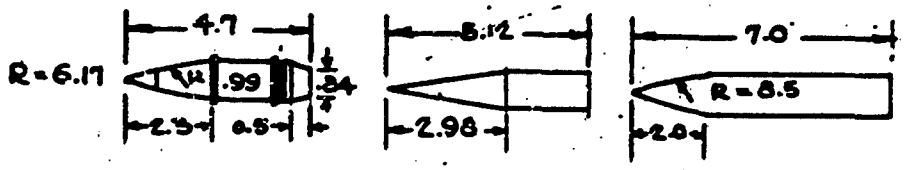

Identification:		*105-mm M1*	*Cone-Cylinder*	*7-Cal A-N Spinner*
C_{D_0} (peak value)		0.40±.01	0.41±0.01	0.46±.01
Constants	a	1.54	1.52	1.50
in Q function	b	0.22	0.20	0.25
(See par. 4-7.7.1)	c	2.70	2.50	2.60
Range of validity		$1.1 \leq M \leq 2.5$	$1.2 \leq M \leq 3.2$	$1.1 \leq M \leq 2.6$
$C_{D_0}{}^2$ (avg)		6.0	7.0	8.0
Coefficients at M = 1.3: determined by free flight measurements				
C_{N_α}		2.3±0.2	2.6±0.1	2.65±0.15
c.p. (cal. from base)		3.45±0.2	2.7±0.1	5.4±0.1
c.g. (cal. from base)		1.75	1.65	2.95
C_{M_α}		3.9±0.1	2.75±0.05	6.2±0.05
$C_{M_q} + C_{M_{\dot\alpha}}$		−7±1	−9	−26±0.5
$C_{M_{p\alpha}}$		0.03±0.05	0.25	0.40±.08
C_{l_p}				−0.19±.001
Coefficients at M = 1.3: estimated by Simmons-Wood methods				
C_{N_α}		2.40	2.80	2.80
c.p. (cal. from base)		3.10	2.60	4.90
C_{M_α}		3.25	2.65	5.40

3—6. METHODS OF ESTIMATING THE COEFFICIENTS

Since it is wasteful to construct a projectile or projectile model for range or wind tunnel test which has no chance of success, and which may even destroy walls or instrumentation of the ballistic range when fired, it is necessary to make preliminary estimates of the principal aerodynamic coefficients before testing. The methods of making such estimates are given in the list of reports, Table

TABLE 3—3
PARTIAL LIST OF BALLISTIC TEST RANGES IN NORTH AMERICA

Location	*Reference*	*Comment*
Ballistic Research Laboratories Aberdeen Proving Ground Maryland	Ref. 19 BRL Report 1048, W. Braun	Two ranges. Projectiles up to 8 inches max. diameter
Naval Ordnance Laboratory White Oak, Maryland	NAVORD 4063	Three ranges, two pressurized
NASA Ames Research Center Moffett Field, California	NACA Report 1222	Several ranges
Canadian Armament Research and Development Establishment Quebec City, Canada	*Canadian Aeronautical Journal*, May 1956	Large range

TABLE 3—4
PARTIAL LIST OF WIND TUNNELS IN NORTH AMERICA*

Location	*Equipment*	*Mach Number Range*
Arnold Engineering Development Center (AEDC) Arnold Air Force Station, Tennessee	Two transonic tunnels Three supersonic Three hypersonic	0.5–1.6 1.5–6 5–8, 10, 12
Ballistic Research Laboratories Aberdeen Proving Ground, Maryland	Two supersonic tunnels One hypersonic	1.25–5 6, 7.5, 9.2
NASA Ames Research Center Moffett Field, California	Three subsonic tunnels Four transonic Four supersonic Seven hypersonic	0–1.0 0–2.2 0.65–6.15 5–20, 25, 28
NASA Langley Research Center Langley Field, Virginia	Three subsonic tunnels Eight transonic Six supersonic Sixteen hypersonic	0–0.6 0–1.4 1.25–7 2–25
NASA Lewis Research Center Cleveland 35, Ohio	One subsonic tunnel One transonic Seven supersonic One hypersonic	0–0.45 0.5–3.1 1.3–5 7
Naval Ordnance Laboratory White Oak, Maryland	Four transonic tunnels One hypersonic	0.2–5 5–8, 10

*This list is intended to include only facilities which do a large amount of projectile testing. Not all of the tunnels listed are used for projectile work. Some tunnels appear more than once in the list. More information about these and many other wind tunnels will be found in the *NATIONAL WIND TUNNEL SUMMARY*, 1961, prepared by the Aeronautics and Astronautics Coordination Board, Department of Defense.

(27)

TABLE 3—5
LIST OF REPORTS CONTAINING METHODS OF ESTIMATING COEFFICIENTS

Quantity	*References*	*Comment*
C_{M_α} and C_{M_α}	Simmons (Ref. 20) Hitchcock (Ref. 81) Wood (Ref. 21) Kelly (Ref. 16)	Not readily available Limited range of usefulness Based on Simmons; used in this handbook (See Appendix III-A)
$C_{M_q} + C_{M_{\dot{\alpha}}}$	Hitchcock (Ref. 81)	Conventional spin-stabilized projectiles of length L $C_{M_q} + C_{M_{\dot{\alpha}}} = 0.9 \left(\frac{L}{d}\right)^{1.5}$ (fairly good for $3 < \frac{L}{d} < 5$)
	Dorrance (Ref. 15)	Reproduced in Murphy and Schmidt (Ref. 49)
$C_{M_{pa}}$	Martin (Ref. 40) Kelly (Ref. 39)	See also Ref. 49

3-5. Sample calculations are shown in the Appendixes.

These methods are fundamentally based on an interpolation of data from very many wind tunnel and ballistic range tests of a wide variety of projectile shapes. Use is made of linear aerodynamic theory in constructing formulas for performing the interpolations. While these formulas should of course not be used for shapes which lie outside of the range of the data on which they are based, it may be necessary to use them for unusual shapes when no other method of estimation is available. Such shapes should be tested in a wi' tunnel; most ballistic range operators would ref to fire them.

Estimated coefficients of typical projectile shapes, for comparison with values obtained in ballistic range tests, are presented in Table 3-2.

CHAPTER 4

TRAJECTORY CALCULATIONS

4—1. GENERAL

The purpose of a calculation of a trajectory, the curve in space traced by the center of gravity of the projectile, is usually the prediction of the expected point of impact of the projectile, when fired at a given muzzle velocity and quadrant elevation, along with the prediction of associated quantities such as time of flight, angle of fall, and velocity at impact. Sometimes the range is stated, and the purpose of the calculation is to find the corresponding muzzle velocity and/or quadrant elevation; the three collateral quantities are still of interest. Or the trajectory may be a ground-to-air type, as for an antiaircraft projectile, for which maximum altitude, time to reach a given altitude, and trajectory curvature are important results.

4—2. DIFFERENTIAL COEFFICIENTS OR SENSITIVITY FACTORS

One can, by varying the inputs to the trajectory calculation by small amounts, one at a time, compute the change in expected range, time of flight, or other quantity of interest, caused by a small change in each input parameter. The percent change in range (or other output quantity) produced by a 1% change in an input parameter is called by some writers a "differential coefficient", by others a "sensitivity factor." The factors are different for each design, as well as for different intervals of the values of the input parameters, which is why they must be determined by small perturbations and the particular set of conditions for which they are valid must be stated. A sample set of sensitivity factors for a rocket-assisted projectile fired for maximum range is given in Table 9-1.

4—3. DIGITAL COMPUTER PROGRAMS FOR TRAJECTORY CALCULATIONS

Innumerable trajectory calculations have been made, and are still being made, for the production of firing tables. Up to the advent and general adoption of the high speed digital computer, these calculations were performed by approximate methods which employed average or effective values of the drag coefficient. The various methods were named for their developers, the Gavre Commission, Sinsci, and Mayevski among others. These methods are still useful for rapid estimations of the effects of variations in projectile shape, muzzle velocity and quadrant elevation on range and time of flight. The necessary charts and tables, with directions for their use, are given in AMCP 706-140 (Ref. 97). Digital computer programs fall into two classes, particle trajectories and six-degree-of-freedom trajectories; each is discussed below.

4—3.1 Simple Particle Trajectory

The relatively simple particle trajectory program assumes that the only forces on the projectile are gravity, drag, and, if present, thrust. The horizontal and vertical accelerations due to these forces are computed at successive points in time, and the resulting horizontal and vertical components of the projectile's velocity and position are computed for each time point. If the time interval is small enough, the simulation of the trajectory can be very good. With a time interval of 0.25 second, the time required to simulate a typical trajectory on an IBM 1620 computer was about ten times the time of flight of the projectile being simulated. This resulted in an accuracy of

29

simulation better than 1%, assuming that the drag coefficient curve used averaged within 2% of the true C_D at all Mach numbers traversed. If no computation of yaw is made, C_{D_0}, the axile drag coefficient, is the coefficient used. Since projectile velocity and altitude are known at each time point, Mach number is always available for entering a stored table of C_{D_0} vs Mach number.

The particle trajectory is very useful in computing trade-offs of range, time of flight, and lethality, particularly in case of a rocket-assisted projectile. Extensions of the program to compute muzzle velocity under the limitations on muzzle energy and muzzle momentum, and then the maximum set-back acceleration, can further automate the design process.

4—3.2 Six-Degree-of-Freedom Particle Trajectory

The six-degree-of-freedom system is seldom coded for anything smaller than the equivalent of an IBM 704. This program computes the position and velocity of the projectile relative to all three axes of the coordinate system(s) chosen, as well as the pertinent angles and angular velocities. All of the aerodynamic coefficients can be used (although many second order terms are usually left out), and the resulting simulation of the trajectory is complete, down to yaw angle, yaw orientation, and swerving motion. Aerodynamic jump is an automatic by-product of this system. Wind can be introduced as a variable.

If roll rate, C_{l_p}, and the variation of C_{M_0} with Mach number were included in the particle trajectory program, then either program could continuously check the gyroscopic stability of the projectile and calculate the yaw of repose. The six-degree-of-freedom system could also continuously check the dynamic stability of the projectile.

4—3.3 Example of Simple Particle Trajectory Calculation (FORTRAN Program)

The FORTRAN particle trajectory program presented below was written for an IBM 1620 computer with 20,000 units of memory. It will compute trajectories of conventional and single-stage rocket-assisted projectiles, either spin- or fin-stabilized, and single-stage rockets. The spin, yaw of repose, and gyroscopic stability computations do not allow for the presence of fin cant or nozzle cant.

The limited memory available made it necessary to read the headings for the output (see Table 4-1 for a sample output) from cards. Appendix IX describes the input cards forming the data deck; the numbers on the input cards describe the projectile and its launching environment. Heading cards are a part of the data deck and follow the numerical data, except that the first card of the data deck identifies the projectile being processed.

An experienced programmer, or one having access to a computer having a larger memory, will be able to make many improvements in and extensions to the program presented here. For example, this program interpolates linearly in finding C_{D_0} or C_{M_0} from the tables provided by the data deck; it may be difficult to represent a given curve sufficiently well with only nine data points. Furthermore, while the computer will print out UNSTABLE when S_g is less than unity, dynamic stability must be computed by hand.

A typical output produced by the program given below is presented in Table 4-1. Projectile data are for the sample projectiles used to illustrate the methods of estimating gyroscopic stability (Appendixes I-VII).

The form factor relating the drag of the sample projectile to that of the 5-inch/54 Navy projectile stored in the computer memory was estimated to be 1.05 since the only significant difference in shape is the shorter ogive of the sample projectile. The form factor relating the static moment coefficient of the sample projectile to the C_{M_0} table stored in memory was estimated to be 1.142, based on the Wood-Simmons estimate at $M = 1.72$.

The last line of the computer output gives the time of flight in seconds, the range in meters, the velocity at impact, angle of fall, and the spin and gyroscopic stability factor at impact. The target is at the same elevation as the gun (sea level) in this example, but any desired target elevation can be fed with the data.

The fundamental equations underying the computer program presented below are:

$$\Delta V = \left(\frac{\text{Thrust} - \text{Drag}}{\text{Projectile Mass}} - g \sin \Theta\right) \Delta t$$

$$\Delta \Theta = \frac{-g \cos \Theta}{V} \Delta t$$

$$\Delta X = (V \cos \Theta) \Delta t$$

$$\Delta Z = (V \sin \Theta) \Delta t$$

Averaging techniques are used to improve the accuracy of the simulation.

4—4. DESK COMPUTER METHOD FOR TRAJECTORY CALCULATION

Reference is made to Table 4-2 for the format of the desk computation. Note that the conditions, Θ_o and V_o, appear in columns 2 and 5 in the first row. Starting with these initial conditions, we now proceed with the computation as follows:

a. Compute the remaining entries in first row.
b. Proceed to next row: locate C_D on the drag curve of the projectile; calculate the drag, D, acceleration, D/m, where m is the projectile mass in slugs.
c. Compute:

(1) $$\frac{dV_x}{dt} = -\frac{D \cos \Theta}{m}$$

(2) $$\frac{dV_z}{dt} = -\frac{D \sin \Theta}{m} - g$$

d. Multiply the above derivatives, dV_x/dt and dV_z/dt, by the currently chosen time interval. The results are ΔV_x and ΔV_z in the third row.
e. Compute V_x and V_z at the end of the time interval (they appear in the fourth row) and use average velocities over the first time interval to compute Δx and Δz (third row) and the new x and z (fourth row).
f. Compute the new V from $V = \sqrt{V_x^2 + V_z^2}$ determine Θ from $\Theta = \tan^{-1} V_z/V_x$; find cos Θ and sin Θ; and complete the fourth row, using $\rho/\rho_0 = \exp\{-3.2 \times 10^{-5} z\}$ and $V_s = 1116 - 0.004z$.
g. Continue as above for remaining entries to complete the table.

4—5. METHOD OF CALCULATING DIRECTION OF TANGENT TO TRAJECTORY

It may be of interest to discuss the equation used in the computer program for the calculation of the direction of the tangent to the trajectory at the end of each time interval. In a particle trajectory, where lift and magnus forces are neglected and drag is assumed to act in line with the velocity vector, the only force acting to change the direction of motion is the weight of the projectile.

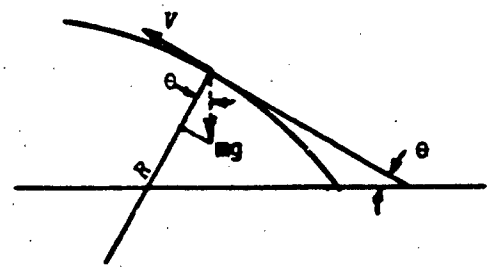

Figure 4—1. Diagram of Gravity Force on Projectile

The inertial force, or centrifugal force, arising from the curvature of the trajectory, is given by mV^2/R, where m is the projectile mass and R is the local radius of curvature of the trajectory. This is balanced (Figure 4-1) by the component of the projectile weight in the direction of the radius of curvature, $mg \cos \Theta$, so we can write

$$\frac{mV^2}{R} = -mg \cos \Theta$$

But V/R is the time rate of change of the direction of the radius, and is therefore also the time rate of change of the direction of the trajectory tangent, since the tangent is always normal to the radius vector. Denoting the rate of change of direction by $d\Theta/dt$, we have

$$mV \frac{d\Theta}{dt} = -mg \cos \Theta$$

or, as it appears in the computer program,

$$\Delta\Theta = -g \cos \Theta_o \Delta t/V$$

TABLE 4-1
TYPICAL OUTPUT OF FORTRAN SIMPLE PARTICLE TRAJECTORY PROGRAM

5-INCH SAMPLE PROJECTILE (SEE APPENDIX I)

FFD	FFM	TYPF	RGA	RGT	D,FT
1.050	1.142	5.540	.381	1.030	.4150

WTO	VO	SPIS	SBT	DTM	TWIST	QE
46.08	1925.	.	.0	.400	28.00	45.000

WTB	ZO	TEMP	DTL	DTE	CDO2	CLP
46.08	.	59.	4.0	.350	6.00	-.014

.001189 1116.0

TIME THETA	X Z	DIST THRUST	V DRAG	CD YAW	CMA DR MACH SPIN	MASS SG
.00	.	.	1925.0	.331	3.59	1.000	1.43
.78	.	.	197.4	.000	1.72	.224	1.49
.11							
2.56	3210.	4469.	1578.0	.362	3.79	.905	1.43
.75	3109.	.	131.3	.001	1.42	.261	2.11
.14							
5.85	6682.	9110.	1265.9	.398	4.14	.820	1.43
.69	6188.	.	84.1	.002	1.16	.311	3.03
.18							
10.38	10713.	14166.	993.0	.290	4.91	.744	1.43
.58	9235.	.	34.3	.004	.92	.379	4.20
.29							
17.72	16400.	20596.	786.3	.168	4.32	.676	1.43
.34	12203.	.	11.3	.010	.73	.456	7.57
.40							
25.72	22088.	26412.	684.8	.169	4.21	.654	1.43
.00	13269.	.	8.3	.016	.64	.502	9.76
.40							
26.12	22361.	26686.	682.4	.169	4.20	.654	1.43
-.01	13267.	.	8.2	.016	.64	.503	9.80
.40							
34.12	27631.	32099.	686.1	.168	4.20	.677	1.43
-.38	12171.	.	8.6	.014	.64	.481	8.66
.40							
42.12	32522.	37859.	762.2	.168	4.28	.745	1.43
-.69	9173.	.	11.7	.009	.70	.414	5.73
.40							
50.12	37001.	44371.	866.5	.176	4.42	.866	1.43
-.91	4464.	.	18.4	.004	.78	.344	3.29
.40							

TIME,S	RANGE,M	V,FPS	THETA,D	SPIN	SG
56.13	12201.	929.	-59.5	.303	2.19

TABLE 5—2

SAMPLE TRAJECTORY CALCULATED ON DESK COMPUTER

5-INCH SAMPLE PROJECTILE (SEE TABLE 5—1 FOR SAME TRAJECTORY USING ELECTRONIC COMPUTER)

t, sec	θ, deg	cos θ	sin θ	V, fps	V_x / dV_x/dt / ΔV_x	V_z / dV_z/dt / ΔV_z	x, ft / Δx	z, ft / Δz	ρ/ρ_0 / D/m	V_a / D, lb	M / C_D
0.0	3.00	.9986	.0523	1925	1922	101	0.0	0.0	1.0	1116	1.72
					-138	-39			138	197	.331
					-124	-35	1674	76			
0.90	2.10	.9993	.0367	1799	1798	66	1674	76	.998	1116	1.61
					-124	-37			124	178	.342
					- 17	- 5	251	9			
1.04	1.95	.9994	.0342	1782	1781	61	1925	85	.997	1116	1.60
					-122	-36			122	175	.344
					- 85	-25	1217	34			
1.74	1.21	.9998	.0212	1696	1696	36	3142	119	.996	1116	1.52
					-113	-35			113	162	.351
					-135	-42	1955	18			
2.94	-0.02	1.00	-.0038	1561	1561	- 6	5097	137	.996	1115	1.40
					- 99	-32			99	142	.365
					-114	-37	1730	-28			
4.09	-1.70	.9996	-.0297	1447	1447	-43	6827	109	.996	1116	1.30
					- 89	-30			89	127	.378
					- 94	-32	1484	-62			
5.15	-3.17	.9985	-.0554	1355	1353	-75	8311	47	.998	1116	1.21
					- 80	-28			80	115	.390
					- 46	-16	758	-47			
5.72	-3.98	.9976	-.0696	1310	1307	-91	9069	0			

= 2765 meters

2.6% error compared with result in Table 5-1

This relationship is also used in deriving the equation for p/V which is presented in paragraph 5.2.2.5.

4—6. EFFECT OF PROJECTILE MASS ON TRAJECTORY

Since C_{D_0} does not vary greatly with increasing length to diameter ratio, a long, and therefore heavy round will experience a lower drag deceleration than a lighter round of the same caliber and general shape. This is the reason for the use of subcaliber or "arrow" projectiles for antitank or antiaircraft fire, where a short time of flight to a given target is of great importance. The manner in which the mass of the round affects the velocity, time of flight, range, and terminal velocity is shown in the treatment which follows.

4—6.1 Horizontal Trajectory

In this case C_D is assumed to be a constant, and the gravity curvature of the trajectory is assumed to be negligible.

$$V = \frac{dx}{dt}$$

$$\frac{dV}{dx} = \frac{dV}{dt} \cdot \frac{dt}{dx} = -\frac{D}{m} \cdot \frac{1}{V} = -\frac{C_D \rho V^2 S}{2mV}$$

So $$\frac{dV}{V} = d \ln V = -\frac{C_D \rho S}{2m} dx$$

Integrating gives

$$\ln V = -\frac{C_D \rho S}{2m} x + C \qquad (4\text{-}1)$$

4—6.1.1 Velocity

If we substitute the initial conditions, $V = V_o$ when $X_o = 0$, into Equation 4-1:

$$C = \ln V_o$$

and

$$V = V_o \exp\left[-\frac{C_D \rho S}{2m} x\right] \qquad (4\text{-}2)$$

which shows the importance of a small C_D and a large mass if a high velocity is to be maintained as X, the range, increases. Replacing the frontal area S by $(\pi/4)d^2$ and m by W/g, we have

$$V = V_o \exp\left[-\frac{\pi}{8}\frac{C_D \rho g}{W/d^2} x\right] \qquad (4\text{-}3)$$

The ratio W/d^2 is called "sectional density", and in most of the older publications is written as m/d^2, using m as a symbol for weight.

4—6.1.2 Time of Flight

The time of flight to a given range can be obtained by substituting dx/dt for V and rearranging Equation 4-3

$$dt = \frac{1}{V_o} \exp\left[\frac{C_D \rho S}{2m} x\, dx\right]$$

Integrating

$$t = \frac{2m}{V_o C_D \rho S} \exp\left[\frac{C_D \rho S}{2m} x\right] + C$$

and substituting intial conditions, $x = 0$ at $t = 0$

gives $$C = -\frac{2m}{V_o C_D \rho S}$$

or $$t = \frac{2m}{V_o C_D \rho S}\left\{\exp\left[\frac{C_D \rho S}{2m} x\right] - 1\right\} \qquad (4\text{-}4)$$

If T is the time of flight to a given range X, then

$$\frac{\partial T}{\partial m} = \frac{T}{m} - \frac{X}{mV_o} \exp\left[\frac{C_D \rho S}{2m} X\right] = \frac{1}{m}\left(T - \frac{X}{V_T}\right) \qquad (4\text{-}5)$$

where V_T = terminal velocity, or velocity at $x = X$.

Since $T = X/V_{av}$ and $V_{av} > V_T$, the quantity in the parentheses of Equation 4-5 is negative and the time of flight to a given target decreases in proportion to the relative increase in the mass or weight of the projectile, $\Delta m/m$, providing that V_o is independent of projectile weight.

However, when designing a round to fit an existing gun, muzzle velocity depends in a very direct manner on projectile weight. If it is desired to make the mass of the projectile greater than the

mass, m_{std}, of the standard projectile fired from that gun, then V_o will be less than the muzzle velocity, V_{std}, of the standard projectile. This is due to the necessity of keeping the muzzle momentum, and therefore the load on the recoil system, at or below the capacity of the system. We can write

$$V_o = \frac{m_{std}\, V_{std}}{m} \text{ for } m \geq m_{std}$$

and substituting this in the Equation 4-4 for time of flight we get

$$t = \frac{2m^2}{m_{std}\, V_{std}\, C_D \rho S}\left\{ \exp\left[\frac{C_D \rho S}{2m} x\right] - 1 \right\}$$

$$\text{and } \frac{\partial T}{\partial m} = \frac{2T}{m} - \frac{X}{m V_T}$$

$$= \frac{X}{m}\left(\frac{2}{V_{avg}} - \frac{1}{V_T}\right)$$

Since the average velocity is usually not much different from the terminal velocity for the flat trajectories of interest to the designer (and indeed cannot be if the assumption of constant C_D is to be be valid), we can conclude that increasing the projectile weight in a momentum limited situation will usually increase the time of flight. If the projectile mass is less than m_{std}, then V_o is limited by chamber pressure (a constant energy constraint, $mV^2_o = m_{std}V^2_{std}$) and $\partial T/\partial m = 1/m\ (3T/2 - X/V_T)$. Here there is more likelihood of decreased time of flight.

4—6.1.3 Terminal Velocity

Increased projectile weight can, however, improve the terminal velocity. If we substitute $V_o = \frac{m_{std}\, V_{std}}{m}$ in the velocity equation, 4-2,

we get

$$V = \frac{m_{std}\, V_{std}}{m} \exp\left[-\frac{C_D \rho S}{2m} x\right]$$

and

$$\frac{\partial V_T}{\partial m} = \frac{m_{std}\, V_{std}}{m^2}\left(\frac{C_D \rho S}{2m} X - 1\right) \exp\left[-\frac{C_D \rho S}{2m} X\right]$$

So $V_{terminal}$ decreases with increased projectile weight for ranges which are shorter than $2m/(C_D \rho S)$, and increases for longer ranges. For a typical 20-mm projectile weighing 0.22 lb, $C_D \rho S$ might be $0.4 \times .002378 \times \pi/4\ (0.066)^2 = 4.1 \times 10^{-6}$ and the range beyond which increased projectile weight will give increased terminal velocity will be about 1000 meters. At this range V/V_o will be e^{-1}, which makes the assumption of constant C_D questionable. The accuracy of the estimate of the cross-over range could be improved by performing the calculation in steps. Since projectile weight generally increases faster than frontal area with increasing diameter ($m = kd^3$, approximately), the cross-over range generally increases with projectile caliber; for a 105-mm projectile weighing 32 lbs, $2m/(C_D \rho S)$ would be about 7000 meters on the assumption of a constant C_D of 0.40.

4—6.2 Curved Trajectory, Antiaircraft Fire

The analysis of antiaircraft fire is complicated by the changing air density and the inability to neglect gravity and trajectory curvature; it will not be attempted here.

4—7. EFFECT OF DRAG ON TRAJECTORY

4—7.1 General

The drag of a projectile has a direct effect on its range, time of flight, and wind sensitivity; and less directly affects both static and dynamic stability. In order to obtain long range, short time of flight, and minimum lateral deflection due to side winds; the drag of the projectile should be as small as possible. Sometimes stability considerations will lead to the acceptance of a high zero-yaw drag. A reduction in yaw, obtained by improving stability decreases the yaw drag and may improve accuracy by decreasing aerodynamic jump.

The material on drag which follows is confined to the drag of a projectile flying in line with the tangent to the trajectory of its c.g., i.e., at zero yaw. The drag coefficient at zero yaw, C_{D_0}, can in this situation be called the axial drag coefficient. The increase in drag with yaw, and its coefficient, $C_{D_{yy}}$, will be discussed in paragraph 4-7.9. For a well behaved projectile the initial yaw damps rapidly to

a small value, so that by far the greater component of C_D is C_{D_0}. The minimization of C_{D_0} is, therefore, of primary importance in nearly all cases.

The designer must seek a projectile shape which will have a small axial drag coefficient, C_{D_0}, and yet have sufficient internal volume to carry the required lethal charge. He must also avoid, as far as possible, surface irregularities such as slots, depressions or protrusions. The effect of general surface roughness varies with the velocity regime of the projectile; this will be discussed later.

4—7.2 Axial Drag

The axial drag at zero yaw may be divided into three components: wave drag, friction drag, and base drag. The relative importance of the various components depends strikingly on the Mach number regime. For example, wave drag is absent in subsonic flight. For this reason the designer will choose different shapes for rounds which fly predominantly in different regimes; however, many artillery projectiles fly in all three regimes and a trajectory calculation of some sort must be made if the optimum drag shape is to be found.

Wind tunnel testing with pressure surveys will provide a division of C_{D_0} into its components; ballistic range testing gives only the overall value. The designer is urged to refer to Hoerner, *Fluid-Dynamic Drag* (Ref. 27) in all matters relating to drag.

4—7.3 Effect of Mach Number

The simplest way to discuss drag is from the point of view of a person observing a projectile fixed in a wind tunnel, with air flowing around it. The airspeed of the projectile is then clearly the velocity of the tunnel air far enough upstream of the model not to be significantly altered by the presence of the model. The speed of sound, V_a, in the tunnel air at the point at which the air velocity is measured then gives the Mach number, V/V_a, at which the test is being conducted. At points in the neighborhood of the model the air velocity is altered in magnitude and direction but the speed of sound is assumed to be unchanged, so that the local Mach number varies from point to point over the surface of the model in a way which depends on its shape.

4—7.3.1 Subsonic Region, $0 < M < 0.8 \pm$

The aerodynamic coefficients of a conventional projectile are fairly constant when the projectile is flying (or being tested in a wind tunnel) at Mach numbers less than some critical number, which is usually in the vicinity of 0.8. This is the model or "free stream" Mach number at which the flow over some part of the model reaches $M = 1.0$.

4—7.3.2 Transonic Region, $.08 \pm < M < 1.1 \pm$

At a free stream Mach number slightly above the critical value, the coefficients such as C_{M_α} or C_{D_0} begin to increase rapidly and the projectile is said to have passed from the subsonic to the transonic regime.

4—7.3.3 Supersonic Region, $1 \pm < M < 5$

At some free stream Mach number greater than 1.0 the wave system characteristic of compressive flow is fully established, and the projectile is said to be in the supersonic regime.

4—7.3.4 Hypersonic Region, $M > 5$

Above $M = 5$ the flight is termed hypersonic. This regime will not be discussed as very few conventional artillery projectiles fly at such high speeds.

4—7.4 Effect of Reynolds Number on Drag Coefficient

Drag coefficients are also influenced by Reynolds number; geometrically similar projectiles of different calibers will have slightly different C_{D_0} vs Mach number curves.

4—7.5 Subsonic Drag

In the subsonic range ($0 < M < 0.8 \pm$) we would like to have a rounded, but not necessarily pointed, nose and as small a base diameter as can be provided in view of the many considerations which affect projectile shape, such as required internal volume, wall strength, propulsive method,

type of stabilization, fuzing, etc. The effect of projectile shape is discussed below.

4—7.5.1 Surface Roughness and Irregularities

Surface roughness corresponding to ordinary industrial practice will have little effect on the drag coefficient. Surface irregularities, such as slots, shallow holes, and protuberances may increase the drag very greatly, depending on their location and orientation. Fuzes are often poorly designed in this respect and consideration may be given to covering them by a windshield.

4—7.5.2 Blunt Nose

Blunting the nose of a projectile will, in the subsonic regime, have little effect on overall drag. The important effect of blunting (short of a completely flat face) is to lower the critical Mach number. Small flat faces, such as appear at the nose in many point-detonating fuzes, have little effect on drag. The integral of the dynamic pressure forces over a properly shaped head will be close to zero, and the forebody drag will accordingly be close to zero. The base drag is thus the result of a pressure deficiency over the base of the projectile; the existence of this sub-static (less than atmospheric) pressure is evident in everyday life in the wake of trains and automobiles.

4—7.5.3 Boattailing

Reducing the diameter of the base below that of the cylindrical body, called "boattailing", is a very effective way of reducing base drag in the subsonic regime. Boattailing also reduces the lift coefficient and changes the position of the center of pressure of the normal force, moving it forward. This reduces the stability of the projectile, placing another limit on the amount of boattailing that can be tolerated.

The extent to which this can be done on a spin-stabilized projectile is limited by the necessity of applying a rotating band, which must be supported by a relatively thick wall, and by the fact that the projectile walls aft of the rotating band are ordinarily exposed to the full chamber pressure so that they must also be thick. These considerations limit the length of the boattail and may also limit the amount of reduction in base area. Use of a hollow boattail avoids these limitations, but sacrifices internal volume.

Use of a large boattail angle (greater than about 16°), without a rounded transition from the cylindrical body, can cause the air flow to separate at the junction, cancelling all of the drag reduction.

4—7.5.4 Fin-Stabilized Projectiles

The zero-yaw drag of fins is, of course, related to their shape and size, but these are dictated primarily by stability considerations. While it is true that some fin profiles have less drag than a simple flat plate, the extra cost of manufacturing the double wedge or streamline profile fins must be weighed.

4—7.6 Transonic Drag

4—7.6.1 Spin-Stabilized Projectile

The transition from the subsonic to the supersonic drag regimes is clearly illustrated, for a typical low-drag spin stabilized projectile, in E. D. Boyer, *Aerodynamic Properties of the 90-mm HE M71 Shell* (Ref. 79). The ogive of this projectile extends over about half its length, the boattail is half a caliber long and the boattail angle is 7°. Its subsonic C_{D_0} is 0.15, even though the rotating band area has four circumferential slots.

Shadowgraphs at $M = 0.88$, $M = 0.97$, and $M = 1.05$ show the initiation of the shock waves at the points of abrupt change in diameter and their growth to fully developed waves. C_{D_0} rises from 0.15 to 0.39 in this Mach number interval, as can be seen from the drag curve in Appendix VIII-E. No shock wave appears over the nose of the projectile before photograph at $M = 1.05$, when a separated bow wave is present. So we can say that for this projectile the transonic regime covers the Mach number range from approximately 0.88 to 1.05. Note this is only one example; the numbers would be different for a different projectile. The development of the shock waves on the body and fins of an arrow projectile is shown by the shadowgraphs in BRL Report 934 (Ref. 89).

The greatest part of the increase in drag in the transonic regime can be attributed to the presence of the shock waves and is called "wave drag". The base drag peaks at about $M = 1.0$; the friction

drag becomes relatively small as the total C_{D_0} increases.

4—7.6.2 Fin-Stabilized Projectile

The drag of typical fin-stabilized projectiles in the transonic regime increases in about the same way as described above, as may be seen from the drag curves presented in Appendixes VIII-T through VIII-Z. The designer should obtain and study a number of shadowgraphs or schlieren photographs of projectiles of varying shapes in conjunction with their drag curves.

4—7.7 Supersonic Drag

4—7.7.1 Decrease of C_{D_0} with Mach Number

After the shock wave system is fully developed, which usually occurs at a free stream Mach number between 1.1 and 1.2, we find that C_{D_0} decreases with increasing Mach number.

In fact, we can use $Q = \sqrt{c + C_{D_0} M^2} = a + bM$ as an interpolation formula: a typical set of values of the constants might be $a = 1.6$, $b = 0.2$, $c = 2.7$.

4—7.7.2 Effect of Nose Shape on C_{D_0}

The size of C_{D_0} in the supersonic regime depends largely on the shape of the nose. By the Taylor-Maccoll formula (Ref. 30) we have:

$$C_{D_p} = \left(.0016 + \frac{.002}{M^2}\right)\epsilon^{1.7}$$

where C_{D_p} is the forebody pressure drag (wave and drag) component of C_{D_0}, ϵ is half of the cone angle, in degrees, and M is Mach number.

While by this formula the lowest drag shape for the nose would be a cone, an ogival nose having a large ogival radius will have slightly lower drag (and also afford a greater warhead volume). R. R. Dickinson (Ref. 24) found from ballistic range firings at $M = 2.44$ that the minimum drag head shape of a caliber .50 projectile ($d = 0.0417$ ft) was a secant ogive having a radius twice that of the tangent ogive of the same length and maximum diameter (ratios between 1.7 and 2.5 were nearly as good).

The presence of a small flat (or rounded) surface at the front of the nose, called the méplat, has only a small effect on C_{D_0}, and indeed, if not too large, may reduce C_{D_0} slightly below that for a pointed nose of the same length.

4—7.7.3 Effect of Boattailing on C_{D_0}

Boattailing reduces the drag of supersonic projectiles as long as the airflow is able to follow the contour of the body. For each projectile shape there is a critical angle (generally about 8°) and a critical boattail length (about 1 caliber at the critical angle, longer for smaller angles) beyond which the flow will separate from the projectile forward of the base, reulting in a C_{D_0} which is greater than the minimum attainable, and which varies from round-to-round with consequent degradation of accuracy. See Refs. 25 and 26.

4—7.8 Dual Flow

As a general rule, we assume that projectiles having the same shape and c.g. location will have the same set of aerodynamic coefficients when fired at the same Mach number (and Reynolds number), and that small differences in shape and surface finish will produce only small differences in the coefficients. The few outstanding exceptions to these rules are discussed below.

4—7.8.1 Spike-Nosed Projectiles

It was found some time ago that replacing the ogival head of a projectile by a slender cylinder protruding from the flat forward face of the body would move the c.p. of the normal force rearward, reducing C_{N_α} and reducing the spin rate required to stabilize a spin-stabilized round, or reducing the length of the tail required on a fin-stabilized round. These spike-nosed projectiles had higher drag coefficients than the corresponding projectiles with ogival heads. Also, for some designs, projectiles from the same lot, fired under the same conditions, exhibited drag coefficients which fell in one or the other of two groups, with the averages of the two groups as much as 30% apart.

Examination of spark photographs showed that the low drag coefficients were associated with rounds on which the airflow separated from the spike at its tip, while on the high-drag rounds the flow separated at a point about half-way down the spike. This phenomenon was called "dual

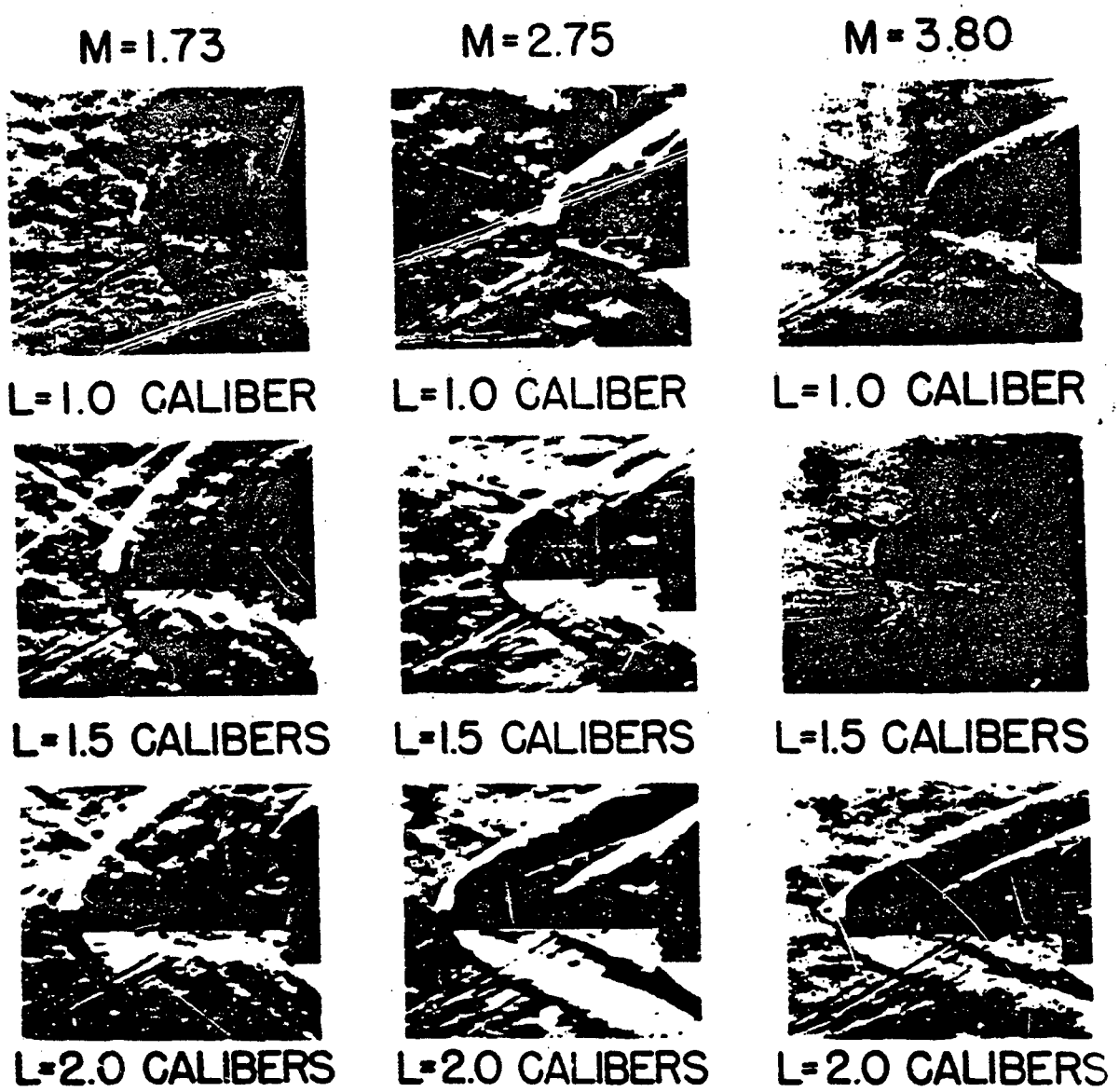

The pictures, taken in the BRL supersonic wind tunnel, show that the character of the flow over a spike nose depends on Mach number and nose length. The flow separation is delayed, with consequent increase in drag, on the three photographs at the lower right hand corner(*). Thicker spikes showed delayed separation at shorter lengths (Ref. 35b).

Figure 4—2. Flow Patterns on Varying Length, Constant Caliber .33 Diameter Spike Noses at Supersonic Velocities

flow"; its existence was a function of the geometry of the spike. In order to avoid the occurrence of dual flow, with its serious effect on accuracy, modern spike-nosed rounds are furnished with a small ring near the tip of the nose which insures the early separation of the flow.

Figure 4-2 shows the effect of Mach number and nose length on the flow pattern produced by a spike-nosed projectile.

4—7.8.2 Undercut Projectiles

Another example of dual flow was found in ballistic range firings of projectiles having the central part of the body deeply undercut; drag and moment coefficients varied from round-to-round by as much as 50%. The flow pattern, whether high- or low-drag, was stable; i.e., once established, it persisted throughout the observed flight of the projectile. The possibility of dual flow may sometimes be detected by wind-tunnel tests when ballistic range firings do not reveal its existence.

4—7.8.3 Hemispherical or Sharply Conical Base Projectiles

The point of separation of the airflow from the base of a projectile having a hemispherical or sharply conical base will also vary from round-to-round, but in a continuously distributed manner, so that this behavior is *not* classified as "dual flow". The hemispherical shape allows the wall of the base to be thinner, so that more HE can be carried, but extra care must be taken to insure dynamic stability (see Appendix VIII-H).

4—7.9 Drag Variation with Yaw

The increase in drag when the attitude of the projectile changes from zero yaw to a yawed position is called by some writers "induced drag." This term is borrowed from airplane terminology, and is equivalent to "drag due to lift." For small yaws, the axial drag is very nearly unchanged from its zero-yaw value, and its component parallel to the trajectory is also very little changed, since $\cos \delta \doteq 1$ when $\delta \doteq 0$. The normal force is inclined rearward at an angle δ, so it has a component in the drag direction which is given by $C_{N_\alpha} \delta^2 qS$ when $\delta \doteq \sin \delta$. The expression for the drag coefficient then becomes

$$C_D \approx C_{D_0} + C_{N_\alpha} \delta^2$$

However, the observed coefficient of variation of drag with yaw squared, $C_{D_{\delta^2}}$, is usually about twice as large as C_{N_α}.

While the induced drag may be reduced somewhat by choosing a body shape having a small C_{N_α}, dynamic stability may be impaired so that the net effect on drag may be unfavorable.

The above observations apply to fins as well as to bodies. It will be seen that over-stabilizing a finned projectile by means of a large fin lift may result in a C_D penalty as well as increased muzzle blast sensitivity.

4—7.10 Muzzle Blast

4—7.10.1 Yawing Velocity Due to Transverse Vibration of Muzzle

Nearly all projectiles emerge from a gun with essentially zero yaw. Even mortar projectiles, which have large bore clearance to facilitate drop firing, can lie in the tube no more than 0.3° out of line with the tube axis. The possibility exists that transverse vibrations of the muzzle may move the rear end of the projectile after the c.g. has passed the muzzle; this action, as well as any overall motion of the gun tube, can impart yawing velocity to the projectile*, but no significant exit yaw.

Equations for aerodynamic jump, which is one of the two primary flight characteristics, will be presented later in this handbook. It is noted here that jump is primarily a function of initial yawing velocity, and not of initial yaw.

4—7.10.2 Transverse Pressure Gradients

Transverse pressure gradients in the muzzle blast can impart some yawing velocity to the projectile if the c.g. of the projectile does not coincide with the center of pressure of the transverse force. This effect is most prominent when firing with a worn gun tube. These transverse pressure gradients are probably related to the bore yaw of the projectile. Good obturation reduces the pressure differences in the blast and shortens the effective blast zone, thus reducing initial yawing velocity, aerodynamic jump, and dispersion at the target. An improvement in accuracy of hot rounds over cold

*For a theoretical and experimental study of the effects of gun motion, see Ref. 3.

rounds of the same projectiles arises chiefly from their better fit in the tube, partly because bore yaw is reduced and partly because obturation is improved.

4—7.10.3 Fin-Stabilized Projectiles in Reversed Flow

Fin-stabilized projectiles are affected by the muzzle blast in yet another way. For a short time after emergence from the muzzle the blast gases are flowing forward over the fin surfaces, resulting in a large destabilizing moment which can impart a significant yawing velocity even though the time of action is short. It is of great importance that the aerodynamic moment coefficient of the fins in reversed flow be kept as small as possible.

Many photographs of the muzzle blast are available in firing test reports of the Development and Proof Services, Aberdeen Proving Ground, Maryland.

Since the camera usually takes thousands of pictures per second, the emergence of the projectile from the smoke cloud can be observed, and the time spent in reversed flow estimated. The data from the photographs can be correlated with the dispersion of hits on the target; these correlations clearly show the importance of obturation for fin-stabilized rounds.

4—7.10.4 Obturation

Extrusion of the rotating band material into the grooves of the rifling is usually considered to furnish adequate obturation for spin-stabilized rounds. However, some recent projectile designs have included special obturating rings or discs, similar to the devices commonly used on fin-stabilized rounds. These devices are described in paragraph 5-3.4.

4—7.11 Crosswind

4—7.11.1 Wind Sensitivity

While the projectile designer cannot do anything about the wind, he can do something about the sensitivity of his projectile to the effect of wind. A stable projectile will nose into the wind, i.e., the equilibrium position of the longitudinal axis of the projectile, neglecting yaw of response and trim, will be in line with the resultant of projectile velocity and wind velocity. The net drag force (drag minus rocket thrust) will then have a component at right angles to the projectile velocity. In the absence of rocket thrust, or if drag exceeds thrust, the projectile will acquire a downwind lateral velocity and displacement; if thrust exceeds drag, the projectile will move upwind.

4—7.11.2 Lateral Deflection

With no rocket thrust, a constant crosswind, and making the usual assumption that the projectile aligns itself with the resultant air-stream as soon as it leaves the muzzle of the gun, we can write a very simple expression for the deflection of a fin trajectory by a crosswind (see H. P. Hitchcock, *The Motion of a Very Stable Shell at Short Ranges*, BRL Report 1047, April 1958, p. 19).

$$Y = V_w \left(T - \frac{X}{V_o}\right)$$

where

Y = lateral deflection at impact, ft
V_w = crosswind velocity, fps
T = time of flight, sec
X = range, ft
V_o = muzzle velocity, fps

The only variable in the above expression is the time of flight. Substituting for T its equivalent, as given in paragraph 4-6.1.2, we have

$$Y = \frac{V_w}{V_o}\left[\frac{2m}{C_{D0}S}\left\{\exp\left[\frac{C_{D0}S}{2m}X\right] - 1\right\} - X\right]$$

From this equation we can find that the lateral deflection in mils decreases with increased projectile weight or muzzle velocity, and increases with increase in C_D.

These relations furnish the designer with additional reasons for seeking low drag and high sectional density (unless his projectile contains a rocket motor, when the trade-off situation becomes more complex).

4—7.12 Values of C_{D_0} vs Mach Number

Curves of C_{D_0} vs Mach number for typical projectiles are shown in Appendices VIII-A through VIII-E. The configuration of the projectile is shown on each page in order to enable the designer to interpolate between shapes.

41 42 Blank

CHAPTER 5

CHOICE OF METHOD OF STABILIZATION

5—1. STABILITY

5—1.1 General

In order to have a small induced drag, a projectile must be stable, i.e., the yaw of the projectile must damp to a small equilibrium angle early in its flight. If not statically stable nor gyroscopically stable, the projectile will commence to tumble as soon as it leaves the muzzle of the gun; if not dynamically stable, the yaw of the projectile will grow continuously with time, so that the projectile will tumble or go into a flat spin unless the expected time of flight is very short.

5—1.2 Static and Gyroscopic Stability

Static stability is related to the position of the center of pressure of the normal force with respect to the c.g. of the projectile. If the c.p. is aft of the c.g., the projectile is statically stable, i.e., any yaw of the projectile produces a moment about the c.g. which tends to return the axis of the projectile to the zero-yaw position. If the c.p. is ahead of the c.g., the normal force produces an overturning moment tending to increase the yaw. However, if the projectile is spinning rapidly enough about its own axis, the yaw will not grow rapidly but mainly change direction; the projectile is said to be gyroscopically stable, even though statically unstable.

Since the c.p. of a cylindrical body of revolution is usually ahead of its centroid, a typical projectile shape is unstable unless:

a. Mass of the projectile is so concentrated at the forward end as to move the c.g. ahead of the c.p. (this is rarely a practical solution), or
b. Projectile is provided with a flaring rear end or with flat surfaces (fins) at the rear of the body which move the c.p. rearward of the c.g., or
c. Projectile is made gyroscopically stable by spin.

5—1.3 Factors to be Considered in Choice of Fin-Stabilization

5—1.3.1 Against

Fixed fins take up length without adding to the payload volume of the projectile, except in the special case of an arrow, or subcaliber, projectile. Folding fins either add to the length or reduce the volume, depending on the design adopted, but in any case add to the complexity of the projectile. Since the usefulness of a projectile of a given maximum diameter and overall length is reduced when its payload volume is reduced, and, in general, spin-stabilized projectiles are cheaper than and as accurate as the corresponding fin-stabilized projectile having equal payload, projectiles are stabilized by spin unless there are overriding reasons to the contrary.

5—1.3.2 For

Some of the reasons for choosing fin-stabilization are:

a. A fin-stabilized projectile can be larger in proportion to its diameter (have a greater fineness ratio) than one which is spin-

(43)

stabilized. If the logistic limitations on length (storing, handling, loading into the gun) are not exceeded, the fin-stabilized projectile may be long enough to have an internal volume greater than that of the corresponding spin-stabilized round.

b. The lethality or other terminal usefulness of the round may be impaired by spin. An example in this category is the shaped charge round.

c. The mission of the projectile may require that it be fired at high quadrant elevations. Conventional spin-stabilized rounds suffer severe degradation in accuracy when fired at quadrant elevations greater than about 65°; fin-stabilized rounds do not.

d. The internal structure of the projectile may be such that the round becomes dynamically unstable when spun, or even such that it cannot be spun rapidly enough for gyroscopic stability by the guns available.

e. The projectile may be designed to be fired from a smooth-bore gun.

f. Fin-stabilized projectiles can be fired from a rifled gun without picking up enough spin to lose accuracy. This is done by the use of an obturator which engages the rifling but slips on the projectile.

5—2. SPIN-STABILIZED PROJECTILES

The first requirement we place on a projectile is that it be stable. It must be statically or gyroscopically stable; it must also be dynamically stable unless its expected trajectory is very short. The stability of spin-stabilized projectiles is treated in the paragraphs which follow.

5—2.1 Gyroscopic Stability

5—2.1.1 Gyroscopic Stability Factor

The gyroscopic stability of a spin-stabilized projectile can be assured by computing s_g, the gyroscopic stability factor.

$$s_g = \frac{I_x^2 p^2}{4 I_y \mu}$$

where

I_x = axial moment of inertia, slug-ft²
I_y = transverse moment of inertia, slug-ft²
p = axial angular velocity, rad/sec
μ = static moment factor, lb-ft/radian

On the assumption that the static moment varies linearly with yaw, the expression for the static moment per radian of yaw is

$$\mu = \frac{\pi}{8} \rho d^3 V^2 C_{M_\alpha}$$

ρ = air density, slug/ft³
d = maximum body diameter, ft
V = airspeed, ft/sec
C_{M_α} = static moment coefficient, per radian

Close attention must be paid to the units used in these expressions, as some of them are not the units customarily employed in reporting measurements of the quantities.

5—2.1.2 Conditions on Value of s_g for Stability

If $0 \leq s_g \leq 1$ the projectile is unstable and will "tumble" within a few hundred feet of the gun.

If s_g is greater than one, the projectile is gyroscopically stable, and we then investigate its dynamic stability, as described later. Since s_g is inversely proportional to the density of the air, projectiles which are stable at standard atmospheric conditions may be unstable when fired under arctic or other nonstandard conditions of temperature and pressure. Possible environments must be taken into account in computing s_g; this fact, coupled with the uncertainties in the other factors entering into s_g, has led some designers to set 1.3 as a lower limit on s_g in the preliminary design stage, using standard air density in the computation.

Note that at the muzzle we can write

$$s_g = C_1 \left(\frac{p}{V}\right)^2 \qquad \text{where } C_1 = \text{constant}$$

but $p/V = 2\pi/nd$, where n is the twist of the rifling at the muzzle, in calibers per turn. Hence the initial stability of the projectile depends on the rifling twist and only indirectly on muzzle velocity. If this were not so, mount fire, i.e., firing with re-

duced propelling charge, would be impractical. The indirect influence of muzzle velocity arises from the dependence of C_{M_α} on Mach number; this dependence can cause instability at reduced muzzle velocities.

Conventional projectiles lose airspeed much more rapidly than they lose spin. The value of s_e thus nearly always increases as the projectile flies down range.

The stability factors of projectiles fired at high quadrant elevations can, unless projectile velocity is maintained by rocket thrust, reach quite large values at the summit of the trajectory, owing to decreases in both velocity and air density. These large values are not detrimental in themselves, but the conditions which produce them also bring about large increases in the equilibrium yaw of the projectile.

5—2.2 Yaw of Repose

5—2.2.1 General

The gravity curvature of the trajectory gives rise to an angle of yaw large enough to create a precession rate which will permit the axis of the projectile to follow the tangent to the trajectory. This equilibrium requirement causes the projectile to point to the right of its flight path (right-hand yaw of repose) when the spin of the projectile is clockwise as viewed from the rear, which is the case with nearly all United States artillery ammunition. The lift force associated with this angle causes a drift to the right, and an estimate of the magnitude of this drift is given in the firing tables for the projectile. The designer is interested in keeping this drift small, and uniform, from round to round, as possible.

The yaw of repose is proportional to p/V^2. If it becomes large, the projectile may become dynamically unstable with resulting loss in range and accuracy.

5—2.2.2 Formula for Angle of Repose

An approximate expression for the usual right-hand yaw of repose is

$$\delta_r = \frac{I_x pg \cos\Theta}{\frac{1}{2}\rho S d\, C_{M_\alpha} V^2}\left(1 + i\frac{C_{M_{p\alpha}}}{C_{M_\alpha}}\frac{pd}{V}\right)$$

This equation shows that at the summit of a high angle trajectory, where $\cos\Theta = 1$ and ρ is considerably less than its sea level value, if V is small the yaw may be very large; it may even shift over to the left-hand equilibrium angle with disastrous results for the trajectory prediction. See Ref. 66, p. 392.

5—2.2.3 Trailing

An analysis of the first (and most significant) term of the expression for yaw of repose may shed

$$\delta_r = \frac{I_x pg \cos\Theta}{\frac{1}{2}\rho S d\, C_{M_\alpha} V^2} + \ldots$$

some light on the mechanism by which a spinning projectile "trails" as it moves along its trajectory. Rearranging the above equation gives

$$\tfrac{1}{2}\rho V^2 S d\, C_{M_\alpha}\, \delta_r = I_x p \frac{g\cos\Theta}{V}$$

On the left side of the equation we have the static aerodynamic moment, on the right side we have the axial angular momentum, $I_x p$, multiplied by the rate of change of direction of the tangent to the trajectory, $g \cos\Theta/V$ (see paragraph 4-5). The product is a rate of change of angular momentum, caused by the aerodynamic moment; conversely, the aerodynamic moment arising from the yaw of repose is just sufficient to change the angular momentum of the projectile at the rate required for the axis of the projectile to remain tangent to the trajectory (in the vertical plane the yaw is in a plane normal to the trajectory plane and the static moment is at right angles to the rotation, or 'precession', of the projectile axis, which is the well known gyroscopic behavior).

5—2.2.4 Projectile Asymmetries

Asymmetries of a projectile, arising from the manufacturing process, will add (vectorially) a small constant yaw to the yaw of repose, increasing the possibility of trouble at the summit. Asymmetry also introduces a forcing function which can lead to resonance; the resulting yaw can be large for fin-stabilized projectiles, and the subject will be discussed further in paragraph 5-3.

5—2.2.5 Method of Computation of Projectile Spin

The gyroscopic stability factor is calculated at the muzzle and is often calculated at the summit of high angle trajectories as an index of summital behavior. It is recommended that the designer compute the yaw of repose at the summit of such trajectories, and compute the stability factor at the muzzle and at impact. If his computer program does not include a running calculation of spin rate, he must estimate as well as he can what the spin rate of the projectile will be at summit and impact, using the expression (in the absence of rocket thrust)

$$\frac{p}{V} \approx \frac{\cos\Theta}{\cos\Theta_o} \exp\left[\frac{\rho S}{2m}\left(k_x^{-2} C_{l_p} + C_D\right)(x - x_o)\right]$$

$$\left(\frac{p}{V}\right)_o$$

where the subscript o refers to conditions at the beginning of the interval over which the change in p/V is being computed, x is distance measured along the trajectory, and $k_x^{-2} = md^2/I_x$. This expression assumes that ρ, C_{l_p} and C_D are constants, which is not likely. Average values of these parameters must be used, and it will be seen that the approximation for p/V may be poor. Designers of spin-stabilized projectiles have been willing to assume that the projectiles retained enough spin to be stable at impact and to accept whatever limitation on quadrant elevation was found to be necessary in test firings of the round.

While C_{l_p} is negative, C_D is usually of sufficient magnitude that p/V increases as the projectile rises to the summit. On the descending limb the cosine of the trajectory angle is decreasing, and p/V will decrease, since obviously V is increasing while p, in the absence of some spin-producing mechanism such as a canted fin, continues to decrease.

Shown in Table 5-1 and Table 5-2 are sample trajectories for a typical 5-inch projectile, with initial conditions differing only in quadrant elevation. The trajectory with Q.E. = 3° offers an opportunity for a simple check on the $(p/V)/(p/V)_o$ equation presented above. Using average values of ρ and C_D, we have, for p, V at impact

$$\frac{\frac{p}{V}}{\left(\frac{p}{V}\right)_o} = \frac{\nu}{\nu_o} \approx \frac{\cos(-3.9°)}{\cos 3°} \exp\left\{\frac{(.001186)\ (0.1355)}{1.435}\right.$$

$$\left.\left(6.89\,(-.014) + 0.365\right) 9530\right\}$$

$$= \frac{.9977}{.9986} e^{.001} = 1.325$$

The trajectory calculation gives $\nu/\nu_o = .295/.224 = 1.32$, so the approximate formula is very good for flat fire.

For the trajectory with Q.E. = 70°, the rough estimates of ρ and C_D obtained by taking simple means values would be .00088 for ρ and .285 for C_D.

$$\frac{\nu}{\nu_o} = \frac{\cos(-77.8°)}{\cos 70°} \exp\left\{\frac{(.00088)\ (0.1355)}{1.435}\right.$$

$$\left.\left(6.89\,(-.014) + 0.285\right) 54100\right\}$$

$$= \frac{.2113}{.3420} e^{.001} = 1.45$$

The trajectory calculation gives $\nu/\nu_o = .289/.224 = 1.29$, so the approximation is only fair. The use of values of C_D weighted by the arc distance traversed, in calculating the means, would make the approximation for ν/ν_o very good.

The high angle trajectory is presented principally to show the magnitude reached by the yaw of repose at the summit. The actual yaw might be much greater because dynamic instability, owing to nonlinearity of the aerodynamic coefficients, is likely to occur at yaws of this magnitude.

5—2.3 Zoning

Conventional projectiles attain their maximum range when fired at a quadrant elevation of about 45°. For rocket-assisted projectiles the Q.E. for maximum range is greater than 45°, running up to 60° or 70° when using a long-burning rocket with a high ratio of fuel weight to total projectile weight. Ranges shorter than the maximum may be obtained by changing the Q.E., reducing the effective rocket thrust, or reducing the muzzle velocity. Reduction of the muzzle velocity in a series of steps, by reducing the charge of gun propellant, is called "zoning"; each level of muzzle velocity is called a "zone", and variations of range within each zone are obtained by varying the quadrant elevation.

A projectile whose range is controlled by muzzle

velocity variation must be stable over a wide range of Mach numbers, which will almost certainly include transonic speeds at sea level air densities. Since C_{M_α} usually peaks in the transonic regime and the gyroscopic stability factor is inversely proportional to C_{M_α}, stability may be at a minimum in the transonic regime. If C_{M_α} data are not available for the full range of speeds, estimates may be made by use of the shapes of the C_{M_α} vs Mach number curves of projectiles similar to the one in question. Use of an estimated C_{M_α} requires a greater margin of safety on the gyroscopic stability factor to insure that it does not become less than unity. However, if trajectory calculations show that the projectile will spend only a short time in the transonic regime, it may be possible to accept a certain amount of instability for that short time.

The gyroscopic stability factor of a conventional spin-stabilized projectile usually has its smallest value at the muzzle. Rocket-assisted projectiles, on the other hand, are more likely to become gyroscopically unstable on the descending limb of the trajectory, near impact. This instability can be avoided by:

a. Distributing the mass of the projectile so that its c.g. is forward of the usual location in a projectile of the given aerodynamic shape.
b. Increasing the rifling twist of the gun.
c. Canting the rocket nozzles, or providing internal means of rotating the jet from a single nozzle.

5—2.4 Dynamic Stability of Spin-Stabilized Projectiles

5—2.4.1 Magnitude of Modal Vectors

The yaw of a symmetric projectile acted on by a linear force and moment system is given by

$$\delta = K_{1_0} e^{\lambda_1 s} e^{i\phi_1} + K_{2_0} e^{\lambda_2 s} e^{i\phi_2} - \delta_e$$

K_{1_0} = initial magnitude of nutation vector
K_{2_0} = initial magnitude of precession vector
λ_1 = nutation damping exponent, per caliber
λ_2 = precession damping exponent, per caliber
s = travel of projectile, calibers
ϕ_j = phase angles of the modal vectors ($j = 1,2$)
δ_e = equilibrium yaw

We are concerned here with the magnitudes and signs of λ_1 and λ_2. It will be seen that the magnitude of a modal vector will increase if its associated λ is positive; the larger the value of λ the more rapid is the increase in the magnitude of the vector. The term $e^{i\phi_j}$ is, of course, simply a sinusoidal oscillation between +1 and −1, and between +i and −i. If neither of the two modal vectors, K_1 or K_2, grows in magnitude as the projectile flies down range, the projectile is said to be dynamically stable. For dynamic stability, therefore, both λ_1 and λ_2 must be equal to, or less than zero.

From Ref. 12a we have

$$\lambda_1 = -1/2\left[H - \frac{2T - H}{\sqrt{1 - 1/s_g}}\right]$$

and λ_2 differs only in having a + sign between the two terms inside the brackets.

$$H = \frac{\rho S d}{2m}\left[C_{L_\alpha} - C_D - k_T^2 (C_{M_q} + C_{M_{\dot\alpha}})\right]$$

$$T = \frac{\rho S d}{2m}\left[C_{L_\alpha} + k_T^2 C_{M_{p\alpha}}\right]$$

So, since s_g is a function of C_{M_α} and (indirectly) of C_{L_α}, we see that all of the major aerodynamic coefficients enter into the determination of the damping exponents.

5—2.4.2 Dynamic Stability Factor, s_d

Murphy (Ref. 12a) recommends that instead of simply requiring that the λ_j be nonpositive, we should set an upper limit on the greater of the two which must not be exceeded if the projectile is to fulfill its mission. This limit, represented by an unsubscripted λ, may be greater than zero because some growth of initial yaw may be tolerable, especially in short flights.

5—2.4.2.1 Stability for $\lambda_{max} \leq \lambda$

Murphy then introduces the stability factor, s_d, where

$$s_d = \frac{2T + 2\lambda}{H + 2\lambda}$$

and by use of the expression for λ_{max} with the restraints that $\lambda_{max} \leq \lambda$ and $H + 2\lambda > 0$, arrives at the identity

$$\frac{1}{s_g} = s_d (2 - s_d)$$

Plotting this expression as a curve with $1/s_g$ and s_d as coordinates, we get

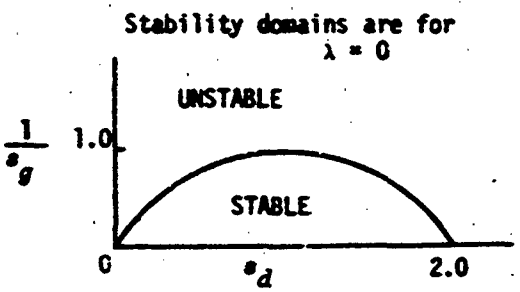

Figure 5—1. Abbreviated Graph of $1/s_g$ vs s_d

Conditions as to stability are a function of the location of the point determined by the intersection of $1/s_g$ with s_d (Figure 5-2), namely:

a. Intersection lies below curve: Projectile is gyroscopically stable and may be dynamically stable, with $\lambda_{max} < \lambda$.
b. Intersection lies on the curve: $\lambda_{max} = \lambda$
c. Intersection lies above curve: Projectile is dynamically unstable with $\lambda_{max} > \lambda$ and may be gyroscopically unstable.

5—2.4.2.2. Stability for $\lambda = 0$

In practice, λ is often set equal to zero. Then the expression for the dynamic stability factor is*

$$s_{d_0} = \frac{2T}{H} = \frac{2(C_{L_\alpha} + k_\alpha^{-2} C_{M_{p\alpha}})}{C_{L_\alpha} - C_D - k_t^{-2}(C_{M_q} + C_{M_{\dot\alpha}})}$$

The curve in Figure 5-1 is now the locus of points where $\lambda = 0$. If the intersection of $1/s_g$ with s_d lies above the curve, we can calculate λ_{max} by measuring Δs_d, the change in s_d required to reach the curve, moving horizontally, and using the following relation:

$$\lambda_{max} = \frac{H/2}{1 - s_{d_0} - \Delta s_d} \Delta s_d \text{ when } \frac{1}{s_g} < 1$$

(Remember that H contains the factor $\rho s_d/2m$.) Note that $H > 0$ is one of the constraints on s_{d_0}, so the λ_{max} computed by the above expression is positive, and one of the yaw vectors is undamped; we can estimate the growth of this vector from $\exp[\lambda_{max} s]$ where s is travel in calibers. Similarly, when the intersection lies below the curve, use of the above expression for λ_{max} will result in a negative value with which the rate of decrease of yaw can be computed.

Returning to the expression for s_{d_0}, we note that C_{L_α} is always positive and usually much greater than C_D. The denominator of s_{d_0} is nearly always positive. If it is not, we should not compute s_{d_0}. The numerator contains the magnus moment coefficient, $C_{M_{p\alpha}}$, which is usually positive for spin-stabilized projectiles at supersonic speeds, but often negative at transonic and subsonic speeds. s_{d_0} is usually positive, and indeed the values of the coefficients and radii of gyration (in calibers) are such that s_{d_0} nearly always lies between 0 and 2; if s_{d_0} is outside these limits, the projectile cannot be stabilized by spin.

In BRL Report 853 (Ref. 48), Murphy discusses the influence of mass distribution on the dynamic stability of statically unstable projectiles. He notes that at supersonic velocities many bodies of revolution cannot be stabilized by spin if the c.g. is more than two calibers aft of the centroid. The centroid is, of course, the point at which the c.g. would be located if the projectile were of uniform density; it is near the geometrical centroid of the silhouette of the projectile. In any case, there is an optimum c.g. location which minimizes the spin rate required for stability, and this optimum location is usually near, and aft of, the centroid.

The complete graph of $1/s_g$ vs s_d, taken from Ref. 12a, appears as Figure 5-2.

Unfortunately $C_{M_{p\alpha}}$ is sensitive to changes in yaw angle. We cannot preserve linearity in the magnus moment by restricting θ to less than 10° as we have assumed that we could for some other aerodynamic coefficients. A large C_{L_α} and k_α will

*Some authors add $C_D + k_\alpha^{-2} C_{L_p}$ to the denominator; however, this sum is effectively zero compared with C_{L_α}.

TABLE 5—1
SAMPLE TRAJECTORY FOR SPIN-STABILIZED 5-INCH PROJECTILE
AT Q.E. = 3°
(SEE APPENDIX I)

FFD	FFM	TYPE	RGA	RGT	D,FT
1.050	1.250	5.540	.301	1.030	.4150
3.0	0.				

IS

WTO	VO	SPIS	SBT	DTM	TWIST	QE
46.08	1925.	.	.0	.400	28.00	3.000
WTB	ZO	TEMP.	DTL	DTE	CDD2	CLP
46.08	.	59.	4.0	.350	6.00	-.014

.001189 1116.0

TIME THETA	X Z	DIST THRUST	V DRAG	CD YAW	CHA DR MACH	MASS SPIN	SG
.00	.	.	1925.0	.331	3.93	1.000	1.43
.05	.	.	197.4	.000	1.72	.224	1.36
.12							
.99	1694.	1695.	1804.4	.342	4.01	.997	1.43
.03	75.	.	178.9	.000	1.61	.234	1.46
.13							
1.04	1937.	1938.	1787.5	.344	4.02	.997	1.43
.03	84.	.	176.3	.000	1.60	.236	1.48
.13							
1.74	3156.	3158.	1704.1	.351	4.07	.996	1.43
.02	118.	.	163.7	.000	1.52	.244	1.57
.14							
2.94	5125.	5127.	1574.8	.364	4.16	.995	1.43
-.00	137.	.	144.6	.001	1.41	.259	1.72
.15							
4.09	6867.	6870.	1465.8	.377	4.23	.996	1.43
-.02	113.	.	129.8	.001	1.31	.273	1.88
.17							
5.15	8375.	8379.	1375.5	.388	4.38	.998	1.43
-.05	55.	.	117.9	.001	1.23	.286	1.99
.18							

TIME,S	RANGE,M	V,FPS	THETA,D	SPIN	SG
5.85	2839.	1316.	-3.9	.295	2.04

TABLE 5—2
SAMPLE TRAJECTORY FOR SPIN-STABILIZED 5-INCH PROJECTILE
AT Q.R. = 70°
(SEE APPENDIX I)

FFD	FFM	TYPE	RGA	RGT	D,FT
1.050	1.250	5.540	.381	1.030	.4150

WTO	VO	SPIS	SBT	DTM	TWIST	QE
46.08	1925.	.	.0	.800	28.00	70.000

WTB	ZO	TEMP	DTL	DTE	CDD2	CLP
46.08	.	59.	8.0	.350	6.00	-.014

.001189 1116.0

TIME THETA	X Z	DIST THRUST	V DRAG	CD YAW	CMA MACH	DR SPIN	MASS SG
.00	.	.	1525.0	.331	3.93	1.000	1.43
1.22	.	.	197.4	.000	1.72	.224	1.36
.22							
5.62	3140.	8749.	1260.0	.397	4.53	.770	1.43
1.17	8166.	.	78.2	.002	1.16	.313	3.00
.35							
15.86	7420.	18531.	739.1	.168	4.69	.581	1.43
1.02	16951.	.	8.6	.013	.70	.496	9.64
.68							
31.25	13064.	26588.	360.4	.304	4.21	.487	1.43
.27	22465.	.	3.0	.151	.35	.971	48.95
.80							
34.45	14159.	27696.	336.7	.375	4.18	.485	1.43
-.02	22606.	.	3.3	.186	.32	1.033	56.07
.80							
44.85	17496.	31575.	450.3	.196	4.33	.513	1.43
-.81	20841.	.	3.2	.069	.43	.757	27.51
.80							
60.85	22170.	41728.	819.9	.168	4.79	.683	1.43
-1.23	11890.	.	12.4	.007	.76	.390	4.95
.80							
65.65	23443.	45896.	911.0	.220	4.97	.775	1.43
-1.28	7931.	.	22.8	.004	.84	.340	3.19
.80							
70.45	24617.	50416.	966.5	.253	5.06	.892	1.43
-1.32	3566.	.	33.9	.003	.87	.307	2.23
.80							

TIME,S	RANGE,M	V,FPS	THETA,D	SPIN	SG
74.20	7755.	988.	-77.8	.289	1.82

reduce the effect of changes in $C_{M_{pa}}$, and a small and nearly constant yaw angle will reduce the size of the change in magnus moment. We see immediately the value of good obturation in keeping the initial yaw small, and the value of high projectile velocity in keeping the equilibrium yaw small.

5—2.4.3 Further Discussion of Magnitude of Modal Vectors and Stability

The following paragraph is taken from Murphy (Ref. 12a):

The requirement that the exponential coefficients be negative throughout the flight is much stronger than necessary in a number of applications. This can be seen by the following example. Consider the case of a specific projectile whose exponential coefficients are strongly negative for $M \leq 2.0$ except for the Mach number interval (0.9, 1.1) where both exponents are positive. Exact numerical integration showed that an initial maximum angle of attack of four degrees for the launch Mach number of two will decay to a tenth of a degree before the Mach number decreases to 1.1. The dynamic instability associated with the transonic velocities then will cause the maximum angle to grow to approximately one degree and then decrease a second time when subsonic stability is established. Thus the "dynamically unstable" projectile has maintained a small angle of attack over the entire trajectory.

5—2.5 Aerodynamic Jump of Spin-Stabilized Projectiles

5—2.5.1 General

The path taken by a projectile after leaving the muzzle of the gun is determined principally by wind, gravity, drift, aerodynamic jump, and, of course, by the direction in which the gun is pointing when the projectile emerges from the muzzle.

The designer can reduce the sensitivity of the projectile to wind by reducing C_D, or balancing drag by rocket thrust; he can reduce the round-to-round dispersion due to varying gravity drop by good obturation which reduces round-to-round variations in muzzle velocity. Drift should not vary much from round to round if the projectile yaw is kept small. In this discussion we will simply set wind, gravity, and drift equal to zero, assume that the transverse component of the velocity imparted to the projectile by the gun is negligible, and consider how the designer may reduce the remaining source of inaccuracy, aerodynamic jump.

5—2.5.2 Aerodynamic Jump Defined

In the absence of wind, gravity, and drift, an average line drawn through the swerving path of the projectile, such that the projectile spends equal times on each side (or all sides) of the line, can be visualized as a straight line which intersects the muzzle of the gun. At the muzzle this mean trajectory line will make an angle with the line defining the direction of the bore of the gun; this angle is called the "aerodynamic jump."

Note that the plane of the aerodynamic jump angle can lie in any orientation; jump can be up, down or sidewise. At a vertical target the effect of jump appears as a deviation from the theoretical point of impact, which is computed from the bore sight line, corrected for drift and gravity drop. (In flat firing wind corrections are seldom made; rounds are fired as rapidly as is practical, and the wind effect is assumed to be the same for all rounds).

5—2.5.3 Magnitude of Aerodynamic Jump

The aerodynamic jump of a symmetric projectile, in radians, is given (to a close approximation) by

$$\Theta_J = \frac{C_{L_\alpha} d}{C_{M_\alpha} V_e} \left(k_1^2 \dot{\delta}_e - i k_2^2 p_e \delta_e \right)$$

where V_e = projectile velocity, fps; $\dot{\delta}_e$ = yawing velocity, rad/sec; p_e = spin rate, rad/sec; δ_e = yaw, radians — measured at the end of the blast zone

and the imaginary multiplier, i, shows that the contribution of initial yaw to jump is at right angles to the direction of the yaw. Asymmetry of the projectile adds another term to the expression for Θ_J, a term which depends on the size and initial orientation of the asymmetry; see Murphy, *Comments on Projectile Jump*, Ref. 97. It is important

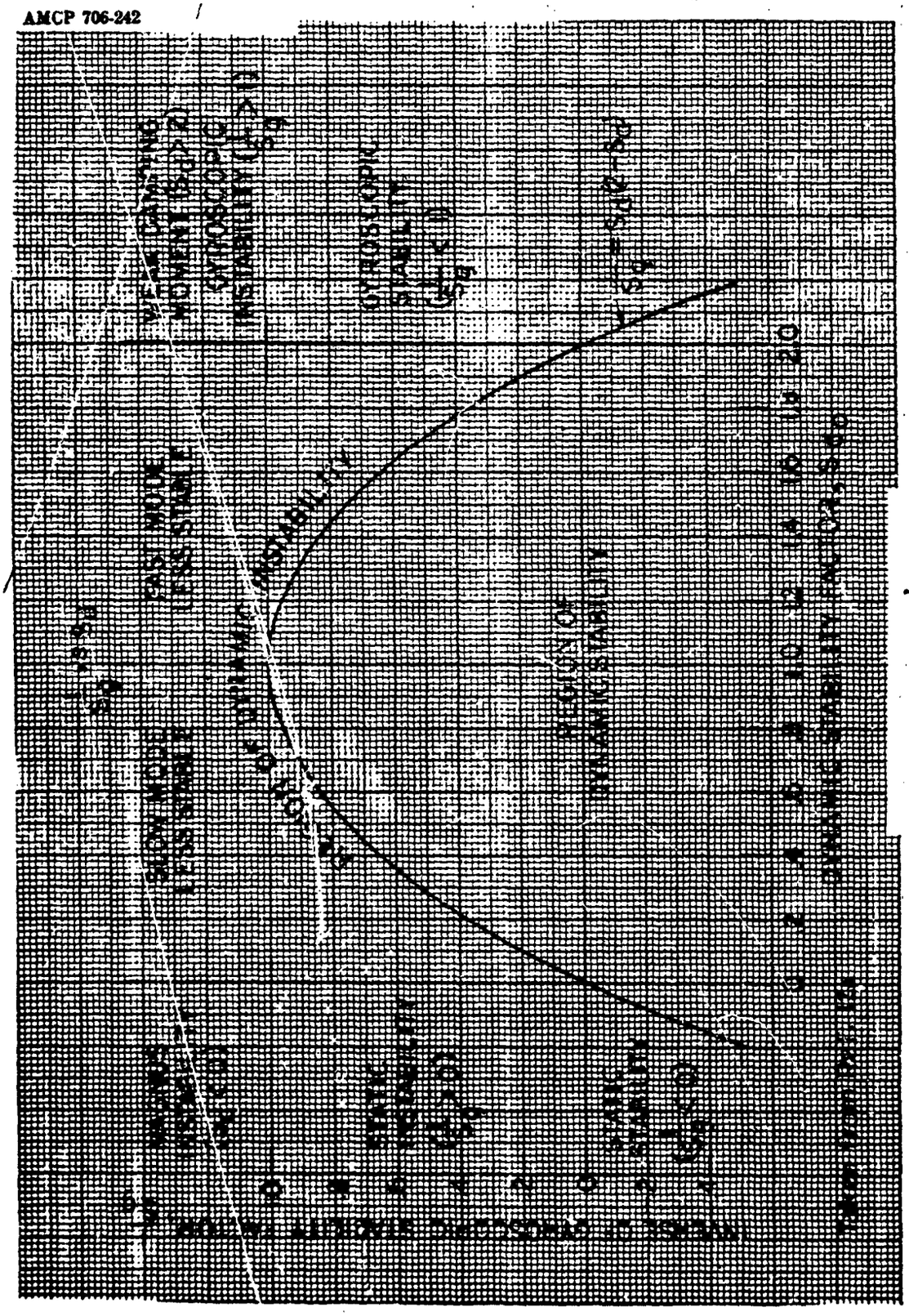

Figure 5—2. Graph of $\frac{1}{\sigma_g}$ vs σ_d

that projectile asymmetries be kept as small as is economically feasible.

$\dot{\delta}_o$ is usually so small that the second term in the jump equation is about an order of magnitude smaller than the first. However, if the bore clearance is unusually large, or if there is a strong cross wind at the gun, the yaw may be large and the second term cannot be neglected.

$\dot{\delta}_o$ varies from round to round. Good obturation will reduce its magnitude and the magnitude of the variation. For a low drag projectile, $C_{M_\alpha}/C_{L_\alpha}$ is approximately equal to the distance, in calibers, between the c.g. of the projectile and the c.p. of the normal force. Increasing this distance will reduce Θ_J for a given $\dot{\delta}_o$ but the design changes which increase the c.p.-c.g. separation, such as an increase in the length of the projectile, often also increase k_t^2. Boattailing will decrease C_{L_α} and increase C_{M_α}, increasing the c.p.-c.g. separation without much change in k_t^2. Since drag is also decreased, boattailing has a very beneficial effect on performance unless the stability of the design is impaired; this must be checked (see paragraph 5-2.4.). This discussion of aerodynamic jump applies only to dynamically stable projectiles.

5—2.5.4 Orientation of Aerodynamic Jump

The orientation of the aerodynamic jump angle also varies from round to round, because $\dot{\delta}_o$ is a vector. The direction of $\dot{\delta}_o$ depends on the pattern of the gas flow in the muzzle blast, which in turn depends on the bore yaw of the projectile. Since projectiles loaded in the gun in the same manner probably ride the lands of the rifling in the same manner (see Ref. 56), the orientation of the blast pressure field, and therefore of $\dot{\delta}_o$, is probably biased in one particular direction. Hence the distribution of jump orientation angles, when a group of rounds is fired, is probably sharply peaked in one quadrant.

5—2.5.5 Distribution of Aerodynamic Jump

The distribution of impact points on the target is really a circular (or elliptical) distribution about the theoretical point of impact of all the rounds, assuming no change in gun direction. The bias described in the preceding paragraph produces a hit pattern which appears to be a rectangular distribution about a mean point of impact which is the "center of gravity" of the pattern. Artillery targets are always analyzed as though this were the true situation, since the center of impact and the vertical and horizontal probable errors are very easy to compute from the coordinates of the hits. The location of the theoretical point of impact is very difficult to obtain from the coordinates of the hits and cannot be computed from the boresight line with any certainty, which makes the derivation of the true Θ_J distribution impractical.

The above discussion is presented because of its implications for design decisions based on the results of firing tests. Since the $P.E._V$ and $P.E._H$ method commonly used is theoretically inappropriate, design changes should not be based on small samples, i.e., groups of fewer than 15 rounds. Furthermore, since most design changes are aimed at reducing only the magnitude of Θ_J and not at reducing its directional dispersion, the statistically indefensible procedure of eliminating "maverick" rounds from the error calculations may be justified by the contention that their points of impact on the target were the result of unusual orientations of the jump angle, not large changes in its magnitude.

5—2.5.6 Relationship Between Aerodynamic Jump and Q.E.

5—2.5.6.1. Vertical Component

In firing for range, the importance of the vertical component of Θ_J depends on the quadrant elevation of the gun. Differentiating the expression for range in a vacuum gives an approximation of the effect of changes in angle of departure on range.

$$X = \frac{V_o^2}{g} \sin 2\Theta$$

$$dX = \frac{2V_o^2}{g} \cos 2\Theta_o \, d\Theta_o$$

$$\frac{dX}{X} = \frac{2}{\tan 2\Theta_o} \, d\Theta_o$$

When $\Theta_o = 45°$, the change in range is negligible. At $\Theta_o = 15°$ the change in range, in mils, is about

3.5 times as great as the change in departure angle (in milliradians) due to aerodynamic jump, so at low quadrant elevations jump is an important factor in range accuracy.

5—2.5.6.2 Horizontal Component

The horizontal component of Θ_J produces a horizontal deviation at the point of fall of the projectile, which is proportional to the arc length of the actual trajectory. Since the deflection dispersion of rounds fired for range is usually reported in mils based on the mean range, the effect of a given horizontal jump is multiplied by the ratio of the arc length of the trajectory to its horizontal projection. Again we can estimate this ratio from the vacuum condition, giving

$$\frac{Arc}{X} = \frac{1}{2}\left[\frac{1}{\cos\Theta_o} + \frac{1}{\tan\Theta_o}\ \ln\left(\frac{\cos\Theta_o}{1-\sin\Theta_o}\right)\right]$$

and at $\Theta_o = 45°$, $\frac{Arc}{X} = 1.15$, while at $\Theta_o = 15°$, $\frac{Arc}{X} = 1.01$. Hence, this factor can be significant in estimating deflection P.E.'s from aerodynamic jump, when $\Theta_o > 40°$.

5—3. FIN-STABILIZED PROJECTILES

5—3.1 General

The inconvenient fact that the center of pressure of the aerodynamic forces on a projectile body is almost invariably forward of the c.g. of the body can be counteracted by placing lifting surfaces (fins) rearward of the c.g. If, when the projectile is yawed, the moment produced by the lift forces on the fins is greater than that produced by the forces on the body, the net moment will oppose the yaw and the projectile will be statically stable. In symbolic notation, we have

$$C_{M_\alpha} = C_{M_{\alpha_B}} + C_{M_{\alpha_T}}$$

$$C_{M_\alpha} = C_{M_{\alpha_B}}(X_{c.p._B} - X_{c.g.}) + C_{M_{\alpha_T}}(X_{c.p._T} - X_{c.g.})$$

$$C.P. - C.G. = \frac{C_{M_\alpha}}{C_{N_\alpha}}$$

where the subscript B refers to the body and the subscript T refers to the tail. Unsubscripted quantities apply to the whole projectile. The X's are distances in calibers, measured from the base of the whole projectile, which is usually the base of the tail. The tail comprises all of the fins and the (usually) cylindrical boom on which they are mounted. Arrow or subcaliber projectiles have the fins mounted directly on the body, so the base of body, base of tail, and base of whole projectile may coincide. Folding fins may require an arbitrary definition of their base location, depending on the design.

5—3.2 C.P.-C.G. Separation

It will be noticed in the above equations that $X_{c.p._T} - X_{c.g.}$ is negative, and C_{M_α} will be negative if the projectile is statically stable. C.P.-C.G. is then also negative, but this quantity is often referred to simply as "c.p.-c.g. separation," in calibers, and treated as though it were unsigned.

The optimum magnitude of the c.p.-c.g. separation is not well defined. For minimum sensitivity to muzzle blast the tail moment coefficient,

$$C_{M_{\alpha_T}}(X_{c.p._T} - X_{c.g.})$$

should be small; to minimize the yaw angle due to projectile asymmetries, the total static moment coefficient, C_{M_α}, should be large. The writer believes that the design value of the c.p.-c.g. separation should be far enough above 0.5 caliber that inaccuracies in estimation of C_{M_α} and C_{N_α}, including the effects of manufacturing variability, will not reduce the c.p.-c.g. separation of any round below 0.5 caliber. On the other hand, c.p.-c.g. separations greater than one caliber have been found to be accompanied by increased dispersion at the target.

5—3.3 Fin Type

The choice of fin type is obviously a trade-off problem, involving the utilities of projectile volume, range, accuracy and cost. Establishing trade-off curves for each design, determining optimum points for each design, and then comparing the optima would be a long process. It is doubtful that the choice will ever be made explicitly in this way, but the intuitive narrowing of choices must follow

these lines. A brief discussion of the types of fins follows.

5—3.3.1 Fixed Fins

Fixed fins of one caliber span are easy to make, and easy to make uniformly; this promotes accuracy. However, space is required between the leading edge of the fins and the location of the full body diameter in order to reduce fin-body interference and allow the fins to develop their expected lift. This reduces the projectile volume-to-length ratio. If low drag is important, the long boattail required further reduces the useful projectile volume.

5—3.3.2 Folding Fins

Folding fins which are bunched behind the projectile when in the gun tube and fanned out to more than one caliber span by some mechanism after the projectile has left the muzzle blast can produce large c.p.-c.g. separations without large muzzle blast effects. They are expensive and conducive to large projectile asymmetry. They need not reduce the volume-to-length ratio of the projectile as much as do fixed fins.

Folding fins which are wrapped around the projectile near its base when in the gun tube and spring out after the projectile leaves the muzzle, can produce the required stability with reduced sensitivity to muzzle blast and very little reduction in projectile volume. They are not cheap; the asymmetry they produce can be offset by a large C_{n_α}.

5—3.4 Obturation

Good obturation is important for both spin- and fin-stabilized projectiles, especially so for the fin-stabilized rounds. It has been achieved by the use of rubber or plastic rings on or near the cylindrical portion of the body, or by the use of a [illegible] of suitable material placed behind the projectile (pusher obturator). The obturator is sometimes given the added function of holding folding fins in the closed position; the obturator must then break up on emergence from the muzzle, usually no problem with rubber or plastic obturators which can be notched or, if necessary, segmented. Obturators on mortar projectiles must break-up into small non-lethal fragments on emergence; this behavior may be required for other weapon systems. Obviously, retaining the obturator in flight increases the drag.

Fin-stabilized projectiles are often fired from rifled guns. The obturator must be designed to fill the grooves of the rifling, but it must not impart a high spin to the projectile. Friction between obturator and projectile will impart a slow spin which is usually remarkably uniform from round to round, and which can to some extent be controlled by the designer by varying the material of the obturator and the area of its surface of contact with the projectile.

5—3.5 Arrow (Subcaliber) Projectiles

5—3.5.1 General

The large muzzle energy obtainable with large caliber guns offers the possibility of launching a light projectile at very high velocity. If the light projectile is reduced in caliber, its weight per unit deceleration due to drag would be so great as to soon reduce its velocity below that of a heavy projectile fired from the same gun. But if the light projectile is reduced in caliber its weight per unit of frontal area (sectional density) can be increased up to the point at which it becomes a useful item for employment against armor, owing to its high striking velocity. Since these subcaliber projectiles are usually very long in proportion to their diameters, they must be fin-stabilized; they are referred to as "arrow" projectiles.

5—3.5.2 Sabot

The space between the subcaliber projectile and the gun barrel is filled by an annular device called a "sabot." The fins, attached to the body near its base, have a span equal to the gun caliber so that they and the sabot, which is usually placed near the c.g. of the projectile, form two riding surfaces which keep the bore yaw of the projectile small.

If the projectile is propelled by a pusher obturator, the sabot has only a centering function and can be relatively light and lightly attached to the projectile. However, the sabot must often provide the obturation and transmit most of the accelerating force to to the projectile since the sabot

area is often greater than the base area of the projectile. The sabot is then heavy, and attached to the projectile by means of grooves around the projectile body. These grooves naturally give rise to shock waves which increase the drag. If fired from a rifled tube, provision must be made for rotational slippage between obturator and projectile. The sabot must leave the projectile by break-up or segmentation shortly after leaving the muzzle because its drag would be intolerable. Fragments of the sabot may strike the fins, so the fins must be strong. For this reason, and to improve the riding of the fins on the interior surface of the gun tube, the fins are often end-plated. While the transverse plates on the tips of the fins increase the drag, they also increase the lift of the fins, permitting a reduction in fin area which largely offsets the drag of the plates. Some interesting sabot designs are described by Allen in BRL Rept. 1005 Part I (Ref. 61).

MacAllister and Rouhke (Ref. 63) compiled and analyzed the drag data obtained in several ballistic range firings of arrow projectiles. They found that the addition of four one-caliber square tail-fins to a two-caliber ogive-cylinder body increased the drag to about 165% of the drag of the body alone, when the fin thickness was 5% of the fin cord. When the fin thickness was 16%, the drag increased to about 220% of the body-alone value. When these fins were canted 2° the drag increased by an additional 10% of the body-plus-tail value. These large C_{D_0} values are made tolerable by the fact that they are based on the diameter of the slender body.

5—3.5.3 Aeroelasticity

Because of the high velocity of the arrow rounds, the aerodynamic forces and moments to which they are subjected can become so large as to cause a long, slender projectile to deform in flight into a slight bow. Since the forces change direction as the projectile yaws and rolls slowly, the bowing deflection becomes an oscillation which leads to the possibility of resonant magnification. Solid bodies are not likely to give trouble but, in the event that a significant portion of the body is thin-walled, the natural frequencies of the body vibrating as a rod should be calculated and compared with the yawing frequency $\sqrt{-M/I_m}$ in radians per second. Large deformations increase the drag of the projectile even if they do not threaten its integrity.

5—3.6 Dynamic Stability of Fin-Stabilized Projectiles

5—3.6.1 General

As discussed (at greater length) in the subsection on spin-stabilized projectiles, a projectile is said to be dynamically stable if its transient yaw does not increase during flight. Statically stable fin-stabilized projectiles having zero spin are always dynamically stable; the yaw, which is planar, decays according to the expression

$$\delta = \delta_0 e^{\lambda s} + \delta_a \qquad \text{(nonspinning)}$$

where

$$\lambda = -\frac{\rho s d}{4m}\left[C_{L_\alpha} - C_D - k_t^2 (C_{M_q} + C_{M_{\dot\alpha}})\right]$$

s is the travel in calibers, and δ_a is the constant yaw due to projectile asymmetry, or "trim angle." The additional yaw which arises from the curvature of the trajectory is negligible for normal trajectories.

5—3.6.2 Zero Spin

A condition of zero spin almost never exists since manufacturing tolerances permit some slight twist of the fins resulting in a spin producing torque. In fact, zero spin is very undesirable, because then the lift produced by the trim angle, δ_a, will steer the projectile away from its predicted trajectory, thus deflection due to asymmetry can be intolerably great if the roll rate of the projectile is near zero over much of the trajectory.

5—3.6.3 Equilibrium Roll Rate

5—3.6.3.1 Equilibrium Spin

Nearly all fin-stabilized projectiles are designed to acquire a certain equilibrium spin, called a slow spin because it is much smaller than the roll rate used for spin-stabilization. The spin torque is

generally produced by "canting" the fins, or, if the projectile is rocket-assisted, may be produced by canting the rocket motors.

5—3.6.3.2 Torque

When the torque is produced by twisting or cambering the fins, or by canting, i.e., bending up a portion of each fin, the spin torque is produced by the lift of the fins, which acts in opposite directions on opposite sides of the projectile axis. The angle at which the air flow over the projectile strikes the fins depends on the spin rate; as the spin rate increases, the angle of attack of the canted portion of the fin decreases and the spin torque decreases until it just balances the decelerating torque produced by skin friction.

5—3.6.3.3 Computation of Equilibrium Roll Rate

This equilibrium roll rate is given by

$$p_e = -\frac{C_{l_0}}{C_{l_p}}\frac{V}{d}\delta_e$$

where p_e = equilibrium roll rate, rad/sec
C_{l_0} = roll moment coefficient due to fin cant (at zero spin)
C_{l_p} = roll damping moment coefficient
δ_e = fin cant angle, radians

C_{l_0} is a function of the percentage of fin area which is canted; C_{l_p} is always negative. This expression is useful when C_{l_0} has been determined in a wind tunnel test. However, C_{l_0}/C_{l_p} may be estimated from the approximation, valid only for fins with a tip radius at least three times as great as the root radius,

$$\frac{C_{l_0}}{C_{l_p}} = \frac{2d}{b\left[\frac{\delta S\, C_{l_{p_B}}}{b\, S_{fin}\, C_{L_{\alpha_f}}} - 1\right]^{\left(\frac{S_{cant}}{S_{fin}}\right)}}$$

where $C_{L_{\alpha_f}}$ is the fin lift coefficient slope based on fin area, $C_{l_{p_B}}$ is the roll damping moment coefficient of the body alone, S_{fin} is the total fin area (not the wetted area, which is twice as great) and S_{cant} is the total canted area. Hence the ratio S_{cant}/S_{fin} is the proportion of fin area which is canted. S is frontal area, b is fin span and d is maximum diameter of the body.

5—3.6.3.4 Sample Calculation

For example, a 6-inch projectile with one-caliber fins ($b = d$) might have the following characteristics:

$C_{L_{\alpha_f}}$ = 2.0 per radian
$C_{l_{p_B}}$ = −0.02
S = 0.196 ft²
S_{fin} = 0.5 ft²
S_{cant} = 0.1 ft²
δ_e = 4° = 0.073 radian
V = 1600 fps

$$\frac{C_{l_0}}{C_{l_p}} = \frac{3}{12\left[\left(\frac{0.196}{0.5}\right)\left(\frac{-0.02}{2.0}\right)\right] - 1}\left(\frac{0.1}{0.5}\right) = \frac{0.6}{-1.05}$$

$$= -0.57$$

and $p_e = 0.57\left(\frac{1600}{0.5}\right)(0.073) = 123$ rad/sec

$= 21$ rev/sec

This calculation is not very sensitive to $C_{L_{\alpha_f}}$, which can be estimated by the expression

$$C_{L_{\alpha_f}} \approx C_{N_{\alpha_f}}\frac{S}{bc}$$

where b = span of fins, and c = average fin chord. If the fins have more than 45° sweepback, the above expression for C_{l_0}/C_{l_p} may not give a usable value.

5—3.6.4 Computation of Dynamic Stability

5—3.6.4.1 General

It is important to have a good estimate of the equilibrium spin since the likelihood of dynamic instability increases with increasing spin rate. This is often expressed by saying "the spin rate must be kept low enough to avoid magnus effects." Murphy's dynamic stability factor, s_m, was discussed in paragraph 5-2.4. This method of displaying the dynamic stability of a projectile can be extended, without change*, to statically stable projectiles; the complete curve of $1/s_p$ vs s_e is shown in Figure 5-2. For fin-stabilized projectiles,

*Except to note that for fin-stabilized projectiles the damping exponents, λ_1 and λ_2, are approximately equal.

s_p is negative since C_{M_α} is negative. For small values of spin, s_p approaches zero and $1/s_p$ becomes a large negative number. Hence, the possibility of dynamic instability is small when the spin is small.

5—3.6.4.2 Sample Calculation

Our 6-inch finner used as an example in the discussion of spin due to fin cant in preceding paragraphs might also have the following characteristics:

$$I_x = 0.15 \text{ slug-ft}^2$$
$$I_y = 3.0 \text{ slug-ft}^2$$
$$C_{M_\alpha} = -2.5 \text{ per radian}$$

Then we have

$$\frac{1}{s_p} = \frac{4 I_y \rho_1^2 V^2 S d\, C_{M_\alpha}}{I_x p^2}$$
$$= \frac{(4)\,(3.0)\,(.00119)\,(1600)^2\,(0.196)\,(0.5)\,(-2.5)}{(0.15)^2\,(132)^2}$$
$$= -22.5$$

Using Murphy's criterion

$$\frac{1}{s_p} = s_{s_0}(2 - s_{s_0}) \text{ for } \lambda_1 = \lambda_2 \leq 0$$

we find that the projectile of this example is dynamically stable if s_{s_0} lies between -3.8 and $+5.8$. It should not be difficult to design a fin-stabilized projectile with a value of s_{s_0} lying between these limits.

5—3.6.4.3 Magnus Moment Coefficients

Platen, Ref. 45, points out that blanketing of the leeward fins by the body, when a slowly rolling projectile is yawed, can create an unbalanced side force which is identified as a magnus force. This force, and the moment associated with it, can be as large as the magnus force and moment on a rapidly spinning body of revolution. If the fins are canted, the fin lift, at equilibrium spin, is in opposite directions on the inboard and outboard sections of the fin, leading to a nonlinear variation of "magnus" moment with yaw.

In any case, the magnus moment coefficients of fin-stabilized projectiles are less predictable than those of spin-stabilized projectiles. For this reason it is wise to allow as great a margin of dynamic stability as can be secured without falling into resonance instability, which is discussed in the next paragraph.

5—3.7 Resonance Instability

While spin-stabilized projectiles can theoretically experience coincidence of spin and yaw frequencies, this phenomenon is so much more likely to occur with fin-stabilized projectiles that it is discussed here.

5—3.7.1 Variation of Magnitude of Yaw with Asymmetry

Murphy (Ref. 12a), in his discussion of the angular motion of a slightly unsymmetric missile, shows that the magnitude of the yaw due to asymmetry is usually well approximated by

$$K_s = \frac{A}{\nu^2 - P\nu + M}$$

where

$$\nu = \frac{pd}{V}, \quad \text{spin in radians per caliber of travel}$$
$$P = \frac{I_x}{I_y}\frac{pd}{V}$$
$$M = \frac{\rho S d^2}{2 I_y} C_{M_\alpha}$$

and A is a constant which depends on the kind and degree of asymmetry.

If the denominator is set equal to zero and solved for ν, the result is

$$\nu = \frac{P}{2} \pm \sqrt{\frac{P^2}{4} - M}$$

but this is precisely the expression for the frequencies of the two modal vectors of yaw (Ref. 12a). So if either the nutational frequency or the precessional frequency is nearly equal to the spin frequency, the magnitude of the yaw due to asymmetry can become very large. The similarity to a spring-mass system subjected to an external alternating force has led to the use of the term "resonance instability" as a label for this mechanism for yaw increase. The increase in yaw, unlike the growth of the amplitude of an ordinary spring-mass system, is bounded not so much by the damping in

the system as by its nonlinearity; the resonant yaw of projectiles may become large enough to cause loss of range and accuracy through large drag increases, but not so large as to cause the projectile to tumble.

5—3.7.2 Resonance Roll Rate, p_r

5—3.7.2.1 Computation

The spin is most likely to coincide with the nutation frequency ϕ_1', which is given by

$$\phi_1' = \frac{P}{2} + \sqrt{\frac{P^2}{4} - M} = \frac{P}{2}\left(1 + \sqrt{1 - \frac{1}{a_0}}\right)$$

Since

$$P = \frac{I_x}{I_y} \quad \text{and}$$

$$\phi_1' = p = \frac{pd}{V}$$

for resonance, then

$$\frac{2I_x}{I_y} = 1 + \sqrt{1 - \frac{1}{a_0}}$$

$$\frac{4I_x^2}{I_y^2} - \frac{4I_x}{I_y} + 1 = 1 - \frac{1}{a_0} = 1 - \frac{4I_x}{I_y^2}\,\frac{\mu}{p_r^2}$$

This reduces to

$$I_x - I_y = \frac{\mu}{p_r^2}$$

where $\mu = qSdC_{n_\alpha}$ is the static moment factor per radian, and p_r is the resonant roll rate in radians per second. When I_x is greater than I_y, which it always is for conventional artillery projectiles, μ must be negative for resonance, and only statically stable ($C_{n_\alpha} < 0$) projectiles can exhibit resonance instability. We can estimate the resonant roll rate from

$$p_r = \sqrt{\frac{-\mu}{I_x - I_y}}$$

which is seen to be just slightly higher than the usual approximation for the yawing frequency of a fin-stabilized projectile, $\sqrt{-\mu/I_y}$ in radians per second.

5—3.7.2.2 Sample Calculation

For the 6-inch finner used as an example in paragraph 5—3.6

$$p_r = \sqrt{\frac{750}{3.0 - 0.15}} = 16.2 \text{ rad/sec} \quad \text{at } V = 1600 \text{ fps at sea level}$$

The equilibrium roll rate p_e for this finner was 133 rad/sec, so p_e is well above p_r. Since both p_e and p_r are directly proportional to airspeed, changes in V along the trajectory do not alter the p_e/p_r ratio.

5—3.7.2.3 Ratio of p_e/p_r to Avoid Resonance Instability

It will be seen from the expression for μ that decrease in air density with altitude decreases p_r; if the equilibrium roll rate is greater than p_r, firing at high quadrant elevations will decrease the chance of resonance instability. Therefore, in firing from a rifled gun, the obturator should be designed to produce a roll rate at emergence from the muzzle at least three times as great as the calculated resonant roll rate, p_r, and the fins should be designed for an equilibrium spin ($s_e = p_e d/V$ about the same as the spin at emergence. The s_e of our 6-inch finner, 0.041, is unnecessarily high in view of its s_r of 0.005; either the fin cant angle or the percentage of fin area canted could be cut in half.

Conventional projectiles fired from a smooth-bore gun emerge from the muzzle with essentially zero spin. Since normal manufacturing asymmetry can produce equilibrium roll rates close to resonance, the fins are usually canted to produce a p_e greater than p_r. The roll rate of the projectile must therefore pass through p_r on its way to p_e; if this passage is rapid enough, the temporary growth in yaw due to resonance will be negligible. The greater the p_e/p_r ratio, the shorter the time spent in the vicinity of p_r, unless the disastrous phenomenon call "roll lock-in" occurs.

5—3.8 Roll Lock-In

Nicolaides and others have made an extensive theoretical and experimental study of the behavior of slightly asymmetric projectiles spinning in the neighborhood of resonance. Some of their work is reported in Refs. 50 and 51. Reference to these reports should be made when designing projectiles which must pass through the resonant roll rate. Nonlinearities and secondary aerodynamic

moments not considered in the discussions in this handbook can offset the fin torque, causing the spin to remain at the resonant frequency long enough for the yaw due to asymmetry to grow catastrophically. Giving the projectile a spin at emergence—and at equilibrium—greater than ν_r, is the method recommended in this handbook for avoiding roll lock-in.

5—3.9 Aerodynamic Jump of Fin-Stabilized Projectiles

All of the material on the aerodynamic jump of spin-stabilized projectiles (paragraph 5—2.5) applies without change to fin-stabilized ammunition, with the exception that the drift of a fin-stabilized projectile is kept small by rolling the projectile slowly. However, it requires very good design and manufacture to keep the aerodynamic jump (and therefore the dispersion) of fin-stabilized rounds to as low a level as that of standard spin-stabilized rounds fired from the same gun. This has been observed many times in test firings of fin-stabilized tank rounds, where spin-stabilized rounds were used as control rounds.

The aerodynamic jump angle Θ_J, is reduced by increasing the c.p.-c.g. separation, as is seen in the equation in paragraph 5-2.5.3. (c.p.-c.g. $\sim C_{N_\alpha}/C_{L_\alpha}$ for small yaw). Unfortunately, if this increase is achieved by increasing the moment coefficient of the tail, as by greater fin area or a longer boom, then the effectiveness of the fins in the reversed flow existing in the blast zone is increased, with resulting increase in initial yawing velocity. If this increase in $\dot{\delta}_0$ is greater than the increase in c.p.-c.g. separation, and it may well be, then the aerodynamic jump is increased, not reduced, by the change in c.p.-c.g. separation.

The c.p. of the normal force on the body alone can be moved rearward by changing the shape of the body: this can increase the c.p.-c.g. separation of the whole projectile with little or no change in the tail moment. If this body change is made by substituting a spike for the ogive, the drag is increased.

Fin-stabilized rounds are probably more sensitive to transverse pressure gradients in the blast zone than are spin-stabilized rounds. Calculations indicate that the effect of these pressure gradients on aerodynamic jump is minimized if the resultant of the transverse pressures on the projectile passes through the normal flight c.p. of the round. However, since little is known about the distribution of muzzle blast pressure in either space or time, the best way to reduce muzzle blast effect is to reduce the magnitude and duration of the blast pressures on the projectile by good obturation.

It will be noticed that aerodynamic jump has been discussed only for dynamically stable projectiles where initial yawing velocity and c.p.-c.g. separation are the quantities of interest. Fin-stabilized projectiles which are statically stable are also dynamically stable unless they have an unusually high roll rate.

5—3.10 Fin Effectiveness at Supersonic Speeds (Ref. 12b)

With low aspect ratio* fins of the order of 1.0 or less, the span is the predominant factor for producing high normal force coefficients. However, when spans are limited to no greater than one full body diameter, the optimum chord length must be determined. For a fixed span there is a definite limit to the chord length that will give the best combination of normal force and most rearward C.P. The normal force based on body frontal area decreases with increasing Mach number for a constant span and constant chord, and it decreases more rapidly as the chord is shortened. This means that as aspect ratio increases, the effect of Mach number is greater on the fin normal forces. The most efficient chord length appears to be between calibers .70 and 1.0, dependent on Mach number. The larger chord should be used for the higher Mach numbers.

The effect of leading-edge sweepback is negligible so far as normal force is concerned if constant area and aspect ratio is held. From the wing theory the lift within the tip Mach cones is approximately ½ of the two-dimensional value.** This is caused by a pressure leakage around the tips from

*Aspect ratio is defined herein as the exposed span squared, divided by the exposed fin area. The exposed fin area is the total plan view area (of a pair of fins) less the area occupied by the boom. The exposed span is the total span less the (average) boom diameter.

**Two-dimensional flow theory states that, for supersonic flow, the normal force coefficient, based on exposed fin area, is given approximately by $C_N = 4/\sqrt{M^2-1}$.

the lower to the upper surfaces. If more of the fin surface is affected by the tip Mach cones, the lower the total normal force will be and the further forward the C.P. will move. If by some method we could prevent this pressure leakage around the tips, we would be able to two-dimensionalize a three-dimensional surface. End plating the fins was attempted. By this method it was found that the fin normal force could be increased as much as 40% depending upon the amount of fin area affected by the end plates and the amount of end plate width. The end plated fin as against the plain tail on the T108 firings had restoring moments 31% greater and much better accuracy. The damping coefficients were also larger for the end-plated tails as against the plain tail, and this caused the more stable round to damp to ½ amplitude in fewer cycles.

A complete end plate width would be classified as a shrouded or ring tail. Experimental evidence at low Mach numbers showed that the shroud had a strong tendency to choke or block the air flow over the fin surfaces, thereby causing poor flow over these surfaces. This in turn caused poor lifting results. However, since the flight velocities have been raised to high Mach numbers, the tendency for the flow to choke between the fins and shroud is eliminated, and fin normal forces are increased and C.P.'s moved rearward.

The number of fins necessary for optimum normal force appears to be six. Theoretically six fins, acting independently of each other, should give 1½ times the force of four fins, however, experimentally they usually produce only 20% to 30% more, dependent upon Mach number. If more than six fins are employed, the fins interfere with one another so far as the flow fields are concerned, and the normal force suffers.

In order to obtain maximum tail effectiveness, one would want the tail to be in a uniform flow region, i.e., outside of any body wake influences. This, however, is only possible when using folding fins whose sweep angles are relatively small. For fixed fin configurations (except in the case of arrow projectiles) the fins are operating mainly in the boundary layer flow from the body. Means of giving the fin the most effective lifting surface are to make the supporting body as small as practical, i.e., keep the span to support body diameter as large as possible so that a greater portion of the fin is outside of the body boundary layer, and boattail the main body so that smooth uniform flow is presented to the surface.

(61) 62 Blank

CHAPTER 6

ROCKET-ASSISTED PROJECTILES

6—1. GENERAL

The kinetic energy which a gun can impart to a projectile is limited by the diameter of the bore, the length of travel of the projectile in the tube, and by the curve of chamber pressure vs travel. The muzzle energy can be increased by using a bigger, longer or thicker gun tube, thus increasing the cost of the weapon and, more important, decreasing its mobility. But range is limited by the kinetic energy supplied to the projectile since each foot of trajectory subtracts from the kinetic energy an amount equal in magnitude to the drag force.

To increase range, or to increase the payload carried to the same range, or to increase the velocity at target impact, without decreasing the mobility of the gun, the first step is to reduce the drag coefficient of the projectile to as low a value as is compatible with the projectile volume required by the projectile's mission. The next step is to add kinetic energy to the projectile in flight.

By increasing the length of the projectile, or by sacrificing some of the warhead volume, a rocket motor can be included in the projectile. The rocket thrust adds kinetic energy to the projectile in flight. The resulting projectile is called a "rocket-assisted projectile," or, equivalently, a "gun-boosted rocket." The burning of the rocket fuel can be controlled, or "programmed," to be less than the drag force, approximately equal to drag, or very much greater for a short period.

The addition of a rocket motor increases the cost of the projectile and increases the storage space required for a given destructive capability. An added limitation on muzzle energy is introduced by the maximum set-back acceleration which the propellant can tolerate without crushing, but this limiting acceleration is surprisingly high.

6—2. MOMENTUM LIMITED SITUATION

6—2.1 Variation of Muzzle Energy, Chamber Pressure and Propellant with Weight of Projectile

Because of the set-back acceleration limit, rocket-assisted projectiles are usually made heavier than the conventional ammunition fired from the same gun. The muzzle velocity is then limited by the capacity of the recoil system, and decreases in proportion to the increase in projectile weight. If we use the subscript "*std*" to identify the symbols relating to a projectile which is launched at the muzzle momentum limit, then

$$mV = m_{std} V_{std} \qquad \text{(constant momentum)}$$

squaring, rearranging, and dividing both sides by two gives

$$\tfrac{1}{2} mV^2 = \left(\frac{m_{std}}{m}\right) \tfrac{1}{2} m_{std} V^2_{std} \quad \text{(muzzle energy decreases).}$$

Equating muzzle energy to the integral of the work done on the projectile by gas pressure in the gun gives

$$A \int_0^L P_c \, dl = \left(\frac{m_{std}}{m}\right) A \int_0^L P_{c_{std}} \, dl$$

where

P_c = chamber pressure
A = bore area
L = bore travel

Assuming the pressure-travel curves have the same shape, $P_o = kP_{c_{std}}$ and $P_c = (m_{std}/m)P_{c_{std}}$ then muzzle energy and chamber pressure, and consequently the weight of gun propellant, are inversely proportional to the weight of the projectile, in a momentum limited situation.

6—2.2 Variation of Setback Acceleration

The setback acceleration, a, is given by

$$a = \frac{P_c A}{m} = \frac{m_{std}}{m^2} P_{c_{std}} A = \left(\frac{m_{std}}{m}\right)^2 \frac{P_{c_{std}} A}{m_{std}}$$

so the setback acceleration is inversely proportional to the square of the mass ratio.

6—2.3 Effect of Rocket Additions on Projectile Design Parameters

The reduction in weight, and volume, of gun propellant allows some of the extra length occupied by the rocket motor to be inserted in the space previously occupied by gun propellant. Whether, and how, this is done depends on the characteristics of the gun tube and loading system involved.

Large increases in range require, if warhead volume is not to be severely reduced, an increase in projectile length. Experience has shown that spin-stabilized projectiles longer than 6 calibers usually require a high spin rate for gyroscopic stability; in the absence of rocket thrust these projectiles slow down so much on a high angle trajectory that their equilibrium yaw becomes dangerously large. However, when the projectile velocity is maintained by a rocket which burns nearly to the summit of the trajectory, spin-stabilization may be used for projectiles as long as 8 calibers, or possibly longer*. At 10 calibers, fin-stabilization is almost certainly required.

6—2.4 Effect of Rocket Additions on Accuracy

Long-burning rockets, sometimes called "sustainer" rockets, with thrust approximately equal to drag, can have a proving ground accuracy (no wind) very little worse than a conventional round fired from the same gun. Thrust malalignment, which contributes heavily to the dispersion of fast-burning rockets, is a minor factor in the low-thrust rocket. Variation in rocket fuel specific impulse contributes to rocket dispersion and accounts for the slightly inferior accuracy of long-burning rockets compared with conventional projectiles when both are fired in the absence of wind. However, a long-burning rocket is less affected by wind than a conventional projectile, so that combat accuracy of the rocket-assisted round might well be better than the conventional.

Accuracy analyses of rocket-assisted projectiles, both spin- and fin-stabilized, are presented in Bullock and Harrington, *Summary Report on Study of the Gun-Boosted Rocket System*, Ref. 69. These analyses, with supporting experimental data, are very useful for design; an extensive bibliography is also included. Initial yawing velocity, dynamic unbalance, and wind are identified as the major sources of dispersion of spin-stabilized rockets; thrust malalignment can be significant in cases of high thrust and slow spin. Dynamic unbalance is not significant for finners, but fin asymmetry and thrust malalignment can be if the roll rate is too low; wind is also a major source of dispersion here. The reasons for the small wind-sensitivity of sustainer rockets are also discussed.

* Special tailoring of the c.g. location may be required in order to reduce dynamic instability at the muzzle and near impact.

CHAPTER 7

LIQUID-FILLED PROJECTILES

7—1. GENERAL

Projectiles having an inner cavity which is partially or completely filled with liquid are a special case of the class of projectiles having a nonrigid internal structure. The yawing motion of a projectile has usually such a low energy content that small transfers of energy between the internal parts and the wall of the projectile can increase the yaw significantly. When the mass of the nonrigid part is large relative to the mass of the projectile, as it is in the case of some liquid-filled projectiles, the yaw may increase very rapidly.

The instability of liquid-filled projectiles has been studied, theoretically and experimentally, by Karpov, Scott, Milne, Stewartson and others. Some of this work is reported in Refs. 71 to 73. The investigation is not complete; the statements made in the following paragraphs represent current (1964) concepts and opinions.

7—2. EFFECT OF SLOSHING OF LIQUID FILLER

Differences in the thermal coefficients of expansion of projectile body and liquid make it impractical to completely fill a projectile cavity with liquid. Mechanical devices for allowing the cavity volume to change with the change in liquid volume are possible, but not much used. Fills of 95% are common; some projectiles may be filled to 98%.

It has been found that the sloshing about of the fill in a fin-stabilized projectile does not increase the yaw. So a simple solution of the problem of liquid fill is to use fin-stabilization. This is not always feasible; limitations on projectile length may reduce the volume of a finner below acceptable limits, or spin-stabilization may be desirable for terminal effects.

7—3 COMPUTATION OF DESIGN PARAMETERS

The discussion which follows applies only to spin-stabilized projectiles.

7—3.1 Gyroscopic Stability Factor

The gyroscopic stability factor of a liquid-filled projectile is given (approximately) by

$$s_g = \frac{I_{x_R}^2 p^2}{4\,(I_{y_R} + c\,I_{y_L})\,\mu}$$

where

I_{x_R} = axial moment of inertia of rigid parts, slug-ft²

I_{y_R} = transverse moment of inertia of rigid parts, slug-ft²

c = a constant related to the viscosity of the liquid; for water, $c = 0.3$

I_{y_L} = transverse moment of inertia of liquid parts, slug-ft²

μ = static moment factor, lb-ft/radian

The rigid parts include both metal parts and high explosive; the transverse moments of inertia are computed about the total c.g. of the projectile, with the liquid fill distributed as a hollow con-

centric cylinder occupying the full length of the cavity.

7—3.2 Dynamic Stability Factor

The dynamic stability factor—computed in the usual way from aerodynamic coefficients, except that k_1^2 is given by $I_{x_B}/(m_B d^2)$ and k_2^2 by $(I_{x_B} + cI_{x_L})/[(m_B + cm_L)\, d^2]$ — must be such that the projectile would be dynamically stable over its trajectory if there were no interaction between the liquid fill and the projectile wall.

7—3.3 Spin Rate

In the transient period, during which the liquid fill is acquiring a spin rate equal to that of the projectile wall, the transfer of angular momentum from wall to liquid will reduce the spin rate of the wall. The reduction in spin rate may be very rapid if the liquid fill has a high viscosity, or if baffles tied to the projectile wall are placed in the liquid. On the theory of paragraph 7-3.1, above, that the angular momentum of the liquid does not contribute to s_p, the projectile may become unstable. However, the transient period is then so short that baffles (or high viscosity) may actually improve the flight. Baffles can be designed simply on the basis of the torque exerted on the liquid in giving it angular velocity and on the shear, due to setback, at the roots of the baffles.

7—4. RIGID BODY THEORY

When all of the liquid is rotating with the same angular velocity as the projectile wall, the projectile is said to be rotating as a "rigid body." If the liquid were not all of the same density, the heaviest fraction would be closest to the projectile wall as a result of the centrifugal field, which resembles a gravitational field. The air space, then, is as far away from the projectile wall as possible, surrounding the axis of the projectile or any solid core, such as a burster tube, which may be positioned along the projectile axis.

Stewartson's theory is concerned with the instability of liquid-filled projectiles rotating as a "rigid body." It was derived for cylindrical cavities completely or partially filled with liquid of uniform density and low viscosity; the behavior of test groups of rounds of varying geometry and percentage of cavity filled has been successfully predicted by the use of this theory. The projectile cavity need not be precisely cylindrical near its ends. The necessary formulas and tables for applying Stewartson's criterion of instability are contained in Karpov, *Dynamics of Liquid-Filled Shell*, BRL Memorandum Report 1477 (Ref. 72).

CHAPTER 8

RANGE TESTING OF PROTOTYPE PROJECTILES

8—1. GENERAL

Very few projectiles are completely satisfactory as first designed. Metal parts failure is rare, but the first test firings usually show that either range or accuracy is not as good as was desired or expected. In instances where the first group of ten or fifteen test rounds fired gave excellent results, a second group has often failed to confirm the good results of the first. Conclusions are drawn from the behavior of the test rounds; design changes are made on the basis of these conclusions; and new prototype rounds are made and fired. This test and change sequence may go on through many cycles before an acceptable design is reached.

The difficulty that a designer may encounter in translating a round from the drawing board into a useful weapon is described in the following excerpt from the report of E. R. Dickinson, *The Effects of Annular Rings and Grooves, and of Body Undercuts on the Aerodynamic Properties of a Cone-Cylinder Projectile of $M = 1.72$* (Ref. 80):

Often, in a projectile's progress from the designer's drafting board to the assembly line, there are many changes made in the details of the projectile's contour. As a result, the actual aerodynamic performance of the projectile may differ from that of the designer's prediction.

Almost all of the basic design data on projectiles concerns itself with smooth contours and simple geometric shapes. When practical considerations enter the picture and fuzes have to be attached, reliefs have to be machined, rotating bands have to be added, a projectile which may have been, originally, an optimum one, often falls short of expectations.

The engineer, who translates the ballistician's design data into a practical piece of ammunition, should be cognizant of the differential corrections that have to be made to the predicted behavior of the projectile. The purpose of this report (Ref. 80) is to show the effect, on drag, lift, and pitching moment, of depressions and protrusions on the surface of a body of revolution. Unfortunately, there were insufficient data to determine effects on the damping and magnus moments and forces.

Obviously important to the designer is the soundness of the conclusions on which the design changes are based. This soundness is directly related to the care taken in preparing for, firing, and analyzing the firing test.

8—2. PRE-FIRE DATA

It is important that the designer know exactly what was fired and how it was fired. He must know what equipment was used for measuring the test parameters, such as velocity, time-of-flight, and target impact, in order to assess the accuracy of the numbers presented to him. Each round fired must be precisely identified so that its performance can be tied to its physical characteristics as determined before firing.

For each round, the following physical characteristics must be determined and recorded before firing:

a. Individual weights and dimensions of all of the significant components of the round.
b. Weight and center of gravity location of the projectile, including its simulated lethal charge.
c. Amount of eccentricity of specific components relative to a chosen reference axis,

67

when assembled into the complete projectile.

d. Axial and transverse moments of inertia. (Moment of inertia data may be omitted if the projectile is fin-stabilized and it is known from a previous test that dynamic stability is not a problem.)
e. Surface irregularities which could cause disruption of proper boundary layer flow.
f. Round number or other identification, which should be permanently marked on the projectile.

Some experiences in the manufacture of prototype projectiles indicates that there should be no difficulty in meeting the following tolerances:

a. Projectile weight: ±0.6% design value
b. Center of gravity location: ± 0.05 inch
c. Eccentricity: ±0.008 inch
d. Moments of inertia: ±2.0% of design value

Practical methods of measurement of projectile characteristics are described in E. R. Dickinson, *Physical Measurements of Projectiles* (Ref. 74).

8—3. TESTING

The primary function of the projectile test facility is to acquire reliable and unbiased test results. Engineering changes must not be based on conclusions that are statistically unsound; accordingly, the test must be planned to provide sufficient data for a statistical analysis (Ref. 76). It is the responsibility of the testing officer to insure completion of the test, as planned, or to record any condition which will make completion impractical. The two types of tests, static testing and flight testing, are described below.

8—3.1 Static Testing

Static testing is an intermediate design tool, which is particularly useful in determination of the following:

a. Shaped charge penetration
   (1) stand-off distance
   (2) liner design: thickness, cone angle, etc.
   (3) high explosive charge: type, volume, density, shape, etc.
   (4) effect of spin
b. Fragmentation studies
c. Smoke tests: chemical type, shape, volume, density, etc.
d. Rocket motor performance
e. Propellant and high explosive ignition systems

Many of these static tests involve design factors which contribute to the mass and mass distribution, and directly or indirectly affect flight characteristics.

8—3.2 Flight Testing

The mission of the projectile determines the type of flight test conducted. The two most common tests are to determine vertical target accuracy and range (distance), each of which is discussed below.

8—3.2.1 Vertical Target Accuracy

8—3.2.1.1 Measurement of Accuracy

For vertical targets, the accuracy is expressed in terms of two probable errors, $P.E._H$ and $P.E._V$. These indicate the distribution, both horizontally and vertically, about a center of impact.

8—3.2.1.2 Temperature Range

Test requests generally specify temperature conditioning of the test projectiles, for a 24-hour period prior to firing. The three temperature ranges usually employed are:

a. Hot: 125°F
b. Standard: 70°F
c. Cold: —40°F

8—3.2.1.3 Data Recorded

In vertical target accuracy tests the projectiles are fired on a flat trajectory and the following data are recorded:

a. Projectile identification; round identification
b. Gun identification and condition
c. Changes in gun elevation or azimuth (if any) between rounds
d. Target distance from gun
e. Muzzle velocity

f. Coordinates of points of impact
g. Ground level meteorological conditions
h. Terminal velocity
i. Time of flight
j. Chamber pressure
k. Early yaw

} Not always observed

8—3.2.2 Range (Distance) Accuracy

8—3.2.2.1 Measurement of Accuracy

When testing projectiles for distance, the accuracy is measured in these two ways:

a. Probable error of range; indicating the distribution forward and aft of a calculated mean range.
b. Probable error of deflection: indicating distribution to the right and left of the center of impact. Deflection P.E. is generally expressed in mils, based on the mean range.

8—3.2.2.2 Data Recorded

These projectiles are generally tested through a range of quadrant elevations and the following data are recorded:

a. Gun and projectile identifications as in flat fire
b. Quadrant elevation and azimuth of gun
c. Muzzle velocity
d. Coordinates of points of impact or burst
e. Meteorological data at ground level and aloft
f. Time of flight
g. Chamber pressure
h. Early yaw

} Not always observed

8—3.2.2.3 Instrumentation

Subsequent field tests may be conducted under localized weather conditions, such as at the Arctic Test Branch, Big Delta, Alaska. Instrumentation available for recording flight data are:

a. Photography: Pictures taken at muzzle show growth of smoke cloud which is related to adequacy of obturation. Sequence photos record discarding sabots or record spin activity.
b. Yaw Cards: The projectile is fired through a series of strategically located soft-cardboard panels to record the attitude of the projectile relative to its line of flight.
c. Radiosondes: A small radio transmitter built into the projectile is actuated upon firing. An on-ground receiver, being sensitive to the roll orientation of the transmitter antenna, is able to record the spin history of the projectile.
d. Radar: Radar tracking can provide position and velocity data throughout the flight.

(69) 70 Blank

CHAPTER 9

MANUFACTURING TOLERANCES

9—1. DIMENSIONAL CHANGES

Cost factors necessitate that tolerances on parts being produced in large quantity be less stringent than prototype manufacturing tolerances. Dimensional changes, to facilitate production, may be made only when the flight results will not be significantly impaired by the change; this implies that standards for high production runs can be established only after statistical analysis of prototype firing test data. A brief example of the type of analysis considered is presented below. Reference should be made to the Engineering Design Handbooks, *Experimental Statistics*, AMCP 706-110 through AMCP 706-114, for a thorough treatment of this important phase of data analysis.

9—1.1 Problem

Fin misalignment relative to the longitudinal axis of the projectile is recorded during preflight inspection. The assemblies accepted at this time must meet the requirements of prototype manufacturing. After test firing the accepted projectiles, the impact dispersion at target is recorded.

9—1.2 Analysis

A simple regression analysis of fin misalignment versus distance of hit from center of impact will produce numbers indicating the effect of misalignment. If the analysis indicates insignificant correlation, the tolerances on the fin dimensions which control alignment may be relaxed.

9—2. PREDICTED PROBABLE RANGE ERROR

Table 9-1 presents estimates of the probable variability of those projectile characteristics which most significantly affect range. These estimates were gathered from ballisticians at Picatinny Arsenal, Aberdeen Proving Ground, and the Naval Ordnance Test Station. The last column in the table presents sensitivity factors for a particular rocket-assisted projectile when fired for maximum range. These sensitivity factors, which represent the percent change in range caused by a one percent change in the associated round variable, were obtained by trajectory computations as described in paragraph 4-2.

The predicted probable error in range, in percent, due to each variable is therefore the product of the probable error of the variable and its associated sensitivity factor. Under the usual assumption that the errors are independent of each other, the resulting range probable error of the projectile, in percent, is the square root of the sum of the squares of the individual products. Vector sums of this type can be significantly reduced only by reducing their large components. Obviously, a significant improvement in the range dispersion of rocket-assisted projectiles could be obtained by reducing the round-to-round variation in specific impulse. In the absence of rocket thrust, variations in drag coefficient become most significant; dispersion might be improved by closer control of the external contour of the projectile.

The foregoing paragraphs apply to high angle indirect fire. As the quadrant elevation is decreased, the relative importance of the various factors changes so that in direct fire the most important items are quadrant elevation and aerodynamic jump.

TABLE 9—1
PROBABLE VARIABILITY OF ROCKET-ASSISTED PROJECTILE CHARACTERISTICS AND SENSITIVITY FACTORS WHICH AFFECT RANGE

Round Variable	*Probable Error as % of Mean of Variable*	*Sensitivity Factor at max. range*
Projectile Weight	.25	.42
Muzzle Velocity	.25	.51
Fuel Weight	.50	.76
Fuel Specific Impulse	1.00	.87
Fuel Burning Rate	.20	.08
Drag Coefficient	.50	.77
Ballistic Density of air	.20	.77
Quadrant Elevation	.35	.81

9—3. DYNAMIC STABILITY OF 175-MM PROJECTILE, M437

The trajectory calculations in Table 9-2 show that the M437 projectile fired at 45° quadrant elevation and 2000 fps muzzle velocity, will fly at a Mach number close to 1.15 over the entire descending limb of its trajectory. Referring to the aerodynamic data in Table 9-3, we see that in this Mach number vicinity the expected value of s_4 is close to 1.0, so that a round having values of the magnus moment and damping moment coefficients near to the average values measured for the rounds tested in the free flight range will be dynamically stable over its whole trajectory.

However, the experimental data from the range firings showed considerable *scatter*, probably because of the small size of the yaw level. As a consequence of this scatter, BRL investigated the sensitivity of the stability of the projectile to variations in the magnus moment and damping moment coefficients. These variations could arise from lot-to-lot variations in projectile shape or center of gravity location.

The results of recent (1964) six-degree-of-freedom computer runs at BRL show that the M437 projectile behaved properly with variations of over four standard deviations from the curve fitted to the experimental values, but variations of five standard deviations produced instabilities. These computations, Table 9-4, indicate that other than minor lot-to-lot variations in shape or c.g. location can lead to trouble even when the basic design of a projectile is quite stable.

TABLE 9—2

SAMPLE TRAJECTORY FOR 175-MM SPIN-STABILIZED PROJECTILE, M437, AT Q.E. = 45°

FFD	FFM	TYPE	RGA	RGT	D,FT	
1.000	1.000	.175	.369	1.297	.5730	
WTO	VO	SPIS	SBT	DTM	TWIST	QE
147.50	3000.	.	.0	.300	20.00	45.000
WTB	Z`	TEMP	DTL	DTE	CDD2	CLP
147.50	.	59.	2.0	.350	5.80	-.015

.001189 1116.0

TIME THETA	X Z	DIST THRUST	V DRAG	CD YAW	CMA DR MACH SPIN	MASS SG
.00	.	.	3000.0	.203	3.62	1.000	4.58
.78	.	.	562.1	.000	2.68	.314	1.95
.06							
3.46	6895.	9621.	2577.8	.222	3.73	.806	4.58
.75	6709.	.	366.5	.001	2.35	.342	2.80
.07							
7.92	14749.	20213.	2198.8	.240	3.87	.642	4.58
.71	13815.	.	229.5	.002	2.07	.379	4.17
.10							
13.64	23745.	31770.	1858.3	.260	4.04	.509	4.58
.64	21066.	.	140.3	.003	1.80	.428	6.38
.12							
21.01	34145.	44262.	1552.6	.279	4.30	.408	4.58
.52	27972.	.	84.4	.007	1.54	.491	9.86
.16							
30.84	46693.	58090.	1282.1	.307	4.61	.322	4.58
.31	33713.	.	50.1	.015	1.30	.572	15.85
.23							
43.01	60831.	72479.	1108.3	.332	4.99	.289	4.58
-.00	36054.	.	36.2	.023	1.14	.641	20.48
.30							
58.01	76566.	88752.	1092.1	.335	5.08	.342	4.58
-.43	32435.	.	42.0	.019	1.10	.627	16.30
.30							
73.01	90373.	105834.	1193.4	.326	4.93	.486	4.58
-.78	22521.	.	69.4	.010	1.16	.545	8.93
.30							
88.01	101738.	124410.	1265.5	.325	4.92	.777	4.58
-1.02	7882.		124.2	.005	1.16	.473	4.21
.30							

TIME,S	RANGE,M	V,FPS	THETA,D	SPIN	SG
95.16	32333.	1247.	-63.6	.452	2.95

TABLE 9—3

AERODYNAMIC DATA SHEET FOR 175-MM PROJECTILE, M437

REPORT	BRL Unpublished Data
DATE	1963
TYPE OF TEST	Free Flight

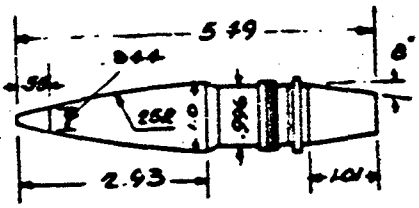

Dimensions, calibers

Muzzle Weight, lb	147.5
Muzzle Velocity, fps	3000
Muzzle Spin rate, rps	260
d, ft	0.573
ν, rad/cal	0.314

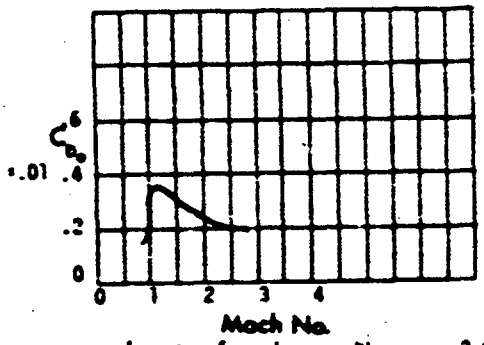

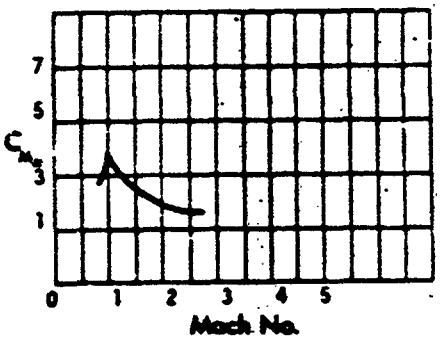

c.g. location from base, calibers 2.0

I_x, slug-ft^2 0.206 I_y, slug-ft^2 2.54

k_x, cal 0.369 k_y, cal 1.297

	M = 0.85	M = 1.0	M = 1.8	M = 2.6	Comments
$C_{M_{p_0}}$	-0.75 ± 0.25	-2 ± 1	-0.7 ± 0.2	-0.6 ± 0.5	
C_{N_0}	5.8 at all Mach numbers				From BRL MR 956 (Ref. 47b)
C_{L_0}	0.75 ± .25	1.25 ± .75	2.4 ± .2	3.0 ± .2	
C_{M_0}	See curve above				
$C_{M_q}+C_{M_{\dot\alpha}}$	-11 ± 10	-5 ± 10	-9 ± 2	-10 ± 4	
$C_{M_{p_\alpha}}$	-0.25 ± .1	0.1 ± .4	0.33 ± .25	0.22 ± .25	
C_{L_p}					
c.p. location	6 ± 2	6.5 ± 2	3.5 ± 0.1	3.1 ± 0.1	calibers from base
s_g	1.42 ± .06	1.30 ± .06	1.75 ± .09	1.98 ± .11	
s_{d_0}	-0.3 ± 0.3	1.0 ± 1.5	1.20 ± 0.5	1.06 ± 0.46	
$y = \frac{C_{M_\alpha}}{C_{M_q}}(2-y_{c.p.})$	-1.56 < y < 0	-1.25 < y < 1.0	0.32 < y < 1.0	0.75 < y < 1.0	
$\frac{1}{s_g}$	UNSTABLE	0.73 ± .03 METASTABLE	0.57 ± .03 STABLE*	0.50 ± .03 STABLE	*In this test

TABLE 9—4
DYNAMIC STABILITY ESTIMATE OF 175-MM PROJECTILE M437

Projectile Type:	175-mm M437	
Mach number:	1.14	
Air density:	$\rho = 0.000688$ slug/ft³ at 26,050 ft above sea level	
Average values of aerodynamic coefficients:	$C_{M_\alpha} = 5.0$	From Unpublished BRL data 1963
	$C_{L_\alpha} = 1.5$	
	$C_{D_0} = 0.33$	
	$C_{M_{D_\alpha}} = 0.25$	
	$C_{M_q} + C_{M_{\dot\alpha}} = -8.8$	

Spin, $p = 0.64$ rad/cal

Diameter, $d = 0.573$ ft

Axial radius of gyration, $k_x = 0.300$ cal

Transverse radius of gyration, $k_y = 1.297$ cal

Projectile mass, $m = 4.58$ slugs

Gyroscopic stability factor, s_g:

$$s_g = \frac{2mk_x^2p^2}{\pi k_y^2 \rho d^3 C_{M_\alpha}} = \frac{2\,(4.58)\,(0.300)^2\,(0.64)^2}{\pi\,(1.297)^2\,(6.88)\,(10^{-4})\,(0.573)^3\,(5.0)} = 29.5$$

Dynamic stability factor, s_d

$$s_d = \frac{2(C_{L_\alpha} + k_x^2 C_{M_{D_\alpha}})}{C_{L_\alpha} - C_{D_0} - k_y^2(C_{M_q} + C_{M_{\dot\alpha}})} = \frac{2(1.5 + 7.38\,(0.25))}{1.5 - 0.33 + 0.6\,(8.8)} = 1.06$$

$s_d\,(2 + s_d) = 1.0$ $\qquad$ $\frac{1}{s_g} = 0.040$

$\therefore$ Dynamically Stable since $\frac{1}{s_g} < s_d\,(2 - s_d)$.

(75) 76 BLANK

GLOSSARY

accuracy. The quality of correctness or freedom from error. Cf. precision.

accuracy of fire. The correctness of fire as judged by the distance of the center of impact from the center of the target.

acoustic velocity. The velocity of sound waves, or similar waves, in a given medium. For variation with altitude, in air, see: Standard Atmosphere.

aerodynamic jump. The average deflection of the trajectory which arises from the alternating lift forces on a yawing projectile. Drift, which arises from a non-zero equilibrium angle, is not included in aerodynamic jump.

airspeed. The speed of a projectile relative to the air in which it is immersed.

AMC *(abbr).* Army Materiel Command.

angle of jump. The angle between the line of elevation and the line of departure.

angle of yaw. The angle between the direction of motion of a projectile and the direction of its axis. In computing aerodynamic forces in the presence of a lateral wind the yaw angle is based on the direction of the relative wind, rather than the direction of motion of the c.g.

atmospheric conditions. *See:* meteorological data.

axial drag. The component of the aerodynamic force on a body in the direction of the longitudinal axis of symmetry.

axis. Unless otherwise specified, the longitudinal axis of symmetry.

ballistic coefficient. A numerical measure of the ability of a projectile to overcome air resistance. It is dependent upon the mass, diameter and form factor, and was widely used in trajectory calculations before the advent of the electronic digital computer.

ballistic range. A suitably instrumented area or enclosure in which projectile trajectories can be closely observed, as by spark photography; analysis of the observations can yield good estimates of the aerodynamic coefficients of the projectile.

blast zone. The zone of turbulent air and propellant gases through which a projectile must fly as it leaves the muzzle of the gun. The blast zone ends where, and when, the projectile enters undisturbed air.

boattail. The base of a projectile when shaped like the frustum of a cone (or like a reversed ogive). Cf: square base.

boom. The central stalk or sleeve to which the fins of a fin-stabilized projectile are attached.

bore. The interior of a gun barrel or tube.

boundary layer. A thin layer of air (or other fluid) next to a body, distinguishable from the main flow by characteristics of its own, set up by friction. The layer within which the major effects of viscosity are concentrated.

bourrelet. The cylindrical surface of a projectile on which the projectile bears while in the bore of the weapon. Conventionally the bourrelet is located just aft of the ogive and has a slightly larger diameter than the main body. In some cases the bourrelet extends the full length of the cylindrical body. In some designs a middle bourrelet is provided just forward of the rotating band. In some other designs a rear bourrelet is provided behind the rotating band, and in fin-stabilized designs a shroud or end plates on the fins provide a rear bourrelet.

bourrelet diameter. The maximum diameter of the projectile. The frontal area used in the computation of aerodynamic coefficients is based on this diameter.

GLOSSARY (cont'd)

bow wave. A shock wave caused by the compression of air ahead of a projectile in flight. When this wave touches the tip of the nose of the projectile, it is called an "attached bow wave" or "attached shock."

BRL *(abbr).* U.S. Army Ballistic Research Laboratories.

burning rate. For solid propellant fuels, the rate of motion of the burning surface (normal to itself).

burnout. The termination of combustion in a rocket motor owing to exhaustion of the propellant supply.

caliber. The diameter of a projectile or the diameter of the bore of a gun. In rifled arms, the caliber is measured from the surface of one land to the surface of the land directly opposite. Often the caliber designation is based on a nominal diameter and represents a close approximation rather than an exact measurement.

Caliber may be used as a unit of length; for example, a 6-inch 50-caliber gun (6"/50) would have a bore diameter of 6 inches and a tube length of 50 calibers or 25 feet, measured from the breech face to the muzzle.

calotte. *See:* **midplat.**

center of impact. Center of the dispersion pattern. Calculated as though it were the center of gravity of a system of discrete unit masses placed at the points of impact of the individual rounds of the group.

center of pressure. The point on the axis of a projectile (or on the chord of a fin) through which the resultant of a given set of aerodynamic forces passes.

chamber pressure. The pressure existent within the gun chamber at any time as a result of the burning of the propellant charge. This pressure normally varies from atmospheric pressure to a peak pressure which is attained when the projectile has traveled a short distance, then decreases steadily until the projectile emerges from the muzzle. In this handbook P_c is identified with the pressure existing at the base of the projectile, although the two pressures are not exactly equal, the base pressure being perhaps 5% smaller than P_c after the projectile has acquired a large fraction of its final velocity.

complete round. All of the components of ammunition necessary to fire a given gun once.

control rounds. *See:* **reference rounds.**

damping exponent. A numerical measure of the rate of change of the amplitude of an oscillating motion.

deflection probable error. The directional error, caused by dispersion, which will be exceeded as often as not, in a large number of rounds fired at a single gun setting. It is approximately one-eighth the greatest width of the dispersion pattern (for large samples).

density of air. The mass of a unit volume of air. It varies with altitude, generally decreasing as the altitude increases, since it varies with the current temperature and barometric pressure. When h is altitude in feet ($h < 30{,}000$) above sea level, $\ln(\rho_o/\rho) \approx 3.2 \times 10^{-5}\,h$, ρ_o the standard density of dry air at 59°F and 14.7 psi, is 0.002378 slug/ft³ (NACA 1942).

derivative. The rate change of one variable with respect to another. In projectile aerodynamics, the rate of change of an aerodynamic coefficient with respect to a change in the magnitude of the yaw angle, e.g., the slope of the C_M vs α curve gives the static moment derivative, C_{M_α}.

differential coefficient. *See:* **sensitivity factor.**

differential effects. The effects upon the elements of the trajectory due to variations from standard conditions.

dispersion. The scattering of shots fired on a target by the same gun (or group of guns).

dispersion error. Chance variation in a series of shots even though firing conditions are kept as constant as possible. For practical purposes the dispersion error of a particular shot is considered the distance from the point of impact or burst of that shot to the center of impact or burst.

dispersion pattern. The distribution of the points of impact of a series of shots obtained under conditions as nearly identical as possible.

distribution. Pattern of projectiles about a point. The set of values taken on by a random variable in successive trials.

GLOSSARY (cont'd)

diverging yaw. In the flight of a projectile, if the angle of yaw increases from the initial yaw, the yaw is said to be diverging.

drag. Component of air resistance in the direction opposite to that of the motion of the center of gravity of a projectile.

drag coefficient. A number relating drag force to the dynamic pressure of the air stream and to the frontal area of the projectile.

drift. The lateral deviation of the trajectory of a spin-stabilized projectile, due to the equilibrium yaw.

dynamic pressure. The pressure exerted by a fluid solely by virtue of its relative motion when it strikes an object. Proportional to density and the square of relative velocity [$q = (1/2)\rho V^2$], it is obviously related to the kinetic energy possessed by, or imparted to, the fluid. Sometimes called "velocity head."

end plate. A narrow rectangular plate integral with the tip of a fin, forming a *T* when viewed in the chordwise direction. The other surface of the plate is curved to conform to the radius of the gun bore, as the end plate supplies a riding surface for the fin in the barrel, as well as increasing the lift of the fin by preventing the flow of air around the fin tip from the lower to the upper surface.

equilibrium yaw. The yaw angle to which the yaw of a dynamically stable projectile decays. Part of this angle is due to asymmetry of the projectile, part to the effect of gravity.

error. *1.* The difference between an observed or calculated value and the true value. *2.* In gunnery, the divergence of a point of impact from the center of impact.

fineness ratio. Ratio of length to diameter (l/d) of a projectile.

fin-stabilized. Of a projectile, made statically stable by the aerodynamic moment arising from the presence of lifting surfaces aft of the c.g.

firing table. Table or chart giving the data needed for firing a gun accurately on a target under standard conditions and also the corrections that must be made for special conditions, such as winds or variations of temperature.

flat base. Descriptive of a projectile with a cylindrical base section, as opposed to a **boattail**, which see. Sometime called "square base."

form factor. Factor introduced into the denominator of the ballistic coefficient (q.v.), based on the shape of the projectile.

free stream. The flow of air or other fluid undisturbed by the presence of a (relatively) moving body; specifically the relative flow of air ahead of a shock wave.

fringing groove. A groove cut into a rotating band to collect metal from the band while it travels through the bore. Excess metal so collected is prevented from forming a fringe behind the rotating band. Fringe formation has been a cause of excess dispersion and short range.

frontal area. The area of the greatest circular cross-section of the body of a projectile [$S = (\pi/4)d^2$]; used as the reference area in defining the aerodynamic coefficients.

gravity drop. In ballistics, the vertical drop due to gravity; equal to one-half the acceleration due to gravity multiplied by the square of the time of flight.

HEAT *(abbr.)*. High explosive antitank. A term used to designate high explosive ammunition containing a shaped charge.

hit. An impact on a target by a projectile.

hit probability. The expected ratio of number of hits to number of projectiles fired at the target.

HVAP *(abbr.)*. Hypervelocity armor-piercing.

hypersonic. Of or pertaining to the speed of objects moving at Mach 5 or greater.

impact velocity. The velocity of a projectile at the instant of impact on the target or target area. Also called "striking velocity."

impulse, total. In rocketry, the product of the average thrust (in pounds) developed by the motor, times the burning time (in seconds).

increment. An amount of propellant added to, or taken away from, a propelling charge of semi-fixed or separate loading ammunition to allow for differences in range.

indirect fire. Gunfire delivered at a target which cannot be seen from the gun position.

inhibitor. A material applied to surfaces of propellant grains to prevent burning on the coated surfaces.

GLOSSARY (cont'd)

initial mass. The mass of a rocket-assisted projectile at the start of burning of the rocket propellant.

initial yaw. The yaw of a projectile as it leaves the muzzle blast zone.

initial yawing velocity. The rate of change of the yaw of a projectile as it leaves the muzzle blast zone.

jump. *1.* Movement of a gun tube when the gun is fired. *2.* Angle of jump (q.v.). *See:* **aerodynamic jump.**

kill probability. Probability (P_K) that, given a hit, a single projectile will kill (i.e., destroy) the target against which it is fired. The overall kill probability of a single shot is the product $P_H P_K$, where P_H is the hit probability, assumed to be independent of P_K.

laminar flow. A nonturbulent airflow.

land. One of the raised ridges in the bore of a rifled gun barrel.

lateral deviation. Horizontal distance (normal to the line of fire) between the point of impact of a single round and the center of impact of the group.

lift. The component of the total aerodynamic force perpendicular to the relative wind, and acting in the plane of yaw.

line of departure. The path of the projectile as it leaves the muzzle; the direction of the projectile at the instant it clears the muzzle of the gun, providing it has no swerving motion.

line of elevation. The prolongation of the bore when the gun is set to fire.

logarithm, natural. Defined by $x = e^{\ln x}$, where $e = 2.71828\ldots$.

lot. Quantity of material, the units of which were manufactured under identical conditions.

M *(abbr). 1.* Mach number. *2.* In such usage as M29, designates a standardized item.

Mach. (Named for Ernst Mach, 1838-1916, Austrian physicist.) Frequently used for Mach number, which see.

Mach angle. The acute angle between a Mach line and the line of flight of a moving body.

$$\theta_M = \tan^{-1} \frac{1}{\sqrt{M^2 - 1}}$$

Mach effect. An effect resulting from the fact that an object is moving at transonic or supersonic speed; a compressibility effect. Mach effect may be considered in terms of (a) The changes in the air brought on by a shock wave, i.e., changes in pressure, velocity, density and temperature and (b) Changes in aerodynamic coefficients, such as drag, lift, and moment coefficients.

Mach line. A theoretical line representing the backsweep of a cone-shaped shock wave made by an assumed infinitely small particle moving at the same speed and along the same flight path as an actual body or projectile. This line, as represented on any plane bisecting the shock-wave cone, forms an angle with the flight path usually somewhat more acute than the angle formed by the shock wave of the actual body, which depends among other things upon the shape of the body.

Mach number. The ratio of the velocity of a body to that of sound in the medium being considered. Thus, at sea level in the U.S. Standard Atmosphere, a body moving at a Mach number of one ($M = 1$) would have a velocity of 1116.2 fps (the speed of sound in air under those conditions).

Mach number, critical. The free stream Mach number at which the relative speed of air and projectile attains sonic velocity at some point on the projectile.

Mach number, free stream. The Mach number computed on the basis of the velocity of the projectile relative to air which is undisturbed by the presence of the projectile.

magnus force. The lateral thrust on a rotating body when acted on by an airstream having a velocity component normal to the body's axis of rotation.

magnus moment. The moment about the body c.g. produced by the magnus force.

mass. The constant of proportionality between the force on a body and the resulting acceleration. $m = W/g$. Unfortunately, in previous references, "mass" is sometimes used as synonymous with "weight."

material. In a restricted sense, those things used in combat or logistic support operations, such as weapons, ammunition, motor vehicles, etc.

GLOSSARY (cont'd)

mean range. Average distance reached by a group of shots fired with the same firing data.

méplat. The flat nose formed by truncation of the ogival portion of a projectile or point fuze. Sometimes the méplat is convex, and may be called a "calotte."

meteorological data. Facts pertaining to the atmosphere, especially wind, temperatures and air density, which are used in determining corrections to basic firing data. Often shortened to "metro data."

modal vectors. A pair of rotating arms, called the precession vector and the nutation vector, which when added together give the magnitude and orientation of the variable part of the yaw of the projectile at any instant. Adding the equilibrium yaw to the variable part gives the total yaw. The precession vector is often visualized as originating on the tangent to the trajectory, and rotating slowly. The outer end of this precession vector is taken as the origin of the nutation vector, which rotates more rapidly, and the resulting epicyclic motion of the outer end of the nutation vector represents the motion of the nose of the projectile (neglecting the equilibrium yaw).

muzzle blast. Sudden gas pressure exerted at the muzzle of a weapon by the rush of hot gases and air on firing. Muzzle blast precedes the emergence of the projectile, and forms a zone of turbulent air, gas, and smoke through which the projectile must fly. The length of the projectile's path in the blast zone varies from about 20 feet to 200 feet, depending on the size of the gun and the amount of gas leakage past the projectile while in the bore.

muzzle energy. Kinetic energy of the projectile as it emerges from the muzzle (plus a small amount of energy picked up in the muzzle blast, where for a short distance the muzzle gases outrun the projectile). This is a measure of the power of the weapon.

muzzle momentum. The momentum of the projectile (i.e., product of mass and velocity) as it leaves the muzzle. Limited by the capacity of the recoil system built into the gun mount.

muzzle velocity. The projectile velocity at the moment that the projectile ceases to be acted upon by propelling forces (other than the thrust of a rocket motor). It is obtained by measuring the velocity over a distance forward of the gun, and correcting back to the muzzle for the retardation in flight.

NBS *(abbr)*. National Bureau of Standards.

NOL *(abbr)*. Naval Ordnance Laboratory.

normal force. The component of the total aerodynamic force perpendicular to the longitudinal axis of the projectile, and acting in the plane of yaw.

NOTS *(abbr)*. Naval Ordnance Test Station.

nutation. The oscillation of the axis of a rotating body such as a spinning projectile. This oscillation is superimposed on the slower motion of the projectile axis which is known as precession, which see.

obturation. The act of, or means for, preventing the escape of gases.

obturator. *1.* A device (usually a ring or pad) incorporated in a projectile to make the tube or a weapon gas-tight. *2.* A device incorporated in a rocket motor to prevent unwanted gas leakage.

ogive. The curved or tapered front of a projectile. The fuze may or may not be included as a part of the ogive

ogive, secant. An ogive generated by an arc not tangent to, but intersecting at a small angle, the cylindrical surface of the body. A secant ogive may have any radius of curvature greater than that of a tangent ogive for the same projectile, up to an infinite radius of curvature (i.e., a straight, conical ogive); a radius twice that of the tangent ogive is common.

ogive, tangent. An ogive generated by an arc tangent to the generator of the cylindrical surface. Called "true ogive" by the British.

orientation of yaw. The direction of the plane of yaw (q.v.) relative to some reference direction such as a vertical plane containing the tangent to the trajectory.

overturning moment. An aerodynamic moment tending to increase the yaw of the projectile.

particle trajectory. The trajectory determined by gravity and zero-lift drag which would be described by a projectile which maintained zero

GLOSSARY (cont'd)

angle of yaw. A useful approximation to the trajectory of an actual projectile.

piezometric efficiency. The ratio of the work done on the projectile by the propellant gases to the work that could have been done if the maximum chamber pressure had acted on the projectile base for the full travel in the bore; i.e., the ratio of average pressure to peak pressure.

plane of yaw. The plane containing both the longitudinal axis of the projectile and the tangent to the trajectory.

precession. A circular motion of the axis of rotation of a spinning body which is brought about by the application of a constant torque about an axis perpendicular to the axis of rotation. A nonconstant torque produces a noncircular precession.

precision. The property of having small dispersion about the mean. Cf: accuracy.

pressure front. *See:* shock front.

pressure-travel curve. Curve showing chamber pressure plotted against the travel of the projectile within the bore of the weapon.

probable error. In general, a value that any given error will as likely fall under as exceed. In gunnery, a measure of the dispersion pattern around the center of impact; half of the observed impacts will fall within a band two probable errors wide and centered on the center of impact.

quadrant elevation. Vertical angle between a horizontal plane and axis of bore of gun, just prior to firing.

radius of gyration. The distance from the axis of rotation at which the total mass of a body might be concentrated without changing its moment of inertia about that axis. In this handbook radii of gyration are usually expressed in calibers.

range correction. Changes of firing data necessary to allow for deviations in range due to weather, material, or ammunition.

range deviation. Distance by which a projectile strikes beyond, or short of, the target measured along a line parallel to the gun-target line.

range error. Difference between the range to the point of impact of a particular projectile and the range to the center of impact of the group of shots fired with the same data.

range probable error. *1.* Error in range that a gun or other weapon may be expected to exceed as often as not. Range probable error given in the firing tables for a gun may be taken as an index of the accuracy of the piece. *2.* In describing the dispersion pattern of a group of shots, the probable error in the range direction.

range wind. Horizontal component of true wind in the direction of the line of fire.

reference rounds. Ammunition rounds of known performance which are fired during ballistic tests of ammunition for comparative purposes. Also called "control rounds."

relative velocity. The velocity of relative motion, especially in respect to a projectile and the airstream.

relative wind. The velocity of the air with reference to a body in it. Usually determined from measurements made at such a distance from the body that the disturbing effect of the body upon the air is negligible. Equal and opposite to the relative velocity of a projectile.

restoring moment. A static moment (q.v.) which is negative when the angle of attack is positive, and vice versa.

reversed flow. Flow of the airstream from the base toward the nose of the projectile, such as exists in the muzzle blast where the blast gases are moving faster than the projectile.

Reynolds number. (Named after Osborne Reynolds, 1842-1912, a British physicist and engineer.) An index of similarity used in the analysis of the fluid flow about scale models in wind tunnel tests to determine the results to be expected of the flow about full-scale models. The Reynolds number is expressed in a fraction, the numerator consisting of the density of the fluid multiplied by its velocity and by a linear dimension of the body (as for example its diameter), the denominator consisting of the coefficients of viscosity of the fluid ($RE = \rho Vl/\mu$).

RMS error. *See:* standard error.

rocket motor. A nonairbreathing reaction propulsion device that consists essentially of a fuel chamber(s) and exhaust nozzle(s), and that carries its own solid oxidizer-fuel combination from which hot gases are generated by combustion and

GLOSSARY (cont'd)

expanded through a nozzle(s). (If the fuel is liquid the device is called a "rocket engine.")

roll. An angular displacement about the longitudinal axis of a projectile.

roll rate. The time rate of projectile rotation about its longitudinal axis.

roll rate, nondimensional. The product of roll rate and a reference length, as for example a diameter, divided by the airspeed ($\nu = pd/V$). Usually called "spin."

rolling moment. An aerodynamic moment about the longitudinal axis of a projectile, tending to change the roll rate.

rolling velocity. Angular velocity; roll rate.

root mean square. The square root of the arithmetical mean of the squares of a set of numerical values.

rotating band. Soft metal band around a projectile near its base. The rotating band centers the projectile and makes it fit tightly in the bore, thus preventing the escape of gas, and by engaging the rifling gives the projectile its spin.

round (of ammunition). *1.* Short for **complete round**, which see. *2.* A shot fired from a weapon.

scale effect. An effect in fluid flow that results from changing the scale but not the shape of a body around which the flow passes. Reynolds number is useful in the assessment of scale effect.

schlieren. *1.* Gradients or variations in gas density, from the German word. *2.* An optical system which either cuts off or passes a large change in light intensity, owing to the slight refraction of the light passing through the gas. This phenomenon is often used to make turbulence and shock waves visible by photographic means; hence, "schlieren photographs."

sectional density. The ratio of the weight of a projectile to the square of its diameter. A measure of the mass per unit of frontal area, and therefore of the deceleration due to drag.

sensitivity factor. The percent change in range (or deflection) produced by a one percent change in a parameter affecting range (or deflection), such as muzzle velocity or initial yawing velocity. Also called "differential coefficient." *See:* **differential effects.**

separation. *1.* The phenomenon in which the boundary layer of the flow over a body placed in a moving stream of fluid (or moving through the fluid) separates from the surface of the body. *2.* The point on the body at which the separation begins. Also called "separation point."

setback acceleration. The peak acceleration experienced by the projectile during launching. Usually expressed in terms of the acceleration due to gravity, e.g., "the setback acceleration was 40000 g's" or about 1,286,400 ft/sec^2.

shock front. The outer side of a shock wave, at which the pressure rises from zero up to its peak value. Also called a "pressure front."

shock wave. *1.* A boundary surface or line across which a flow of air or other fluid, relative to a body or projectile passing through the air or fluid, changes discontinuously in pressure, velocity, density, temperature and entropy within an infinitesimal period of time. *2.* Such a boundary surface or line that comes into being when an object moves at transonic or supersonic speeds. *3.* Such a surface or line produced by the expansion of gases away from an explosion (or through a nozzle).

shroud. A tubular section encircling the tips of the fins, and usually integral with the fins. The shroud often forms a rear riding surface for the projectile in the bore of the gun.

slug. The engineering unit of mass, chosen such that a force of one pound acting on a unit mass will produce an acceleration of one foot per second per second. Since the weight of a body is equal to the product of its mass and the acceleration of gravity, the weight of a body having a mass of one slug is 32.17 lbs (at sea level at 45° latitude).

span. The maximum dimension of an airfoil (e.g., a coplanar pair of fins) from tip to tip.

spark range. A firing range in which projectiles in free flight can be photographed by the light from an electric spark which is triggered by passage of the projectile. *See:* **ballistic range.**

specific impulse. The total impulse produced by burning a pound of rocket fuel. At constant thrust and mass burning rate, the thrust pro-

GLOSSARY (cont'd)

duced per unit of mass burning rate, i.e., pounds per lb/sec.

specific weight. Weight per unit volume.

spike. A subcaliber cylinder, often slightly tapered, which replaces the ogive of a projectile, increasing the drag but moving the center of pressure of the lift force nearer the base of the projectile.

spin. *See:* **roll rate, nondimensional.**

spin rate. *See:* **roll rate.**

spin stabilization. Method of stabilizing a projectile during flight by causing it to rotate about its own longitudinal axis.

spotting charge. A small charge such as black powder, in a projectile under test, to show the location of its point of functioning (usually its point of impact).

square base. Descriptive of a projectile with a cylindrical base section, as opposed to a boattail, which see. Also called "flat base."

stability. A characteristic of a projectile that causes it, if disturbed from its condition of equilibrium or steady flight, to return to that condition.

stability factor, dynamic. A number related to the yaw damping characteristics of a projectile.

stability factor, gyroscopic. A number relating the angular momentum of a projectile to the slope of its aerodynamic overturning moment. Long used as a sole criterion of projectile stability and called simply the "stability factor," s. A necessary, but not sufficient, condition for stability is that this factor be greater than unity, or negative.

stability, static. Stability in the absence of spin. In general, a mechanism is statically stable if any displacement from a rest position creates a force or moment opposing the displacement.

Standard Atmosphere. The standard atmosphere for the United States Armed Services is the U.S. Standard Atmosphere which is that of the International Civil Aviation Organization (ICAO). This standard atmosphere assumes a ground pressure of 760 mm of mercury (14.69 psi) and a ground temperature of 15°C (59°F). The temperature throughout the troposphere extending up to 11 kilometers (approx. 36,000 ft) is given by:

$$T(°F) = 59 - 0.00356\,h$$

where h is the height above sea level measured in feet. In the stratosphere, extending from 11 kilometers to 25 kilometers (approx. 82,000 ft) the temperature is assumed to be a constant 216.66°K (−69.7°F). Above the stratosphere other laws are assumed. Temperature is significant because the acoustic velocity in feet per second is given by

$$V_a = 49.1\sqrt{460 + T} \qquad T \text{ in } °F$$

standard deviation. In the field of testing, a measure of the deviation of the individual values of a series from their mean value. The standard deviation of a sample is expressed algebraically by the formula

$$s = \sqrt{\frac{\Sigma(x_i - \bar{x})^2}{N}} \quad \text{where } \Sigma \text{ means}$$

the sum of N individual squared differences, the x_i are the individual values, $\bar{x}$ is the mean ($\bar{x} = \sum_i x_i/N$), and N is the number of individuals in the sample. The best estimate of σ, the standard deviation of the lot from which the sample was drawn, is obtained by multiplying the sample value, s, by $\sqrt{N/(N-1)}$.

standard error. The square root of the average of the squares of all the errors. When error is identified as the difference between an observed point and the means of the observations, standard error becomes identical with the sample standard deviation. It might also be called the "RMS error."

standard muzzle velocity. Velocity at which a given projectile is supposed to leave the muzzle of a gun. The velocity is calculated on the basis of the particular gun, the propelling charge used, and the type of projectile. Firing tables are based on standard muzzle velocity.

standard projectile. That projectile which a given gun was primarily designed to fire.

static moment. An aerodynamic moment related only to angle of yaw.

static pressure. The pressure which is exerted by

a fluid at rest, or which would be indicated by a gage placed in the stream and moving with the same velocity as the stream. It is the pressure arising from the random motions of the molecules of the fluid, rather than their organized motion in the direction of the flow.

steady state. The condition of a system which is essentially constant after damping out initial transients or fluctuations.

sting. A rod or type of mounting attached to, and extending backward from, a model, for convenience of mounting when testing in a wind tunnel.

subsonic. Pertaining to relative motion between a body and a surrounding fluid at a speed less than the speed of sound in the same fluid.

summit of trajectory. Highest point that a projectile reaches in its flight.

swerving motion. In flight, the motion of the center of gravity of a projectile perpendicular to its particle, or zero-lift, trajectory.

system reliability. The probability that a system will perform its specified task under stated tactical and environmental conditions. This will include accuracy.

T (subscript). In aerodynamic data, relating to tail alone configuration.

terminal velocity. *1.* The constant velocity of a falling body attained when the resistance of air or other ambient fluid has become equal to the force of gravity acting on the body. Sometimes called "limiting velocity." *2.* Velocity at end of trajectory, i.e., impact velocity.

time of flight. Elapsed time in seconds from the instant a projectile leaves the gun until the instant it strikes or bursts.

tolerance. The permissible difference between the two extremes in dimension, weight, strength or other quality which will not cause rejection of an item.

trajectory. The curve in space traced by the center of gravity of the projectile.

transition flow. A flow of fluid, about a body, that is changing from laminar flow to turbulent flow.

transonic range. The range of speeds between the speed at which one point on a body reaches supersonic speed (relative to the airflow in the vicinity of that point) and the speed at which the shock wave system is fully developed.

transonic speed. A speed within the transonic range.

transverse axis. In a projectile, any axis normal to the longitudinal axis and passing through the center of gravity.

trim. The equilibrium attitude of the longitudinal axis of the projectile relative to the tangent to the trajectory; equilibrium yaw.

turbulent flow. An unsteady flow characterized by the super-position of rapidly varying velocities on the main velocity of flow, in contrast to the smooth, steady laminar flow in which velocity varies with distance but only slowly with time.

twist (of rifling). Inclination of the spiral grooves of the rifling to the axis of the bore of the weapon. It is expressed as the number of calibers of length in which the rifling (and therefore the projectile) makes one complete turn. A right hand twist is such as to impart a right hand (clockwise) rotation to the projectile when viewed from the rear. Most U.S. guns have right hand twist.

utility. A numerical scale for comparing preferences between alternatives. Usually defined on the interval 0, 1 because of its relation to probability.

vacuum trajectory. The path of a projectile subject only to gravity. A first approximation to the trajectory of an actual projectile.

vector. *1.* An entity which has both magnitude and direction, such as a force or velocity. *2.* In connection with the yawing oscillations of projectiles, the rotating arms which can be used to represent the components of the yaw are termed modal vectors, which see.

velocity. Speed, or rate of motion, in a given direction and in a given frame of reference. In many contexts no distinction in meaning is made between speed and velocity, the symbol V often being used in equations in which the magnitude of the velocity, i.e., the speed, is the only attribute of velocity which is being considered.

velocity head. *See:* **dynamic pressure.**

viscosity, coefficient of. The ratio of the shearing stress to the velocity gradient in a boundary

GLOSSARY (cont'd)

layer. Dependent on the fluid and on its temperature.

μ_{air} at 59° F = 3.72×10^{-7} lb-sec/ft²

wake. The zone of turbulent flow behind the base of a projectile.

wash. The surge of disturbed air or other fluid resulting from the passage of something through the fluid. Includes the wake and bow and side waves.

wave, expansive. An oblique wave or zone set up in supersonic flow when the change in direction of the airflow is such that the air tends to leave the new surface, such as flow around the juncture of a cylinder and a cone (e.g., at the forward end of a boattail). This condition is called "flow around a corner." The air after passing through an expansive wave or zone has a lower density, static pressure, and freestream temperature and has higher velocity and Mach number. Visible as a darkened zone in schlieren photographs, these waves are often called "expansion fans."

wave length. *1.* The distance traveled in one period or cycle by a periodic disturbance. *2.* Of yaw of a projectile, the distance traveled by the projectile during one cycle of yaw.

yaw. *1.* The angle between the direction of motion of a projectile and the direction of the longitudinal axis of the projectile. *2.* The oscillation of the direction of the longitudinal axis (as in "wavelength of yaw"). *3.* To acquire an angle of yaw; to oscillate in yaw.

yaw of repose. That part of the equilibrium yaw which is due to gravity.

yaw drag. Drag due to yaw.

yawing moment due to yawing. Term sometimes used for the damping moment.

yawing velocity. Time rate of change of yaw; the change may be a change in magnitude or direction, or both.

zone charge. The number of increments of propellant in a propellant charge of semifixed rounds, corresponding to the intended zone of fire.

zone of fire. The range interval which can be covered by a round containing a given number of increments of propellant, i.e., the coverage obtainable by changing quadrant elevation at a constant muzzle velocity.

zoned ammunition. Semifixed or separate loading ammunition in which provision is made for adding or removing propellant increments.

APPENDIX I
SAMPLE SPIN-STABILIZED PROJECTILE

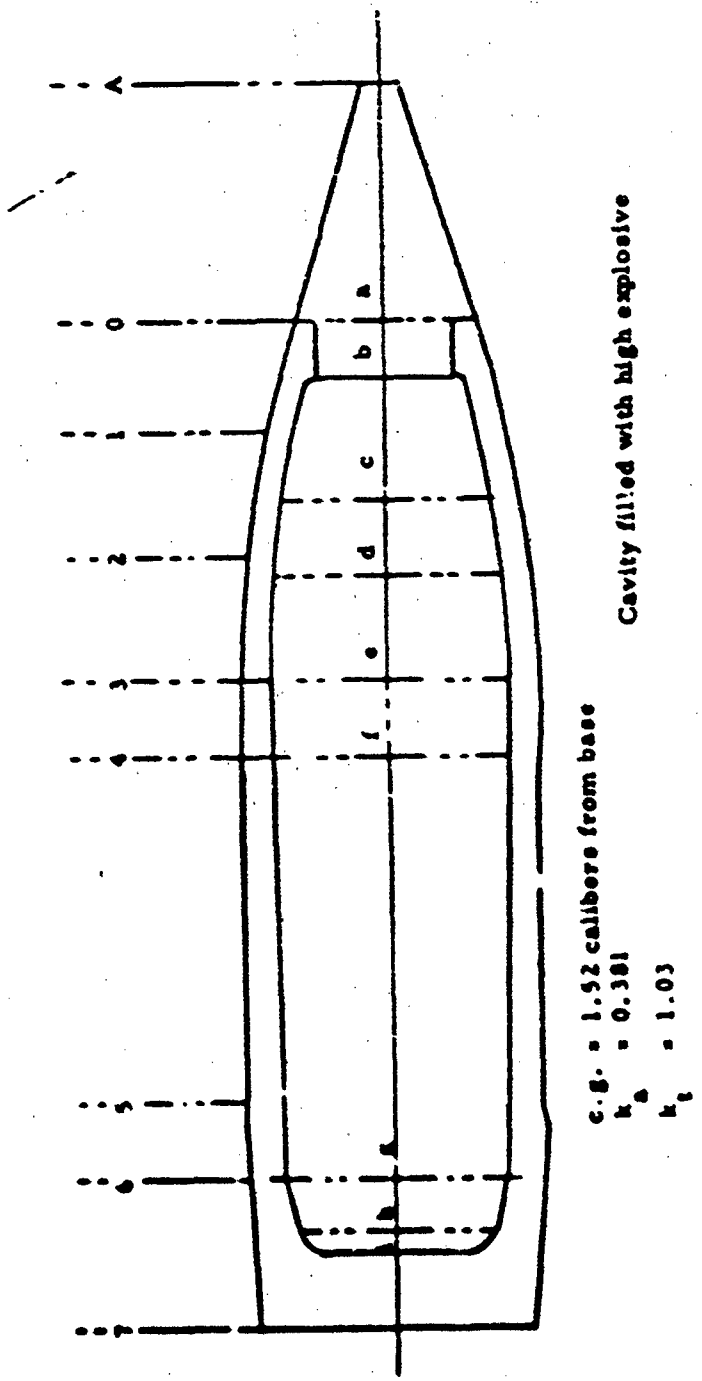

APPENDIX II
CALCULATION OF C. G. AND RADIUS OF GYRATION

Approximate formulas for high explosive projectiles are presented by Hitchcock in BRL Report 620 (Ref. 81).

$$X_{c.g.} = 0.375\frac{l}{d}$$

$$k^2_o = 0.140$$

$$k^2_t = 0.070 + 0.0594\left(\frac{l}{d}\right)^2$$

where $X_{c.g.}$ is the distance from the base of the projectile to its center of gravity, in calibers, and l/d is the fineness ratio of the projectile.

a. *Alternate Method:*

For the sample projectile in Appendix I, the parameters calculated by use of the "Alternate Method" (see Appendix VII) are:

$$X_{c.g.} = 1.55$$

$$k^2_o = 0.145$$

$$k^2_t = 1.07$$

b. *Hitchcock Method:*

By Hitchcock's formulas, we would get

$$X_{c.g.} = 0.375 \times 4.18 = 1.64$$

$$k^2_o = 0.140$$

$$k^2_t = 0.070 + 0.0594\ (4.37)^2 = 1.21$$

APPENDIX III
GYROSCOPIC STABILITY ESTIMATES

A. SPIN-STABILIZED PROJECTILE WITH BOATTAIL

The following is a sample calculation for a spin-stabilized projectile with boattail, using the methods of Wood (Ref. 21) and Simmons (Ref. 20) to estimate the normal force and static moment coefficients. The geometric and mass characteristics of the projectile are given in Appendix I.

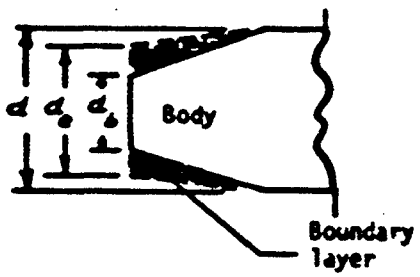

Effective Base Diameter:

$$d_e = \sqrt{\frac{d^2 + d_b^2}{2}}$$

where d = Rear body diam. = 4.98" (0.415 ft)
d_b = Base diam. = 4.22"

$$d_e = \sqrt{21.7314} = 4.66''$$

Effective Base Area:

$$S_b = .7854\, d_e^2$$
$$= .7854\,(4.66)^2 = 17.0554 \text{ in}^2$$

Frontal Area:

$$S = .7854 d^2$$
$$= .7854\,(4.98)^2 = 19.4782 \text{ in}^2$$

Base Area Ratio:

$$\frac{S_b}{S} = \frac{17.0554}{19.4782} = 0.8756$$

Volume of Projectile (including boattail boundary layer):

V_b = 203.5412 in³ (see calculation below)

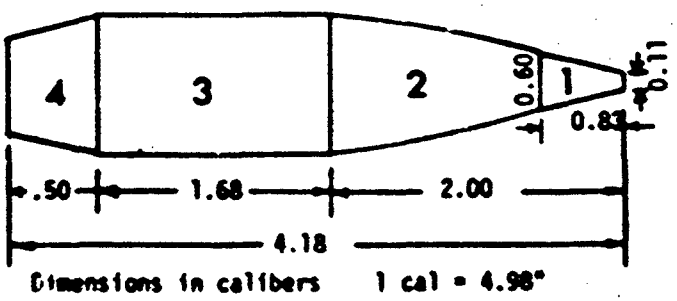

Section	Calculations	Volume, in³
1	.2618 (4.125) [(3.00)² + (3.00) (.55) + (.55)²]	11.8276
2	From Harvard Tables Calculations*	82.8140
3	.7854 (8.262) (4.98)² =	163.2060
4	.2618 (2.50) [(4.98)² + (4.98) (4.66) + (4.66)²]	45.6336
	V_b = Total Boundary Layer Volume =	203.5412

* Reference Appendix VII.

APPENDIX III (cont'd)

Mean Fineness Ratio:

$$\frac{V_b}{Sd} = \frac{383.5412}{(19.4762)(4.98)} = 3.1292$$

Determination of f_1 and f_2:

(See graph Appendix IV)

At supersonic speed:

$$N = \frac{\sqrt{M^2 - 1}}{V_b/Sd} = 0.45 \text{ for } M = 1.72$$

$$\frac{f_1 - 1}{\sqrt{M^2 - 1}} = 0.142 \text{ and}$$

$$\frac{f_2 - 1}{\sqrt{M^2 - 1}} = 0.165$$

$$\therefore f_1 = 1.1987 \text{ and } f_2 = 1.2309$$

Normal Force Coefficient:

$$C_{N_\alpha} = \left(2\frac{S_t}{S} + .5\right) f_1$$

$$= [\,2\,(.8756) + .5\,]\,(1.1987)$$

$$= 2.70 \text{ rad}^{-1}$$

Moment Coefficient (about base):

$$C_{M_\alpha} = \left(2\frac{V_b}{Sd}\right) f_2 = \left[\,2\,(3.1292)\,\right](1.2309)$$

$$= 7.70 \text{ rad}^{-1}$$

Center of Pressure:

$$C.P. = \frac{C_{M_\alpha}}{C_{N_\alpha}} = 2.85 \text{ calibers from base}$$

Center of Gravity (from Appendix I):

$C.G.$ = 1.52 calibers from base

$C.P. - C.G. = 2.85 - 1.52 = 1.33$ calibers

Static Moment Coefficient:

$$C_{M_\alpha} = C_{N_\alpha}(C.P. - C.G.)$$

$$= (2.70)(1.33) = 3.59$$

Gyroscopic Stability Factor, s_g:

Velocity: $Vel = 1925$ fps

Twist: $n = 28$ calibers per turn

Spin rate: $p = 165$ rps

$= 1040$ rad per sec

Max body diam: $d = 0.415$ ft

Air density: $\rho = 0.002378$ slug/ft³

$$I_x^2/I_y = 0.0040 \text{ slug-ft}^2$$

$$\mu = \frac{\pi}{8}\rho d^2 V^2 C_{N_\alpha}$$

$$s_g = \frac{I_x^2 p^2}{4 I_y \mu}$$

$$s_g = \frac{.0040\,(1.0816 \times 10^6)}{4\left(\frac{\pi}{8}\right)(.002387)(.5716)(3.706626 \times 10^6)(3.59)}$$

$$= 1.40$$

APPENDIX III (cont'd)
GYROSCOPIC STABILITY ESTIMATES

B. SPIN-STABILIZED PROJECTILE WITHOUT BOATTAIL (FLAT BASE)

Assume only change from previous example is in volume and $C.\ G.$ location.

New volume: $V = 306.5412$ in.^{3}

Mean Fineness Ratio:

$$\frac{V_b}{Sd} = \frac{306.5412}{(19.4782)\ (4.98)} = 3.1608$$

Determination of f_1 and f_2: (See graph Appendix IV)

$$N = \frac{\sqrt{M^2 - 1}}{V/Sd} = 0.44 \text{ for } M = 1.72$$

$$\frac{f_1 - 1}{\sqrt{M^2 - 1}} = 0.136 \text{ and } \quad \frac{f_2 - 1}{\sqrt{M^2 - 1}} = 0.148$$

$$\therefore f_1 = 1.900 \text{ and } f_2 = 1.2337$$

Normal Force Coefficient:

$$C_{N_\alpha} = \left(2\ \frac{S_b'}{S} + .5\right) f_1 \quad \text{where } S_b' = S$$

$$= [2\ (1.0) + .5]\ (1.900)$$

$$= 3.00 \text{ rad}^{-1}$$

Moment Coe[illegible] (about base):

$$C_{M_\alpha} = \left(2\ \frac{V}{Sd}\right) f_2 = 6.3216\ (1.2337)$$

$$= 7.80 \text{ rad}^{-1}$$

Center of Pressure:

$$C.\ P. = \frac{C_{M_\alpha}}{C_{N_\alpha}} = 2.60 \text{ calibers from base}$$

Center of Gravity: $C.\ G.$ is now located 1.50 calibers from base

$$C.\ P. - C.\ G. = 2.60 - 1.50 = 1.10 \text{ calibers}$$

Static Moment Coefficient:

$$C_{M_\alpha} = C_{N_\alpha}\ (C.\ P. - C.\ G.)$$

$$= (3.00)\ (1.10) = 3.30$$

Gyroscopic Stability Factor, s_g

Since the parameters—Vd, p, n, d, ρ, I_x/I_y—are the same as the example in part A:

$$s_g = 1.49 \left(\frac{C_{M_\alpha} \text{ with boattail}}{C_{M_\alpha} \text{ without boattail}}\right)$$

$$= 1.49 \left(\frac{3.59}{3.30}\right) = 1.62$$

Conclusion: Eliminating the boattail has increased the gyroscopic stability factor (but also increased the zero-yaw drag coefficient).

APPENDIX IV
COMPARISON OF ESTIMATES OF BALLISTIC PARAMETERS BY VARIOUS METHODS

For comparison with the other estimates, calculations by Hitchcock's method, BRL Report 620 (*Ref.* 21), for the same boattailed projectile, Appendix I, are presented below:

a (boattail angle)	= 7.5 degrees
b (boattail length)	= 0.5 calibers
c (cylindrical body length)	= 1.68 calibers
d (ogival head length)	= 2.00 calibers
e (radius of ogival arc)	= 5.12 calibers
	$1.0/e = .1953$

Normal Force Coefficient: (using a, b, c, d, and e above)

$$K_n = .653 + .0223a - .6136b - .0023c + .2635d + .6476\ (1.0/e)$$

$$K_n = .653 + .1673 - .3070 - .0029 + .5270 + .1265$$

$$K_n = 1.1629$$

$$C_{x_0} = \frac{K}{\pi}\ K_n = 2.96 \text{ (vs 2.70 by Wood's method)}$$

Center of Pressure:

$$h = .0747 + .0443a + 1.0196b + .0032c + .2459d + .8083\ (1.0/e)$$

$$h = .0747 + .1323 + .5095 + 1.2494 + .4918 + .1579$$

$h = 2.51$ calibers from the base (vs 2.85 by Wood's method)

This agreement is considered to be better than average. While Hitchcock's estimates are very good for projectiles which lie within the range of his experimental data, the Wood-Simmons estimates will in general be more reliable.

APPENDIX IV (cont'd)

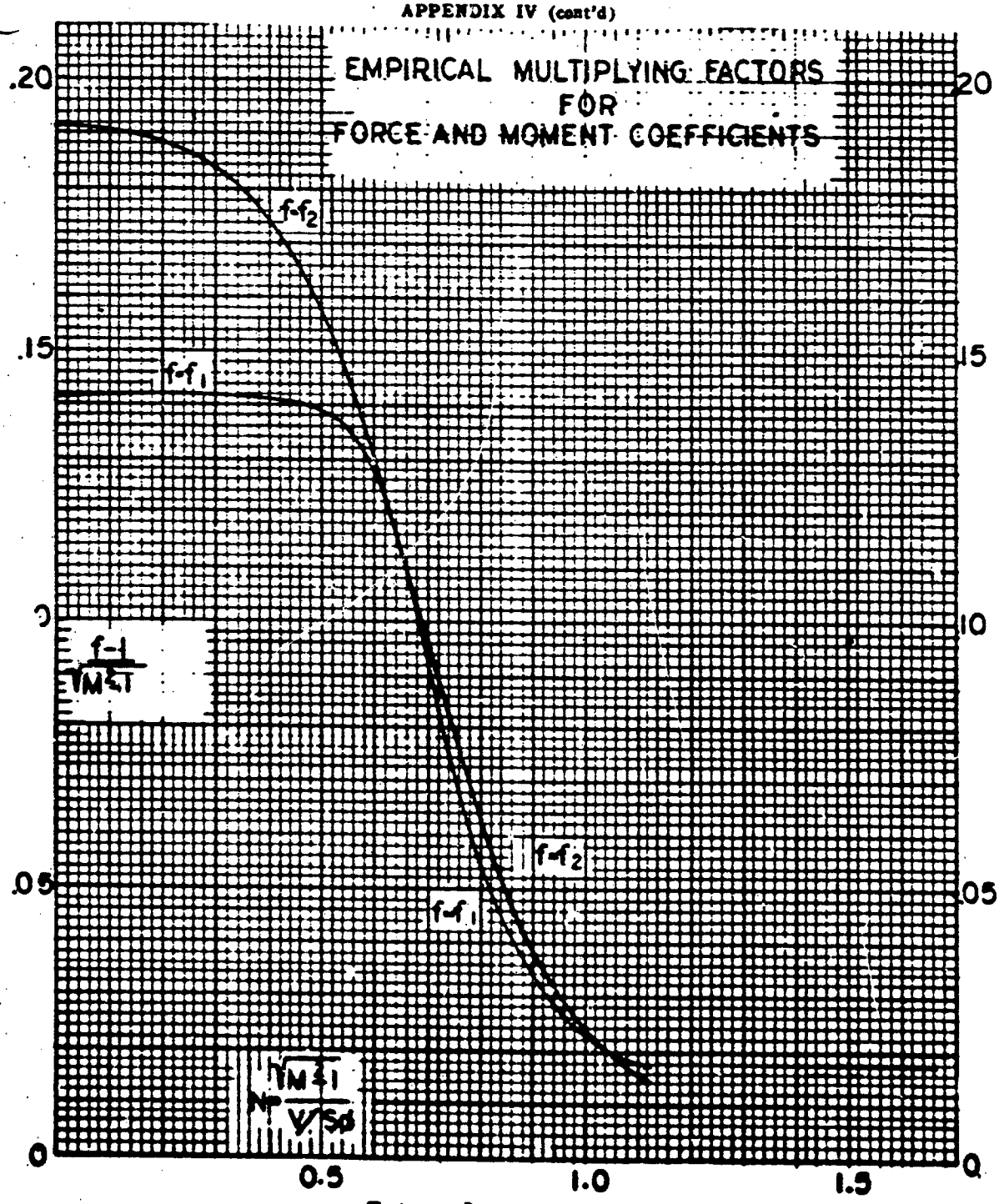

Taken from
R.M.Wood BRL MR 854 (Ref. 21)

APPENDIX V
DYNAMIC STABILITY ESTIMATE

Problem: To determine s_{d_o}. The projectile will be stable if:

$$\frac{1}{s_g} < s_{d_o}(2.0 - s_{d_o}) \quad \text{(Ref. par. 5-2.4.2.1)}$$

Formula: $$s_{d_o} = \frac{2\,(C_{L_\alpha} + k_m^2\, C_{M_{p\alpha}})}{C_{L_\alpha} - C_D + k_t^2\,(C_{M_q} + C_{M_{\dot\alpha}})}$$

Data: For prototype projectile (Appendix I).

$C_{L_\alpha} = 2.70\ \text{rad}^{-1}$
Mach $= 1.72$
$m = 46.08/32.2$ slugs
$d = 0.415$ ft
$I_x = 0.0259$ slug-ft²
$I_y = 0.2640$ slug-ft²

$$k_m^2 = \frac{1}{k_m^2} = \frac{md^2}{I_x}$$

$$= \left(\frac{46.08}{32.2}\right)\frac{(.415^2)}{(.0259)} = 6.854$$

$$k_t^2 = \frac{1}{k_t^2} = \frac{md^2}{I_y}$$

$$= \left(\frac{46.08}{32.2}\right)\frac{(.415^2)}{(.2640)} = 0.933$$

Since our projectile has the same ballistic shape as projectile, 90-mm, HE, M71, the ballistic coefficients for the 90-mm projectile at Mach $= 1.72$ (ref. Appendix VIII-E) may be used, namely:

$$C_{M_{p\alpha}} = 0.20$$
$$C_{M_q} + C_{M_{\dot\alpha}} = -9.0$$
$$C_D = 0.33$$

Solution:

$$s_{d_o} = \frac{2[2.70 + 6.854\,(.20)]}{2.70 - 0.33 - 0.933\,(-9.0)} = \frac{8.14}{10.767}$$
$$= 0.756$$

From Appendix III-A: $s_g = 1.49$

$$\therefore \frac{1}{s_g} = \frac{1}{1.49} = 0.671$$

$$s_{d_o}(2.0 - s_{d_o}) = 0.756\,(2.0 - 0.756) = 0.94$$

Conclusion: Projectile is stable since:

$$\frac{1}{s_g} < s_{d_o}(2.0 + s_{d_o}), \text{ i.e.:}$$

$$0.671 < 0.94$$

APPENDIX VI
STATIC STABILITY ESTIMATE OF A 5-INCH FIN-STABILIZED PROJECTILE

Problem: Determine normal force and center of pressure of the body alone, and normal force and center of pressure of the tail alone in order to solve for static stability:

$$|C.P. - C.G.| > 0.5 \text{ caliber}$$

Solution:

(1) Body alone coefficients at subsonic muzzle velocities

Data: The effective base area, S_b', and total boundary layer volume are determined in a manner similar to that shown in Appendix III-A.

$$d_e = 2.672'' \text{ and } d = 5''$$
$$S_b' = .7854\, d_e^2 = .7854\,(2.672)^2 = 5.6074 \text{ in}^2$$
$$S = .7854\, d^2 = .7854\,(5)^2 = 19.635$$
$$Sd = 19.635\, d = 19.635\,(5) = 98.175$$
$$V_b = 487.0151 \text{ in}^3$$
$$\frac{V_b}{Sd} = \frac{487.0151}{98.175} = 4.9606$$

Solving by Simmons' Equations Ref. 20:

$$C_{N_B} = 2\left(\frac{S_b'}{S}\right) + 0.5 = 2\left(\frac{5.6074}{19.635}\right) + 0.5 = 1.071$$

$$C_{M_B} = 2\left(\frac{V_b}{Sd}\right) = 2\left(\frac{478.0151}{98.175}\right) = 9.9212$$

$$C.P._{body} = \frac{C_{M_B}}{C_{N_B}} = \frac{9.9212}{1.071} = 9.26 \text{ calibers from base of fins}$$

(2) Tail alone coefficients at subsonic velocities:

Data:

effective tail length: $l = 3.0''$
fin span: $S = 5.0''$
effective base diameter: $d_e = 2.67''$

$$\frac{l}{S} = 0.6 \text{ and } \frac{d_e}{S} = 0.53$$

Solving by Simmons' Tables:

$C_{L_T} = 2.20$ (for 6 rectangular fins)

$C_L = C_{L_T}\,(0.74) = 1.628$ (body interference factor = 0.74)

$C_{N_T} = C_L\,(1.80) = 2.9304$ (allowance for end plates and shroud = 1.80)

$C.P._{tail} = 0.60$ caliber from base of fins

(3) Static Stability $|C.P. - C.G.| > 0.5$ caliber (Ref. par. 5-3.2):

Data: From parts (1) & (2):

$C_{N_B} = 1.0710$ at a $C.P.$ located 9.26 calibers from base of fins

$C_{N_T} = 2.9304$ at a $C.P.$ located 0.60 caliber from base of fins

$C_{N_\alpha} = C_{N_B} + C_{N_T} = 4.0014 \text{ rad}^{-1}$

$C.G. = 3.68$ calibers from base of fins

$(C.P._B - C.G.) = 9.26 - 3.68 = 5.58$ calibers

$(C.P._T - C.G.) = 0.60 - 3.68 = -3.08$ calibers

Solving (ref. par. 5–3.1):

$$C_{M_\alpha} = C_{N_B}(C.P._B - C.G.) + C_{N_T}(C.P._T - C.G.)$$

$$C.P. - C.G. = \frac{C_{M_\alpha}}{C_{N_\alpha}} = \frac{(1.071)(5.58) + (2.9304)(-3.08)}{4.0014} = -\frac{3.0494}{4.0014} = -0.76$$

$$|C.P. - C.G.| = 0.76 \text{ caliber}$$

Conclusion: Static stability seems adequate since $|C.P. - C.G.| > 0.5$, i.e., $0.76 > 0.5$

APPENDIX VII
PROJECTILE GEOMETRY

The design parameters related only to the materials and geometry of the projectile are:

Weight
Center of gravity location
Axial and transverse moments of inertia

Methods of Computation:

1. Mechanical Integrator (Ref. 95):
   a. A scale drawing is made of the part or assembly.
      (1) Dimensions in the x direction are not altered
      (2) Dimensions in the y direction are altered by letting $y_1 = y^2/2$
   b. The drawing is traversed by the mechanical integrator (a form of planimeter).
   c. Dial indicators provide numbers, relative to the transformed plane areas.
   d. Equations convert dial readings to weight, center of gravity, and moments of inertia of solids of revolution.
2. Harvard Tables—Standard Method (Ref. 94):
   a. Analyst works from dimensioned sketches, or drawings, to evaluate weight, c.g., and moments of inertia.
   b. Tables provide expedient method to supplement standard equations for solids of revolution.
3. Alternate Method: Analyst uses variations of formulas for limited number of solid shapes, and simplifies summary of parts and assembly.
4. Computer (Ref. 98): The weight, location of center of gravity, volume, polar moment of inertia, transverse moment of inertia and total moment of inertia can be obtained through use of a digital electronic computer.

AUTHOR(S) E. T. Roecker and E. D. Boyer

REPORT BRL MR 1098
DATE 1957
TYPE OF TEST Free flight

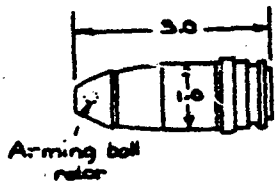

Dimensions, calibers

Muzzle	Weight, lb	0.56
	Velocity, fps	Variable
	Spin rate, rps	Variable
	d, ft	0.098
	ν, rad/cal	0.38

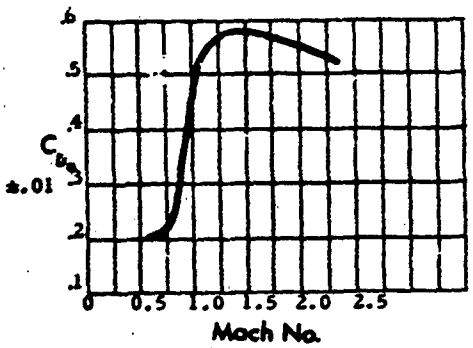

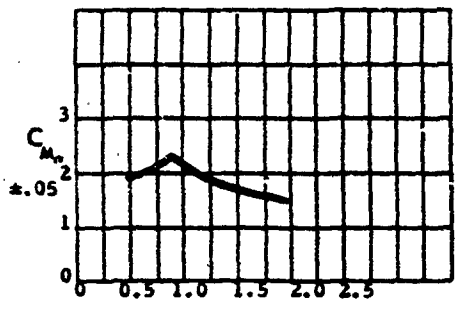

c.g. location from base, calibers 1.33

I_x, slug-ft^2 _____ I_y, slug-ft^2 _____

k_σ, cal 0.372 k_τ, cal 0.845

	Subsonic	Transonic Peak	Supersonic	Comments
M	0.6	0.9	2.0	
C_{D_0}				
C_{L_α}	1.7	2.1±0.2	2.4±0.2	
C_{M_α}	1.9	2.3±.05	1.5±.05	
$C_{M_q}+C_{M_{\dot\alpha}}$			-3.5±1.0	Without arming ball rotor
$C_{M_{pa}}\|_{\alpha=0}$			-0.13±0.10	$\begin{cases} C_{M_{pa}} = C_{M_{pa}}\|_{\alpha=0} + b\,\delta_g^2 \\ M = 2.0 \quad b = 90 \end{cases}$
C_{L_p}				
c.p. location	2.3	2.35±.05	1.85±.05	calibers from base
s_g			5.6±0.1	Computed for standard 1:25 twist (ν = 0.25)
s_{d_0}			0.5±0.[illegible]	Without arming ball rotor and at small yaw (δ_g<2°)
$s_{d_0}(2-s_{d_0})$				
$\frac{1}{s_g}$				STABLE at small yaws w/o arming ball rotor. Usually UNSTABLE with arming ball rotor

APPENDIX VIII—B

20-MM HEI PROJECTILE, T282E1

AUTHOR(S) E. D. Boyer

REPORT BRL MR 813 (Ref. 78); BRL MR 916
DATE 1954 1955
TYPE OF TEST Free flight

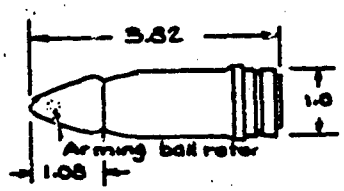

Dimensions, calibers

Muzzle
Weight, lb 0.216
Velocity, fps Variable
Spin rate, rps Variable
d, ft 0.0655
ν, rad/cal 0.209 or 0.251

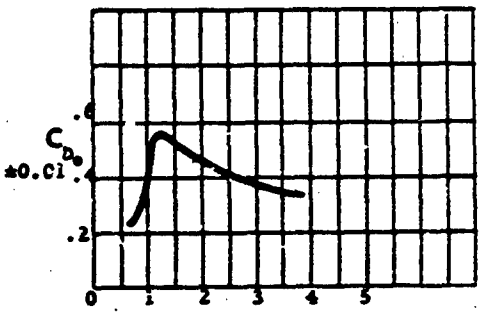

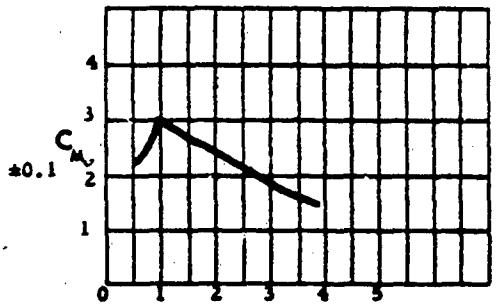

c.g. location from base, calibers 1.57

I_x, slug-ft^2 3.94×10^{-6} I_y, slug-ft^2 29.7×10^{-6}

k_x, cal .370 k_y, cal 1.015

	Subsonic	Transonic	Supersonic	Comments
M	0.98	1.15	2.4	
C_{D_0}	6.6 (estimated)		5.3±1.0	$1.4 \leq M \leq 3.6$
C_{L_α}	1.9±0.1	2.0±0.1	2.6±0.2	$C_{N_\alpha} - C_{D_0}$
C_{M_α}	see curve			
$C_{M_q}+C_{M_{\dot\alpha}}$	-4.8±0.6	-7.5±0.6	-3.8±1.1	-0.7±0.3 @ M= 3.5 -4.3±0.3 @ M= 3.5 w/o arming ball rotor
$C_{M_{p\alpha}}$	-0.20±0.04	0.07±0.04	0.16±0.07	
C_{l_p}	Not measured; assumed to be -0.01 in computations			
c.p. location	2.85±.05	2.70±.05	2.25±.05	calibers from base
s_g	1.75±.06	1.85±.07	2.6±.12	
s_{d_0}	0.15±.12	0.58±.10	1.25±.10	
$s_{u_0}(2-s_{u_0})$	0.26±.20	0.82±.08	0.93±.05	
$\frac{1}{s_g}$	0.57±.02 UNSTABLE	0.54±.02 STABLE	0.38±.02 STABLE	For large yaw ($\delta \leq 43°$) firings at M= 2.3 see E.T. Roecker, BRL MR 888, 1955.

APPENDIX VIII—C

DRAG VS TRUNCATION: CONICAL HEADS

AUTHOR(S) A. C. Charters and H. Stein

REPORT BRL R 624
DATE 1952
TYPE OF TEST Free flight

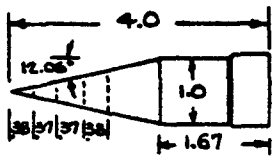

Dimensions, calibers

Muzzle
Weight, lb _____
Velocity, fps _____
Spin rate, rps _____
d, ft 0.0655
ν, rad/cal 0.25

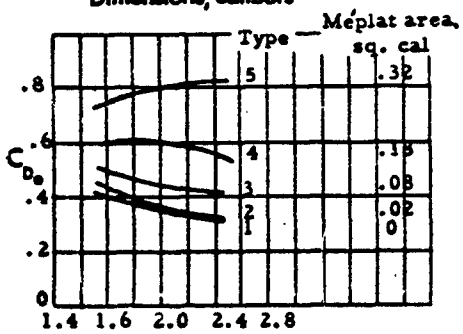

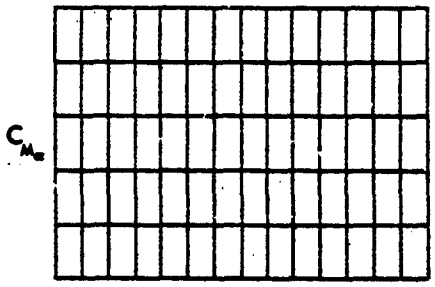

c.g. location from base, calibers _____

I_x, slug-ft^2 _____ I_y, slug-ft^2 _____

k_x, cal _____ k_y, cal _____

	Type 1	Type 2	Type 3	Type 4	Type 5	Comments
C_{D_0}	5.4±1.0	3.6±1.2	2.0 approx.	1.0 approx.	0 approx.	About 10 rounds of each type.
C_{L_α}						
C_{M_α}						
$C_{M_q}+C_{M_{\dot\alpha}}$						
$C_{M_{p\alpha}}$						
C_{l_p}						
c.p. location						
s_g						
s_{d_0}						
$s_{d_0}(2-s_{d_0})$						
$\frac{1}{s_g}$						

APPENDIX VIII—D

2.75-INCH ROCKET, T131

AUTHOR(S) L. C. MacAllister and W. K. Rogers

REPORT BRL MR 948
DATE 1955
TYPE OF TEST Free flight

INERT ROCKET

	Weight, lb	5.3
Muzzle	Velocity, fps	Variable
	Spin rate, rps	Variable
	d, ft	0.228
	ν, rad/cal	0.523

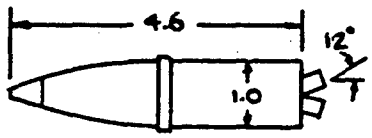

Dimensions, calibers

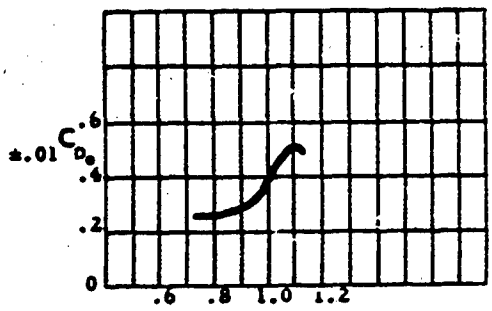

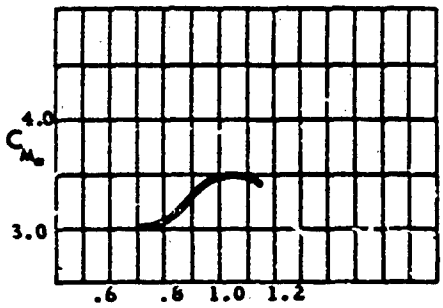

c.g. location from base, calibers 1.77±.01

I_x, slug-ft² .00123 I_y, slug-ft² .01425

k_x, cal 0.376 k_y, cal 1.19

Comments

M	0.85	1.0	1.15
C_{D_0}	5.8 approx.		
C_{L_α}	1.95±.05	2.0±.05	2.0±.08
C_{M_α}	3.15±.05	3.45±.08	3.45±0.1
$C_{M_q}+C_{M_{\dot\alpha}}$	-4.5±0.5	-7.5±1.0	-10±2
$C_{M_{p\alpha}}$	-0.23±0.1	-0.23±0.1	-0.07±0.07
C_{l_p}			
c.p. location			
s_g			
s_{d_0}			
$s_{d_0}(2-s_{d_0})$			
$\frac{1}{s_g}$			

At all 3 Mach nos.

calibers from base

(10d)

AUTHOR(S) E. D. Boyer

REPORT BRL MR 1475 (Ref. 79)
DATE 1963
TYPE OF TEST Free flight

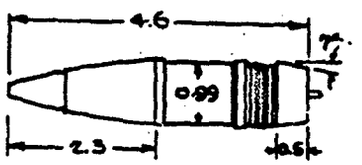

Dimensions, calibers

Muzzle	Weight, lb	23.41
	Velocity, fps	2700
	Spin rate, rps	285
	d, ft	0.295
	ν, rad/cal	0.196

Std

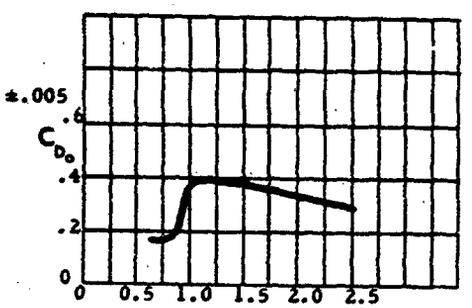

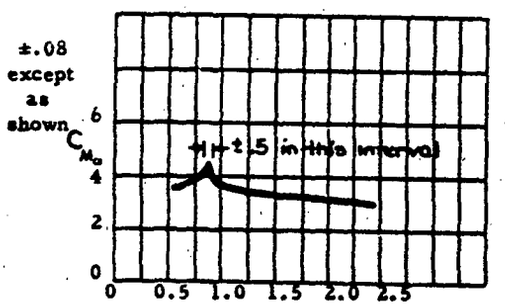

c.g. location from base, calibers 1.66

I_x, slug-ft^2 0.0087 I_y, slug-ft^2 0.0815

k_x, cal 0.369 k_y, cal 1.135

M	Subsonic 0.8	Transonic Peak 0.95	Supersonic 1.8	2.4	Comments
C_{D_0}			5.53±.15	5.17±.05	
C_{L_α}	1.5±0.15	1.4±0.5	2.35±0.05	2.55±0.05	
C_{M_α}	4.0±0.08	4.7±0.5*	3.55±0.08	3.30±0.08	Independent of yaw except in interval stated
$C_{M_q}+C_{M_{\dot\alpha}}$	-6±1	-7.5±1	-9±1	-8.5±1	At M = 1.05 $C_{M_q} + C_{M_{\dot\alpha}}$ = -5.5±2.5
$C_{M_{p\alpha}}$	-0.2±0.15	+0.2±0.15	+0.2±0.05	+0.2±0.05	At M = 1.05 $C_{M_{p\alpha}}$ = 0±0.2
C_{l_p}					
c.p. location	4.0±0.2	4.25±0.25	2.8±0.15	2.7±0.15	calibers from base
s_g	1.07±.02	0.92±.10	1.20±.03	1.30±.03	
s_{d_0}	0.0±0.47	0.85±.50	0.86±.16	0.92±.16	Increasing the twist of rifling to 25 cal/turn (ν = 0.251) stabilizes projectile over whole Mach no. range.
$s_{d_0}(2-s_{d_0})$	$0.0^{+0.72}_{-1.16}$	0.79±.21	0.95±.05	0.97±.03	
$\frac{1}{s_g}$	0.93±.02	1.10±.12	0.83±.02	0.77±.02	
	UNSTABLE	METASTABLE	STABLE	STABLE	

* Strongly dependent on yaw when $0.93 \leq M \leq 0.98$; $C_{M_\alpha} \approx 5.2 - 10\delta_g$

APPENDIX VIII—F

105-MM HE PROJECTILE, M1 (MODIFIED)*

AUTHOR(S) E. T. Roecker; E. D. Boyer

REPORT	BRL MR 929 (Ref. 85);	BRL MR 1144
DATE	1955	1958
TYPE OF TEST	Free flight	Free flight

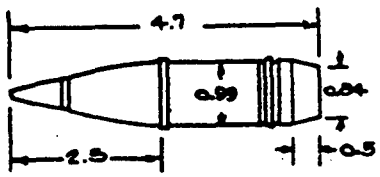

Dimensions, calibers

Muzzle	Weight, lb	32.12
	Velocity, fps	1510
	Spin rate, rps	220
	d, ft	0.344
	ν, rad/cal	0.314 at muzzle
	Rifling twist	20 cal/turn

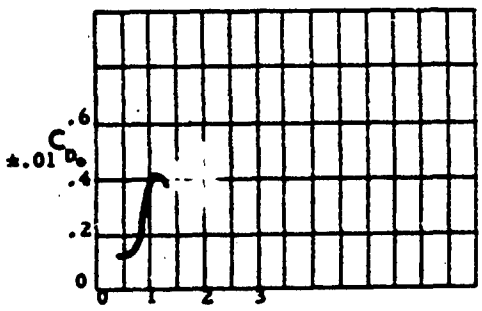

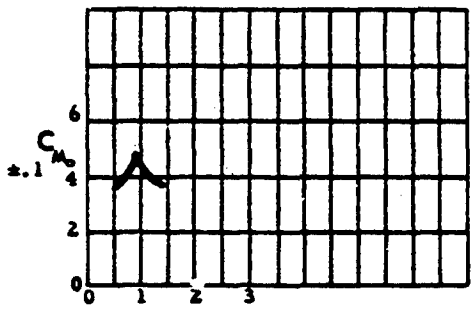

c.g. location from base, calibers 1.74 I_x, slug-ft² 0.017 I_y, slug-ft² 0.167

k_x, cal 0.380 k_y, cal 1.185

M	Subsonic 0.7	Transonic Peak 0.95	Supersonic 1.35	Comments
C_{D_0}	6.1±0.5		8.1±2.0	
C_{L_α}	1.6±0.2	2.0	1.9	
C_{M_α}	3.8±0.1	4.9±0.13	3.85±0.05	
$C_{M_q}+C_{M_{\dot\alpha}}$	-7.6±3.0	-12.7±3.5	-6.9±0.7	Varies markedly with yaw at subsonic and transonic speeds
$C_{M_{p\alpha}}$	-0.3±0.25	0.55±0.07	0.03±0.05	
C_{l_p}	Roecker		Boyer	
c.p. location	3.9±0.2	4.5±0.2	3.4	calibers from base
s_g	2.6±0.15	2.15±0.1	2.7	Subsonically, $C_{M_{p\alpha}}$ and s_{d_0} vary markedly with yaw. Projectile is dynamically unstable at yaws less than 3°.
s_{d_0}	0.15±0.47	0.94±0.14	0.63±0.16	
$s_{d_0}(2-s_{d_0})$	$0.28^{+0.57}_{-1.03}$	0.98±0.02	0.85±0.12	
$\frac{1}{s_g}$	0.38±0.02	0.47±0.02	0.37	
	See comment	STABLE	STABLE	

*The cylindrical body diameter was undercut by .03 inch to increase the yaw.

4.9-CALIBER PROJECTILE AT TRANSONIC SPEEDS

AUTHOR(S) L. E. Schmidt

REPORT BRL MR 824
DATE 1954
TYPE OF TEST Free flight

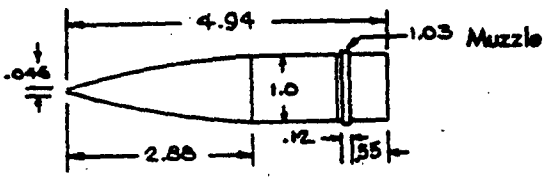

Dimensions, calibers

Weight, lb	42.5
Velocity, fps	Variable
Spin rate, rps	Variable
d, ft	0.341
ν, rad/cal	0.314

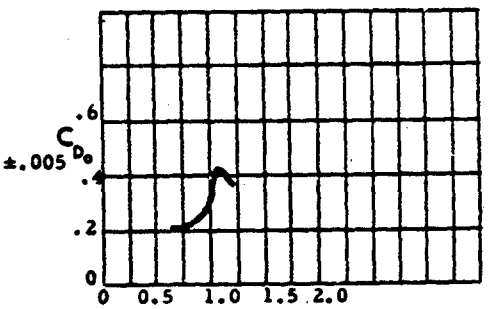

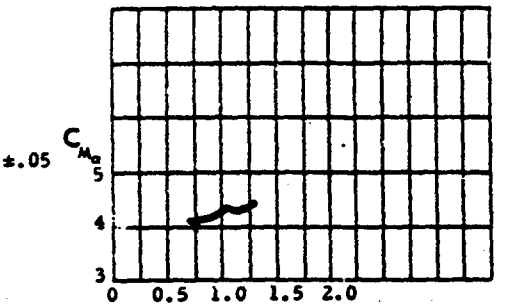

c.g. location from base, calibers 1.23 I_x, slug-ft^2 _____ I_y, slug-ft^2 _____

k_α, cal 0.345 k_p, cal 0.975

M	Subsonic 0.83	Transonic Peak 1.03	Supersonic 1.3	Comments
C_{D_0}		6.? (estimated)		Used over whole Mach no. range
C_{L_α}	2.3±0.1	2.1±0.1		
C_{M_α}	4.4±.04	4.7±.04	4.7±.04	
$C_{M_q}+C_{M_{\dot\alpha}}$	-1.8±0.8	-5.0±1.2	-3.5	
$C_{M_{p\alpha}}$	-0.4±.05	-0.1±0.1	-0.05	
C_{l_p}				
c.p. location	3.0±0.1	3.0±0.1	3.0±0.1	calibers from base
s_g	3.1±0.1	3.0±0.1	3.0±0.1	
s_{d_0}	-0.63±0.40	0.42±0.30	0.71	
$s_{d_0}(2-s_{d_0})$	-1.7±1.4	$0.66^{+0.26}_{-0.43}$	0.92	
$\frac{1}{s_g}$	0.32±.01	0.33±.01	0.33±.01	
	UNSTABLE	METASTABLE	STABLE	

APPENDIX VIII—H

90-MM HE PROJECTILE, T91

AUTHOR(S) L. C. MacAllister

REPORT BRL MR 990 (Ref. 83)
DATE 1956
TYPE OF TEST Free flight

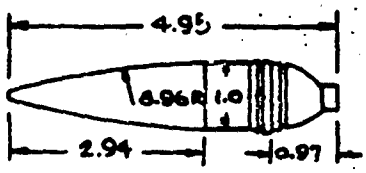

Dimensions, calibers

Muzzle	Weight, lb	18.64
	Velocity, fps	Variable
	Spin rate, rps	Variable
	d, ft	0.292
	ν, rad/cal	0.25

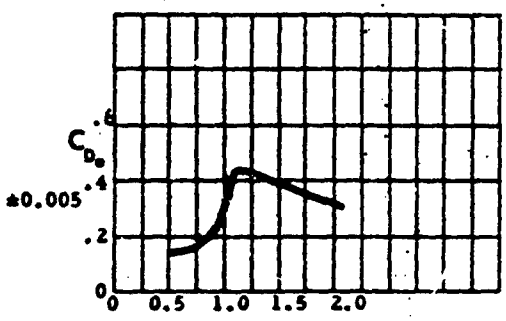

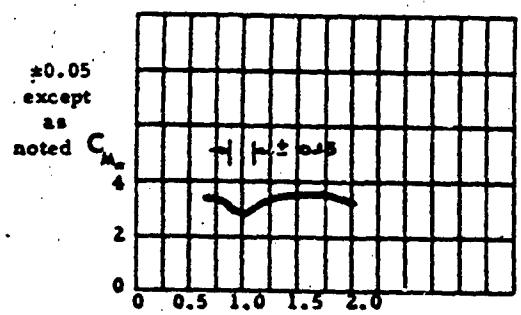

c.g. location from base, calibers 1.95 I_x, slug-ft² 0.0068 I_y, slug-ft² 0.0645

k_x, cal 0.370 k_y, cal 1.14

M	Subsonic 0.7	Transonic 0.95	Supersonic 1.8	Comments
C_{D_0}				Values shown are for tracer not ignited. With tracer ignited, C_{D_0} is reduced about 6%; C_{M_α} is not changed very much; dynamic stability is improved.
C_{L_α}	2.1±0.1	2.7±0.2	2.1±0.1	
C_{M_α}				
$C_{M_q}+C_{M_{\dot\alpha}}$	18±1.1	8±1.5	-6.5±1.0	
$C_{M_{p\alpha}}$	-1.0±0.15	-0.9±0.3	-0.2±0.15	
C_{l_ν}				
c.p. location	3.65±.05	3.35±.15	3.55±.05	calibers from base
s_g				Coefficients vary with yaw. See BRL TN 1119 (Ref. 84) for data on variation.
s_{d_0}				
$s_{d_0}(2-s_{d_0})$				Tracer off--UNSTABLE at all Mach nos. tested (0.6 ≤ M < 2.0)
$\frac{1}{s_g}$				Tracer on--UNSTABLE 0.6<M≤1.6; STABLE above M = 1.6.

APPENDIX VIII—I

EFFECTS OF HEAD SHAPE VARIATION

AUTHOR(S) E. R. Dickinson

REPORT BRL MR 838 (Ref. 24)
DATE 1954
TYPE OF TEST Free flight

Weight, lb
Velocity, fps 2720
Spin rate, rps
d, ft .0416

M = 2.44

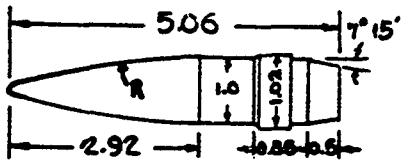

Dimensions, calibers

c.g. location from base, calibers various

						Comments
R	9.47	14.20	18.94	37.88	∞	calibers
R/R_T	1.0	1.5	2.0	4.0	∞(cone)	
C_{D_0}	.235±.007	.210±.006	.205±.005	.210±.005	.217±.005	$C_{D_{0B}}$ = 10.0 for all types
C_{L_α}	2.8±0.1	2.7±0.1	2.65±0.1	2.55±0.1	2.5±0.1	All values are at M = 2.44
c.p. location	3.05±.05	2.93±.05	2.82±.03	2.71±.03	2.57±.05	calibers from base

R_T is the radius of a tangent ogive, in calibers.
For this projectile R_T = 9.47 calibers.

APPENDIX VIII—J

120-MM HE PROJECTILE, M73

AUTHOR(S) H. P. Hitchcock

REPORT BRL R 569
DATE 1945
TYPE OF TEST Free Flight

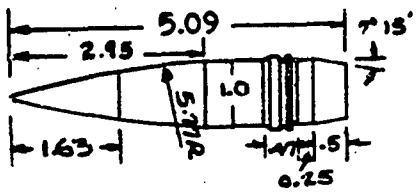

Dimensions, calibers

Muzzle Weight, lb	50 (approx.)
Velocity, fps	3010
Spin rate, rps	256
d, ft	0.392
ν, rad/cal	0.209

M.T. M61 Fuze

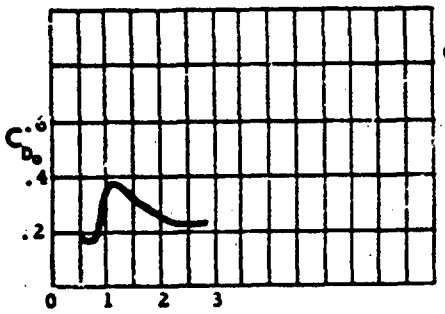

Computed from G_2 drag function

Form factor = 0.89

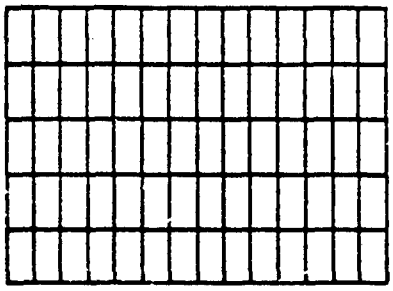

c.g. location from base, calibers _____ I_x, slug-ft^2 _____ I_y, slug-ft^2 _____

k_σ, cal _____ k_f, cal _____

	Subsonic	Transonic Peak	Supersonic	Comments
M			1.2±0.17	
C_{D_0}				
C_{L_α}				
C_{M_α}				
$C_{M_q}+C_{M_{\dot\alpha}}$				
$C_{M_{p\alpha}}$				
C_{l_p}			-0.0125±.0008	Determined by averaging over time intervals as long as 60 sec.
c.p. location				calibers from base
s_g				
s_{d_0}				
$s_{d_0}(2-s_{d_0})$				
$\frac{1}{s_g}$				

CONE CYLINDER

AUTHOR(S) L. E. Schmidt

REPORT BRL MR 759 (Ref. 52)
DATE 1954
TYPE OF TEST Free flight
Type 21 - solid bronze

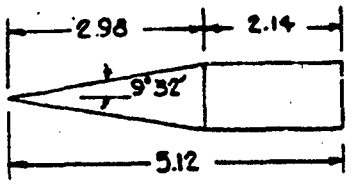

Dimensions, calibers

Muzzle
Weight, lb 0.382
Velocity, fps Variable
Spin rate, rps Variable
d, ft .0655 20mm
ν, rad/cal 0.25

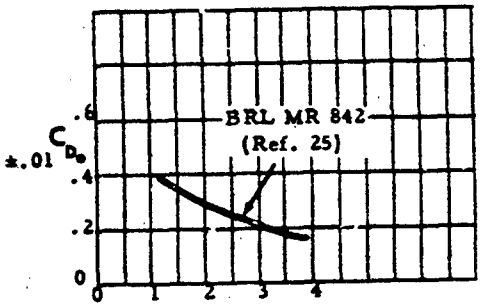

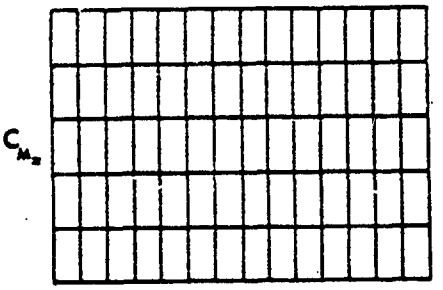

c.g. location from base, calibers 1.65

I_x, slug-ft^2 5.55×10^{-6} I_y, slug-ft^2 57.2×10^{-6}

k_x, cal 0.330 k_y, cal 1.06

	Subsonic	Transonic	Supersonic		
M	0.8	1.25	1.9	2.3	
C_{D_0}					
C_{N_α}	2.3±0.06	2.6±0.06	2.7±0.1	2.9±0.06	
C_{M_α}	2.5±0.03	2.75±0.02	2.3±0.04	2.3±0.02	
$C_{M_q}+C_{M_{\dot\alpha}}$	-0.3±3.1*	-9.0	-4.8	-6.0 (from curve)	
$C_{M_{p\alpha}}$	-0.7±0.1	+0.25	+0.05	0 (from curve)	
C_{l_p}					
c.p. location	2.7±.05	2.75±.05	2.5±.05	2.45	calibers from base
s_g	2.86	2.75	3.24	2.33	
s_{d_0}		0.87	0.87	0.68	Computed from curve data
$s_{d_0}(2-s_{d_0})$		0.98	0.98	0.90	
$\frac{1}{s_g}$		0.36	0.31	0.43	
	UNSTABLE	STABLE	STABLE	STABLE	

* Positive values of $C_{M_q}+C_{M_{\dot\alpha}}$ are reported for 3 rounds.

(107)

APPENDIX VIII—1

EFFECT OF BOATTAILING ON C_{D_o}

AUTHOR(S) E. R. Dickinson

REPORT BRL MR 842 (Ref. 25)
DATE 1954
TYPE OF TEST Free flight

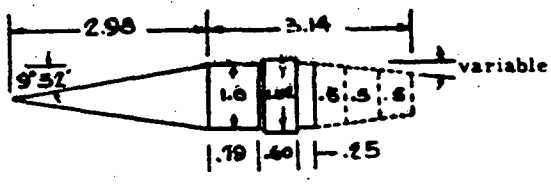

Dimensions, calibers

PART I

Effect of adding to length of projectile, and diminishing the area of the base, by adding boattail.

d = .0417 ft

Boattail Angle	Square Base	Boattail Length, calibers 0.5	1.0	1.5
	C_{D_o} at M = 1.2			
0°	0.42			
4°		0.372	0.350	0.330
7°15'		0.376	0.340	0.324
9°		0.39	0.35	0.345*
	C_{D_o} at M = 1.8			
0°	0.32			
4°		0.288	0.276	0.257
7°15'		0.298	0.270	0.261
9°		0.31	0.275	0.27*
	C_{D_o} at M = 2.4			
0°	0.26			
4°		0.254	0.220	0.220
7°15'		0.246	0.22	0.22
9°		0.25	0.225	0.22*

The C_{D_o} values shown were read from the curves in MR 842. The scatter of the observations averaged about ±0.005. Variation in surface finish, by affecting the boundary layer transition, may account for much of the scatter.

*The 9°, 1.5 caliber boattail was a dynamically unstable configuration; these data are for a 9°, 1.25 caliber boattail.

AUTHOR(S) E. R. Dickinson

REPORT BRL MR 842 (Ref. 25)
DATE 1954
TYPE OF TEST Free flight

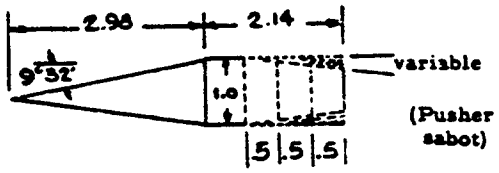

Dimensions, calibers

PART II

Effect of increasing the length of the boattail, and diminishing the area of the base, while keeping the overall length of the projectile constant.

d = .0655 ft = 20mm

Boattail Angle	Square Base	Boattail Length, calibers 0.5	1.0	1.5
	C_{D_o} at M = 2.4			
0°	0.256			
4°		0.243	0.224	
7°		0.237	0.216	0.207
	C_{D_o} at M = 3.2			
0°	0.208			
4°				
7°		0.19*	0.179	0.169
	C_{D_o} at M = 4.0			
0°	0.172			
4°				
7°		0.165*	0.151	0.144

The C_{D_o} values shown were read from the curves in MR 842. The scatter of the observations averaged about ±0.003.

Estimated effect of adding a driving band (rotating ring) is to add 0.01, or less, to the values shown assuming that the band does not extend to within less than 0.25 calibers of the boattail.

*These values were read from an interpolated curve.

APPENDIX VIII—M

EFFECT OF BOATTAIL ON C_{D_0} AT M = 2.44

AUTHOR(S) T. Hailperin

REPORT BRL MR 347 (Ref. 26)
DATE 1945
TYPE OF TEST Free flight

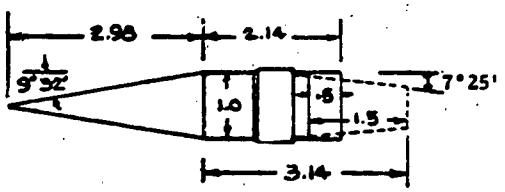

Dimensions, calibers

d = 0.0417 ft

M = 2.44

Base Area	Square Base	Boattail Length, calibers 0.5	1.5
Frontal Area	1.0	0.76	0.39
C_{D_0}	0.263 ±.027	0.248 ±.004	0.228 ±.005
C_{D_0}/A	6.7	5.1	4.5

APPENDIX VIII—N

90-MM MODEL OF 175-MM PROJECTILE, T203

AUTHOR(S) B. G. Karpov, K. S. Krial and B. Hull

REPORT BRL MR 956
DATE 1955
TYPE OF TEST Free flight

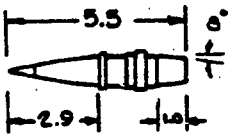

Dimensions, calibers

Muzzle	Weight, lb	21.82
	Velocity, fps	Variable
	Spin rate, rps	Variable
	d, ft	0.295
	ν, rad/cal	0.196 (For standard 175mm gun, ν = 0.314)

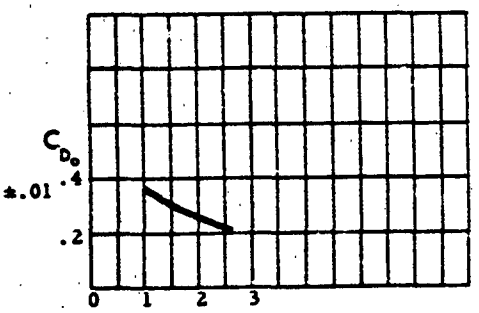

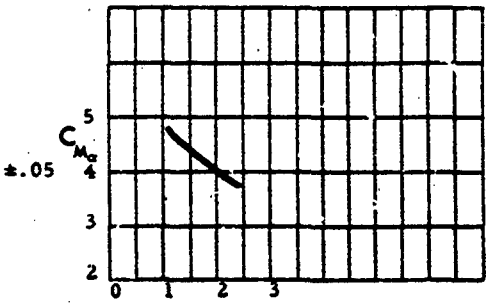

c.g. location from base, calibers 1.94

I_x, slug-ft² .0075 I_y, slug-ft² .0535

k_x, cal 0.356 k_y, cal 0.952

	Transonic		Supersonic	Comments
M	1.15	1.65	2.6	
C_{D_0}	5.8	5.8	5.8	
C_{L_α}	1.4±.08	3.0±.05	3.5±.05	
C_{M_α}	4.75±.05	4.3	3.75	
$C_{M_q}+C_{M_{\dot\alpha}}$	-7.8	-8.0	-6.7±.35	
$C_{M_{p\alpha}}$	0.28±.15	0.28	0.19±.04	
C_{l_p}				
c.p. location	4.7	3.25	2.95	calibers from base
s_g	1.48	1.65	1.90	calculated with ν = 0.314
s_{d_0}				Projectile is dynamically stable over this range of Mach numbers when fired from a gun with 1:20 twist (ν = 0.314).
$s_{d_0}(2-s_{d_0})$				
$\frac{1}{s_g}$				

AUTHOR(S) B. G. Karpov, K. S. Krial and B. Hull

REPORT BRL MR 956
DATE 1955
TYPE OF TEST Free flight

Muzzle
Weight, lb 21.21
Velocity, fps Variable
Spin rate, rps Variable
d, ft 0.295
ν, rad/cal 0.196 or 0.251

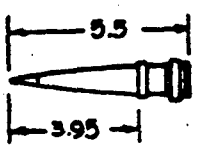

Dimensions, calibers

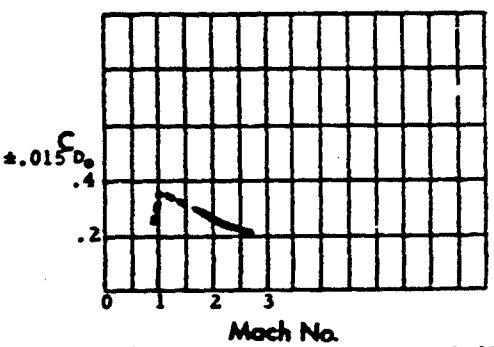

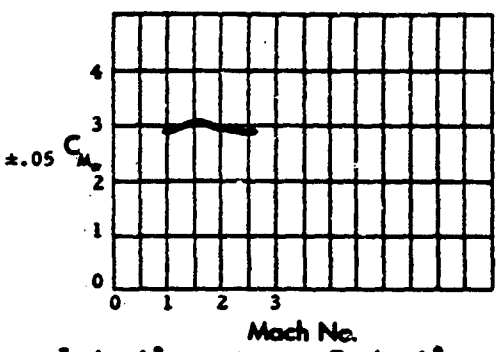

c.g. location from base, calibers 1.85

I_x, slug-ft^2 .0066 I_y, slug-ft^2 .094

k_σ, cal 0.340 k_t, cal 1.065

	Supersonic			Comments
M	1.2	1.6	2.6	
$C_{D_{\nu^2}}$	5.8	5.8	5.8	
C_{L_α}	2.3	2.95	3.5	
C_{M_α}	3.0	3.1±.05	2.8±.02	
$C_{M_q}+C_{M_{\dot\alpha}}$	-9.3	-9.7±0.1	-9.5	
$C_{M_{p\alpha}}$	0.18	0.18	0.16±.05	
C_{l_p}				
c.p. location	2.98	2.80	2.60	calibers from base
s_g	2.37	2.30	2.52	calculated with ν = 0.314
s_{d_0}				Projectile is dynamically stable over this range of Mach numbers when fired from a gun with 1:20 twist (ν = 0.314).
$s_{d_0}(2-s_{d_0})$				
$\frac{1}{s_g}$				

7.2-INCH SPINNER ROCKET, T99

AUTHOR(S) T. Hailperin

REPORT BRL R 572
DATE 1945
TYPE OF TEST Free flight

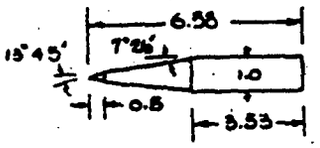

Muzzle	Weight, lb	
	Velocity, fps	1300
	Spin rate, rps	1980
	d, ft (model)	0.0655
	ν, rad/cal	0.63

Dimensions, calibers

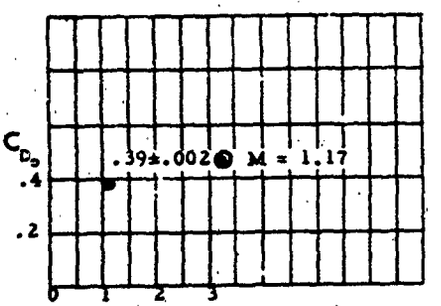

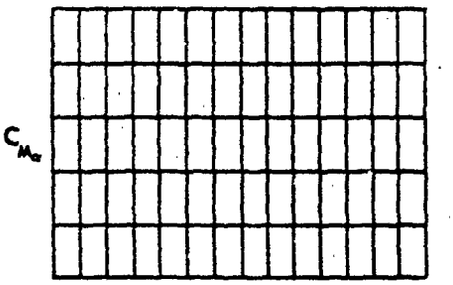

c.g. location from base, calibers various

I_x, slug-ft^2 _____ I_y, slug-ft^2 _____

k_x, cal _____ k_y, cal _____

	Subsonic	Transonic Peak	Supersonic	Comments
M			1.17	
C_{D_0}			9.4±0.5	
C_{L_α}			2.7±0.03	
C_{M_α}				
$C_{M_q}+C_{M_{\dot\alpha}}$				
$C_{M_{p\alpha}}$				
C_{l_p}			-0.025	
c.p. location			3.84	calibers from base
s_g				
s_{d_0}				
$s_{d_0}(2-s_{d_0})$				
$\frac{1}{s_g}$				

APPENDIX VIII—P

5-CALIBER A-N SPINNER ROCKET

AUTHOR(S) C. H. Murphy and L. E. Schmidt

REPORT BRL R 876 (Ref. 49)
DATE 1953
TYPE OF TEST Free flight
Intermediate c.g. location

Muzzle	Weight, lb	Variable
	Velocity, fps	Variable
	Spin rate, rps	Variable
	d, ft	.0655
	ν, rad/cal	

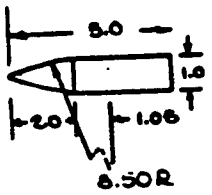

Dimensions, calibers

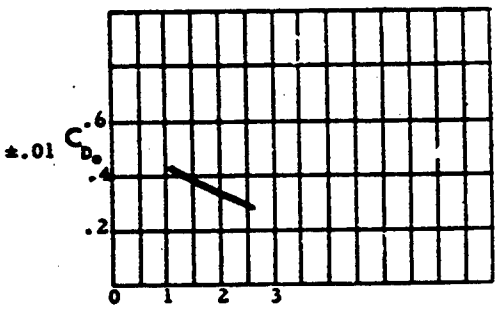

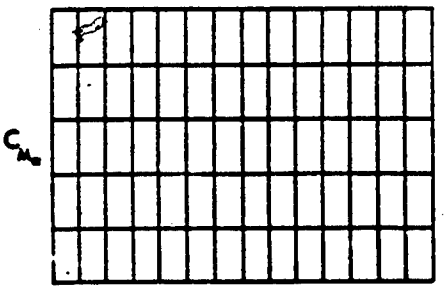

c.g. location from base, calibers 1.96 I_x, slug-ft^2 _____ I_y, slug-ft^2 _____

k_σ, cal 0.340 k_β, cal 1.19

	Supersonic			Comments
M	1.3	1.8	2.5	
C_{D_0}	7.9±1.5	6.6±2.3	6.9±8.4	
C_{L_α}	2.1±0.1	2.5±0.1	2.9±0.15	
C_{M_α}	3.95±.05	3.80±.05	3.35±.05	
$C_{M_q}+C_{M_{\dot\alpha}}$	-13.5±1.5	-12.5±0.5	-11.5	
$C_{M_{p\alpha}}$	0.43±.06	0.19±.08	0.19	
C_{l_p}	-.013±.001	-.011±.001	-.010±.001	
c.p. location	3.5±0.1	3.3±0.1	3.0±0.1	calibers from base
$C_{N_{p\alpha}}$	-0.35	-0.30	-0.15	approximate
s_{d_0}				
$s_{d_0}(2-s_{d_0})$				
$\frac{1}{s_d}$				

(N4)

7-CALIBER A-N SPINNER ROCKET

AUTHOR(S) L. E. Schmidt and C. H. Murphy

REPORT BRL MR 775 (Ref. 53)
DATE 1954
TYPE OF TEST Free flight
Type 2 model: intermediate c.g. location

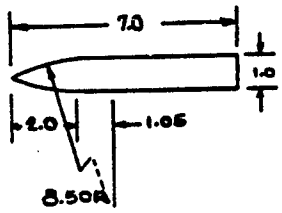

Dimensions, calibers

Muzzle	Weight, lb	0.33
	Velocity, fps	Variable
	Spin rate, rps	Variable
	d, ft	.0655 = 20mm
	ν, rad/cal	0.63

(Pusher sabot)

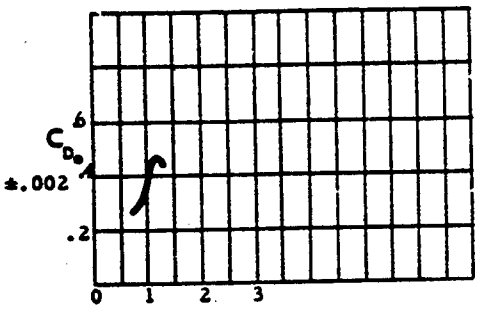

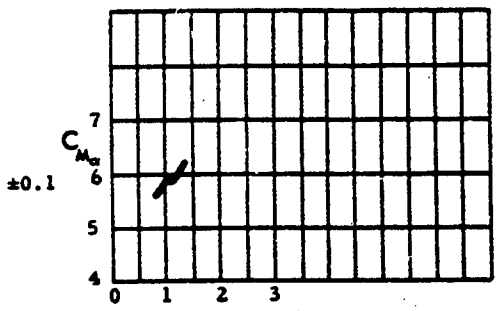

c.g. location from base, calibers 2.96

I_x, slug-ft^2 5.76×10^{-6} I_y, slug-ft^2 95.5×10^{-6}

k_σ, cal 0.364 k_t, cal 1.48

M	Subsonic 0.8	Transonic Peak 1.01	Supersonic 1.28	Comments
C_{D_0}	6.6±1.3	7.1±0.8		
C_{L_α}	2.0±0.05	2.0±0.1	2.2	
C_{M_α}	5.2±0.1	5.7±0.1	6.2	
$C_{M_q}+C_{M_{\dot\alpha}}$	-21±1	-19±1	-25	
$C_{M_{p\alpha}}$	-0.40±.05	-0.35±0.1	+0.40	Change due mainly to change in magnus c.p.
C_{l_p}	-0.024±.0005	-0.021±.001	-0.019	
c.p. location	5.4±.05	5.35±.05	5.3	calibers from base
s_g	6.0±0.1	5.6±0.1	5.0	*Moving the c.g. forward 0.8 calibers makes this shape stable at Mach numbers greater than 0.9.
s_{d_0}	-0.26	-0.20±0.13	0.78	
$s_{d_0}(2-s_{d_0})$	-0.59	-0.46±0.31	0.95	
$\frac{1}{s_g}$	0.17 UNSTABLE	0.18 UNSTABLE*	0.20 STABLE	

APPENDIX VIII—R

7-CALIBER A-N SPINNER ROCKET

AUTHOR(S) C. H. Murphy and L. E. Schmidt

REPORT BRL R 876 (Ref. 49)
DATE 1953
TYPE OF TEST Free flight
Intermediate c.g. location

Weight, lb	Variable
Muzzle Velocity, fps	Variable
Muzzle Spin rate, rps	Variable
d, ft	0.655
ν, rad/cal	

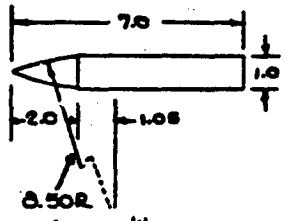

Dimensions, calibers

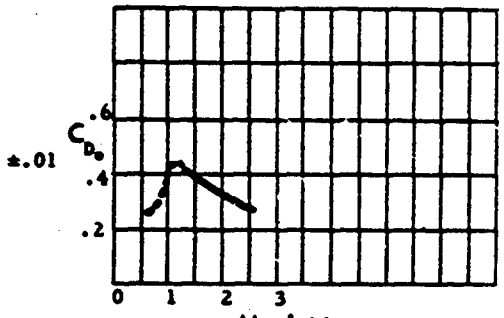

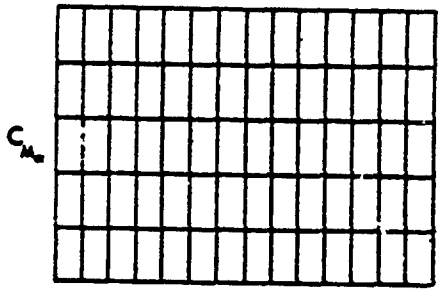

c.g. location from base, calibers 2.96

I_x, slug-ft^2 _____ I_y, slug-ft^2 _____

k_x, cal 0.345 k_y, cal 1.74

Solid dural model

	Supersonic			Comments
M	1.3	1.8	2.5	
C_{D_0}[a]	12.0±4.5	6.6±1.5	6.9±2.3	
$C_{L\alpha}\|_{\alpha=0}$	2.2±0.15	2.5±0.1	2.8±0.1	$C_{L\alpha} = C_{L\alpha}\|_0 + b\delta^2$
C_{M_α}	6.2±.05	6.8±.05	6.6±.05	M = 1.3, 1.8, 2.5; b = 45, 26, 110
$C_{M_q}+C_{M_{\dot\alpha}}$	-26±0.5	-31.5±1.0	-33±0.5	
$C_{M_{p\alpha}}$	0.40±.08	0.50±0.12	0.70±.05	
C_{l_p}	-.019±.001	-.016±.001	-.014±.001	
c.p. location	5.4±0.1	5.4±0.15	5.15±0.05	calibers from base
$C_{N_{p\alpha}}$	-0.50	-0.50	-0.40	approximate
s_{d_0}				
$s_{d_0}(2-s_{d_0})$				
$\frac{1}{s_g}$				

All test rounds were dynamically stable; $s_g \geq 1.5$.

N6

9-CALIBER A-N SPINNER ROCKET

AUTHOR(S) C. H. Murphy and L. E. Schmidt

REPORT BRL R 876 (Ref. 49)
DATE 1953
TYPE OF TEST Free flight
Intermediate c.g. location

Muzzle
Weight, lb — Variable
Velocity, fps — Variable
Spin rate, rps — Variable
d, ft ____
ν, rad/cal ____

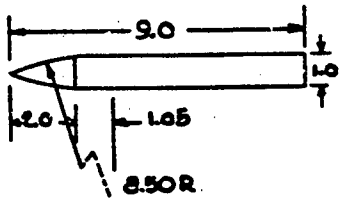

Dimensions, calibers

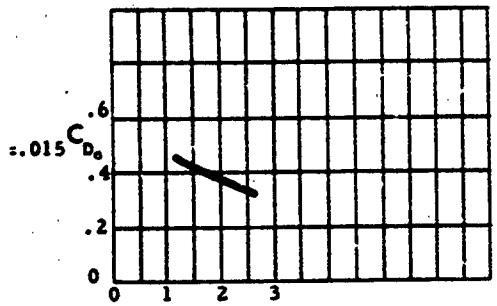

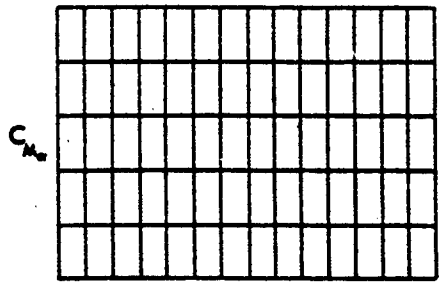

c.g. location from base, calibers 3.95

I_x, slug-ft^2 ____ I_y, slug-ft^2 ____

k_x, cal 0.347 k_y, cal 2.30

Homogeneous models

Comments

M	1.3	1.8	2.5
C_{D_0}	8.6±3.0	5.9±2.3	7.4±7.5
$C_{L_\alpha}\|_{\alpha=0}$	2.3	2.6	2.9
$C_{M_\alpha}\|_{\alpha=0}$	8.5	9.5	10.0
* $C_{M_q}+C_{M_{\dot\alpha}}$	-50±3	-72±4	-74±8
$C_{M_{p\alpha}}\|_{\alpha=0}$	0.5	1.0	1.0
C_{l_p}	-.024±.001	-.021±.001	-.018±.002
c.p. location	7.05±.05	7.1±.05	7.1±0.1 calibers from base
s_g			
s_{d_0}	1.14	1.40	1.35
$s_{d_0}(2-s_{d_0})$	0.98	0.84	0.88

Based on zero yaw values

$C_{L_\alpha} = C_{L_\alpha}|_{\alpha=0} + b\delta^2$

M =	1.3	1.8	2.5
b =	42	60	76
a =	-85	-150	-142

$C_{M_\alpha} = C_{M_\alpha}|_{\alpha=0} + a\delta^2$

$C_{M_{p\alpha}} = C_{M_{p\alpha}}|_{\alpha=0} + 40\delta^2$

$\frac{1}{s_g}$ Dynamically stable (at zero yaw) at all 3 Mach nos. when $s_g > 1.2$.

*$C_{M_q}+C_{M_{\dot\alpha}}$ is also a function of yaw, increasing in magnitude.

APPENDIX VIII—8

10-CALIBER CONE CYLINDER

AUTHOR(S) E. D. Buyer

REPORT BRL MR 1258 (Ref. 37)
DATE 1960
TYPE OF TEST Free flight
Forward c.g. configuration

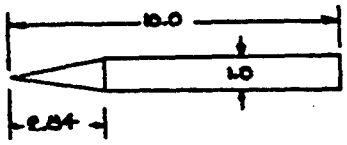

Dimensions, calibers

Muzzle	Weight, lb	0.535
	Velocity, fps	Variable
	Spin rate, rps	Variable
	d, ft	.0655 = 20mm
	ν, rad/cal	0.63

Pusher sabot

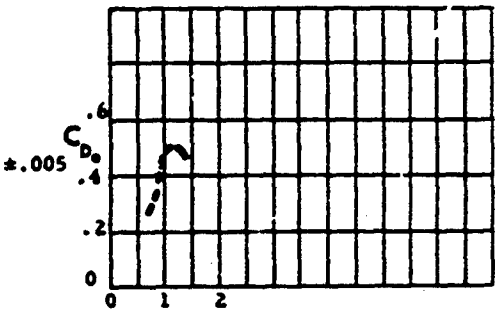

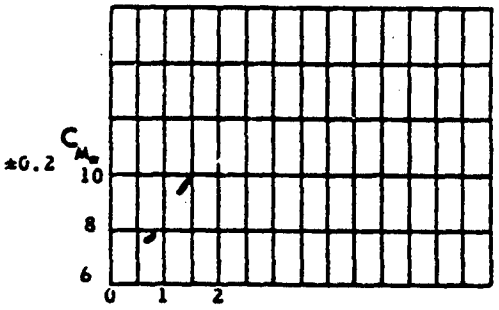

c.g. location from base, calibers 3.752

I_x, slug-ft^2 9.3×10^{-6} I_y, slug-ft^2 2.8×10^{-4}

k_x, cal 0.361 k_y, cal 1.98

	Subsonic	Transonic Peak	Supersonic	Comments
M	0.8		1.3	
C_{D_0}	5.88		11.2 (estimated)	
C_{L_α}	2.3±0.15		2.3±0.15	$C_{N_\alpha} - C_{D_0}$
C_{M_α}	7.85±0.2		9.15±0.2	
$C_{M_q}+C_{M_{\dot\alpha}}$	-42±5		-45±5	$C_{M_{p\alpha}} = C_{M_{p\alpha}}\|_{\alpha=0} + b_{p\alpha}\delta_\alpha^2$
$C_{M_{p\alpha}}\|_{\alpha=0}$	-0.9±0.1		-0.4±0.1	M = 0.8, $b_{p\alpha}$ = 250; M = 1.3, $b_{p\alpha}$ = 340
C_{l_p}	-.032±.0005		-.027±.0005	
c.p. location	6.8±0.2		7.0±0.2	calibers from base
s_g	3.6±0.1		3.0±0.05	
s_{d_0}	-0.75±0.23		-0.13±0.15	calculated at zero yaw
$s_{d_0}(2-s_{d_0})$	-2.1±0.8		-0.30±0.34	
$\frac{1}{s_g}$	UNSTABLE at yaws less than 5°		0.33 UNSTABLE at small yaws	

APPENDIX VIII—T

105-MM HEAT PROJECTILE, T171 (MODIFIED)*

AUTHOR(S) M. J. Fiddington

REPORT BRL MR 1215 (Ref. 91)
DATE 1959
TYPE OF TEST Free flight

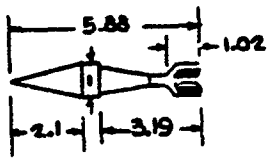

Dimensions, calibers

Muzzle
Weight, lb 17.54
Velocity, fps Variable
Spin rate, rps Variable
d, ft 0.344
ν, rad/cal

Six-finned, end-plated tail

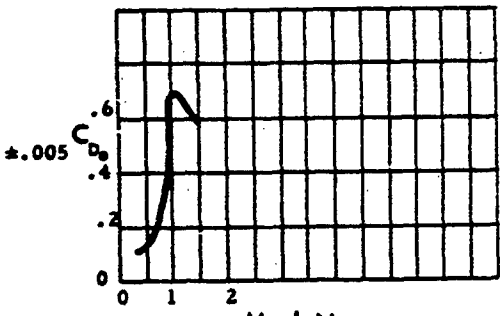

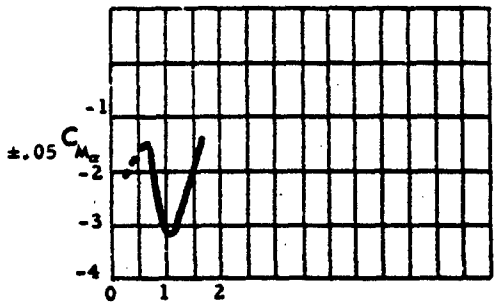

c.g. location from base, calibers 3.22

I_x, slug-ft² 0.0072 I_y, slug-ft² 0.088

k_σ, cal 0.341 k_η, cal 1.17

	Subsonic	Transonic	Supersonic	Comments
M				
C_{D_0}				
C_{L_α}		2.5±0.2	No significant variation with Mach number	5 rounds
C_{M_α}				
$C_{M_q}+C_{M_{\dot\alpha}}$		-28±7.5		14 rounds
$C_{M_{p\alpha}}$				
C_{l_p}				
c.p. location				calibers from base
s_g				Static instability ($C_{M_\alpha} > 0$) is to be expected at about M = 2.
s_{d_0}				
$s_{d_0}(2-s_{d_0})$				The size of the yaw for the rounds tested ranged from about 0.5° to 4°.
$\frac{1}{s_g}$				

*Modified by eliminating the wrench slots in the forward section of the nose.

(119)

APPENDIX VIII—U

60-MM MORTAR PROJECTILE, T24

AUTHOR(S) E. D. Boyer

REPORT BRL MR 1020 (Ref. 87)
DATE 1956
TYPE OF TEST Free flight

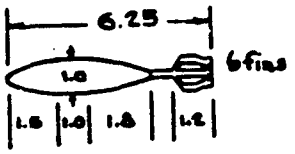

Dimensions, calibers

Muzzle
Weight, lb 4.05
Velocity, fps 500
Spin rate, rps Variable (less than 1 rps)
d, ft 0.197
ν, rad/cal

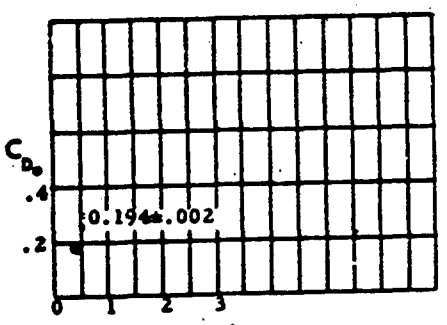

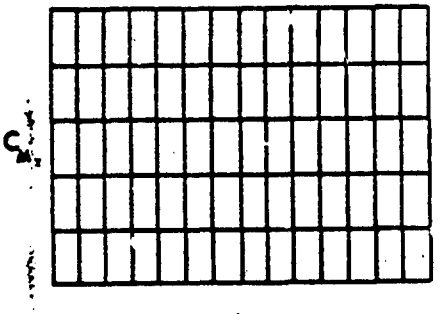

c.g. location from base, calibers 3.81

I_x, slug-ft² 5.9×10^{-4} I_y, slug-ft² 93.5×10^{-4}

k_x, cal 0.347 k_y, cal 1.38

	Subsonic	Transonic Peak	Supersonic	Comments
M				
C_{D_0}	5.3±1.0			
C_{L_α}	2.3±0.1			$C_{L_{\delta^2}}$ = 45 ± 13
C_{M_α}	-2.1±0.05			$C_{M_{\delta^2}}$ = -25 ± 5
$C_{M_q}+C_{M_{\dot\alpha}}$	-20 (approx.)			
$C_{M_{p_a}}$				
C_{l_p}				
c.p. location				calibers from base
s_g				
s_{d_0}				
$s_{d_0}(2-s_{d_0})$				
$\frac{1}{s_g}$				

Based on 5 rounds with no fin cant, and 7 rounds with the aft sections of the fins canted. No apparent effect of cant (up to 4°) on drag, lift or pitching moment.

AUTHOR(S) M. J. Piddington

REPORT BRL MR 1354
DATE 1961
TYPE OF TEST Free flight

8-bladed tail

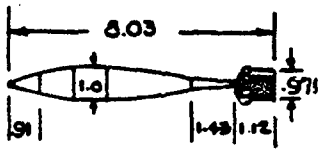

Dimensions, calibers

Muzzle Weight, lb	23.35
Muzzle Velocity, fps	925
Muzzle Spin rate, rps	Variable
d, ft	0.344
ν, rad/cal	0.08
	0.13
	0.16

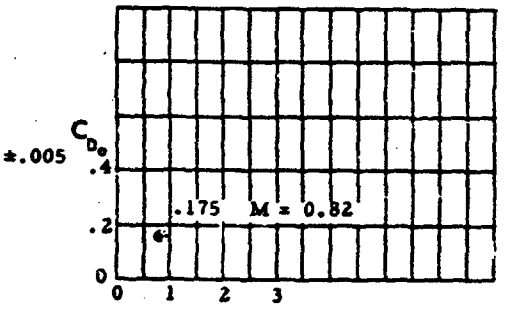

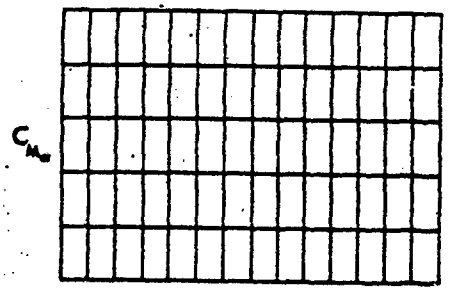

c.g. location from base, calibers 4.87

I_x, slug-ft² 0.011 I_y, slug-ft² 0.253

k_x, cal 0.345 k_y, cal 1.64

	Subsonic	Transonic Peak	Supersonic	Comments
M	0.82			
C_{D_0}	7 ± 2			
C_{L_α}	3.0 ± 0.2			
$C_{M_\alpha}\|_0$	-3.5 ± 0.1 at zero spin			$C_{M_\alpha} = C_{M_\alpha}\|_0 - 4.2\nu$
$C_{M_q}+C_{M_{\dot\alpha}}$	-55 ± 5			
$C_{M_{p\alpha}}\|_0$	-1.4 ± 0.3 at zero spin and yaw			$C_{M_{p\alpha}} = C_{M_{p\alpha}}\|_0 - 25\nu + 385\delta_e^2$
C_{l_p}				
c.p. location	= 0.08	= 0.16		calibers from base
s_g	-0.045±.001	-0.165±.005	at zero yaw	δ_e^2 = effective squared yaw
s_{d_0}	-2.25±.43	-3.70±.57	at zero yaw	For stability at nearly zero yaw, ν should not exceed 0.11 (45 rps at V = 900 fps)
$s_{d_0}(2-s_{d_0})$	-9.75±2.8	-21.4±5.4	at zero yaw	
$\frac{1}{s_g}$	-22.2±0.5	-6.05±0.2	at zero yaw	(Computed from coefficients tabulated above)
	STABLE	UNSTABLE (but STABLE at about δ_e = .094 rad = 5.5°)		

APPENDIX VIII—W

57-MM HEAT PROJECTILE, T188E18

AUTHOR(S) C. P. Sabin

REPORT BRL MR 1112 (Ref. 35)
DATE 1957
TYPE OF TEST Free flight

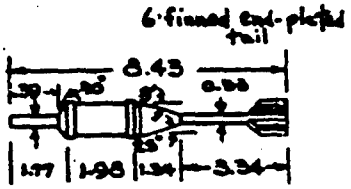

Muzzle	Weight, lb	2.75
	Velocity, fps	1200
	Spin rate, rps	6 ± 1
	d, ft	0.187
	ν, rad/cal	

Dimensions, calibers

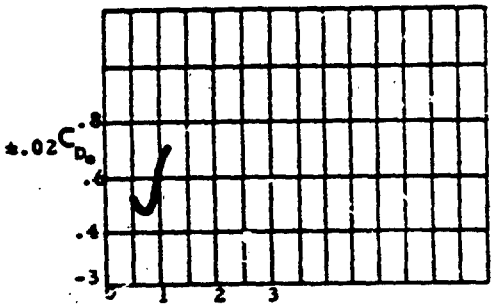

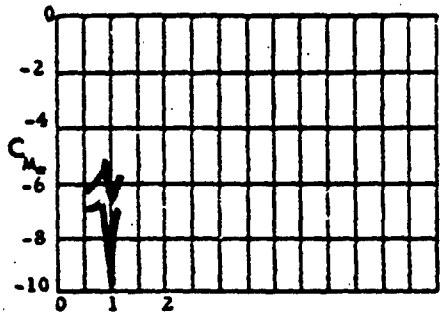

c.g. location from base, calibers 4.95 I_x, slug-ft² .00035 I_y, slug-ft² .0103

k_x, cal 0.343 k_y, cal 1.86

M	Subsonic 0.8	Transonic 0.95	Transonic 1.06	Comments
C_{D_0}	10.0			0.5 ≤ M ≤ 1.07
C_{L_α}	2.8 ± 0.8	3.6 ± 1.2	3.1 ± 0.3	
C_{M_α}	-6.4±0.3	-8.5±1.5	-6.0±0.3	The large variation in C_{M_α} may be due to yaw and to dual flow.
$C_{M_q}+C_{M_{\dot\alpha}}$	-70±10	-62±9	-75±8	
$C_{M_{p\alpha}}$				
C_{l_p}			-0.05±0.05	Computed from curve; fin asymmetry can nullify skin friction.
c.p. location				calibers from base
x_B				
x_{d_0}				
$x_{d_0}(2-x_{d_0})$				
$\frac{1}{x_B}$				

*Cylindrical body undercut 0.22 inch to increase yaw level (to about 3°).

AUTHOR(S) B. G. Karpov

REPORT BRL MR 696 (Ref. 47)
DATE 1953
TYPE OF TEST Free flight

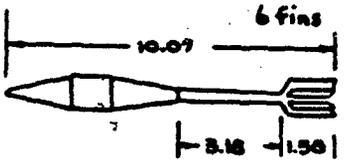

Dimensions, calibers

Muzzle	Weight, lb	14.4
	Velocity, fps	2450
	Spin rate, rps	Variable
	d, ft	0.295
	ν, rad/cal	

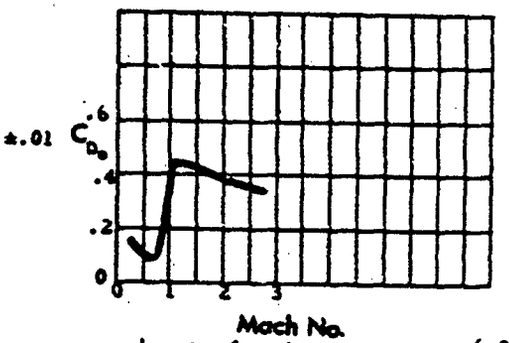

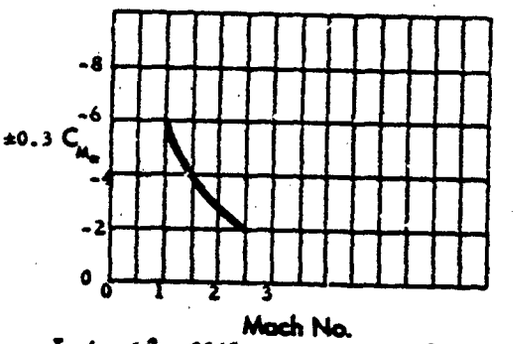

c.g. location from base, calibers 6.21

I_x, slug-ft^2 .0048 I_y, slug-ft^2 .143

k_x, cal .350 k_y, cal 1.91

M	Subsonic	Transonic 0.9	Supersonic	Comments
C_{D_0}			$1.2 < M < 1.8$	
C_{L_α}		2.7	3.0 ± 0.5	
C_{M_α}		-6.5	See curve	
$C_{M_q}+C_{M_{\dot\alpha}}$			-120 ± 10	
$C_{M_{p\alpha}}$				
C_{L_p}				
c.p. - c.g., calibers location		-2.0	-1.1 ± 0.4	
s_g				
s_{d_0}				
$s_{d_0}(2-s_{d_0})$				
$\frac{1}{s_g}$				

APPENDIX VIII—Y

90-MM HEAT PROJECTILE, T108

AUTHOR(S) L. J. Rose and R. H. Krieger; R. Piziali and L. C. MacAllister

REPORT BRL MR 763 (Ref. 93); BRL MR 1076 (Ref. 41)

DATE 1956; 1957

TYPE OF TEST Wind tunnel; Free flight

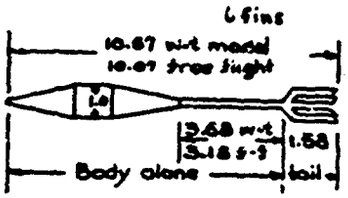

Muzzle
Weight, lb
Velocity, fps 2750
Spin rate, rps 0 to 217
d, ft (full scale) 0.295 d, ft (w-t model) 0.118
ν, rad/cal

Dimensions, calibers

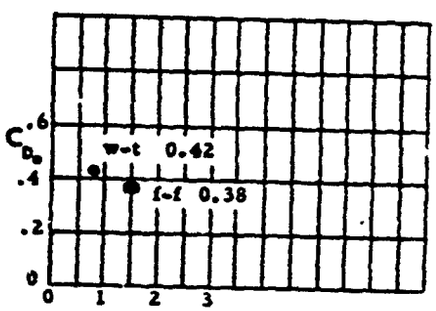

c.g. location from base, calibers 7.13 (w-t) 6.21 (f-f)

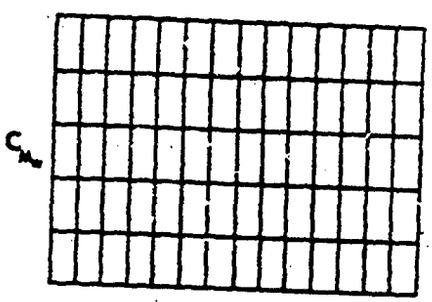

I_x, slug-ft² _____ I_y, slug-ft² _____

k_x, cal _____ k_y, cal _____

M	1.72 Body alone	1.72 Body + tail	2.45	
$C_{L_\alpha}(=C_{N_\alpha}-C_{D_0})$	1.3	2.8	3.0	
C_{M_α}	+5.6	-3.2	$-(1.5 + 75\nu^2)$	ν = roll rate in rad/cal
$C_{M_q}+C_{M_{\dot\alpha}}$			-75 (approx.)	
$C_{M_{p\alpha}}$			-8.3 (approx.)	
C_{l_p}	Wind tunnel		Free flight	
c.p.-c.g., calibers	+3.5	-1.6	$-(0.45 + 22\nu^2)$	

$\frac{s_g}{d_0}$ Reduction of boom length by 1.5 calibers cut C_{L_α} in half (when using shrouded tail). c.p.-c.g. separation was also halved. This relation should hold for the six-fin unshrouded tail as well.

$\frac{s_j}{d_0}\left(2-\frac{s_j}{d_0}\right)$

$\frac{1}{\nu}$

Projectile becomes dynamically unstable above 16[illegible] rps (ν = 0.11).

10-CALIBER ARROW PROJECTILE

AUTHOR(S) L. C. MacAllister

REPORT BRL R 934 (Ref. 89)
DATE 1955
TYPE OF TEST Free flight

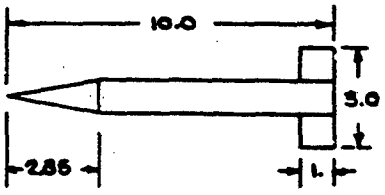

Dimensions, calibers

Weight, lb	Variable
Velocity, fps	Variable
Spin rate, rps	I ±
d, ft	.066
ν, rad/cal	

Cruciform tail
8% thick wedge fins, not canted

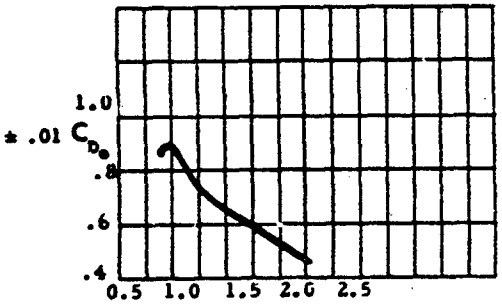

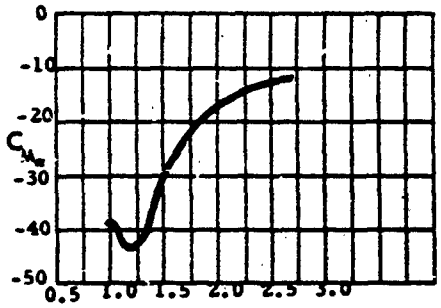

c.g. location from base, calibers 3.90

I_x, slug-ft² _____ I_y, slug-ft² _____

k_x, cal 0.38 k_y, cal 2.4

	Transonic		Supersonic	Comments
M	1.1	1.8	2.4	
C_{D_0}		12±1	9±1	
C_{L_α}	21±3	12±1	8.5±0.5	
C_{M_α}	-42±0.5	-21±0.5	-12±0.5	
$C_{M_q}+C_{M_{\dot\alpha}}$	-220±50	-290±50	-270±50	
$C_{M_{p\alpha}}$				
C_{l_p}				
c.p. location	2.1	2.1	2.6	calibers from base
s_g				
s_{d_0}				
$s_{d_0}(2-s_{d_0})$				
$\frac{1}{s_g}$				

APPENDIX IX
TRAJECTORY PROGRAM IN FORTRAN LANGUAGE

```
C
      DIMENSION CDO(9,2), CMA(9,2)
    1 FORMAT (49H                    HEADINGS
    6 FORMAT (F7.2,F8.0,F8.0,F7.1,F6.3,F6.2,F7.3,F6.2)
    9 FORMAT (F6.3,F6.3,F8.3,F6.3,F6.3,F8.4)
   10 FORMAT (F8.6,F7.1)
    7 FORMAT (2H  )
  100 READ 1
      READ 6,D,ZT,WTO,WTB,SPIS,SBT,QE,VO
      READ 6, FFD,FFM,CDD2,TWIST,CLP,PINT,RGA,RGT,DTE,DTL,DTM,ZO,TEMP
      DO 11 I=1,9
   11 READ 9, CDO(I,1),CDO(I,2),X,CMA(I,1),CMA(I,2)
      PRINT 1
      PRINT 7
      READ 1
      PRINT 1
      PRINT 9,FFD,FFM,X,RGA,RGT,D
      PAUSE
   20 IF (SENSE SWITCH 1) 21,22
   21 ACCEPT 6, QE, SBT
   22 IF (SENSE SWITCH 2) 23,26
   23 ACCEPT 6, FFD, VO,DTL,DTM
   26 READ 1
      PRINT 1
      PRINT 6,WTO,VO,SPIS,SBT,DTM,TWIST,QE
      READ 1
      PRINT 1
      PRINT 6,WTB,ZO,TEMP,DTL,DTE,CD2,CLP
      PRINT 7
      THST = 0.0
      IF (WTO-WTB)29,29,96
   96 THST=(WTO-WTB)*SPIS/SBT
      DMASS=THST/(32.17*SPIS)
   29 TEMPR =  518./(459.+TEMP)
      VAO = 1116./(TEMPR**0.5)
      RHO05 = .001189*TEMPR
      PRINT 10, RHO05, VAO
      PRINT 7
      PAUSE                                          (DR stands for 'Density Ratio')
      IF (SENSE SWITCH 4) 20,97
   97 READ  1     ---> Time  X  Dist  V  CD  CMA DR  Mass
      PRINT 1
      READ 1     ---> Theta  Z  Thrust  Drag  Yaw  Mach  Spin  SG
      PRINT 1
      PRINT 7
      PINTT = 0.0
      TIME = 0.0
      X = 0.0
      DIST = 0.0
```

```
      THT = QE
      Z = ZO
      ZF = ZO
      S = .7854*D**2
      PMASS = WTO/32.17
      THETA = .01745329*QE
      V = VO
      IF (TWIST)30,31,30
   30 SGC =        RGA**4/(4.0*RHO05*S*D*RGT**2)
      GNU = 6.2832/TWIST
      YRC = 32.17*RGA**2/(RHO05*S)
C     END OF INITIALIZATION
   31 IF (Z-30000.) 32,33,33
   32 RHO = EXPF(-3.2E-05*Z)
      GO TO 34
   33 RHO = .38289*EXPF(-4.6E-05*(Z-30000.))
   34 IF (Z-36500.) 35,36,36
   35 VM = V/(VAO-(VAO-970.)*Z/36500.)
      GO TO 37
   36 VM = V/970.
   37 IF (CDO(9,1)-VM) 38,38,39
   38 CD = CDO(9,2)
      GO TO 43
   39 I=2
   40 DIFF = VM-CDO(I,1)
      IF (DIFF) 41,41,42
   41 CD = CDO(I,2)+DIFF*(CDO(I,2)-CDO(I-1,2))/(CDO(I,1)-CDO(I-1,1))
      GO TO 43
   42 I=I+1
      GO TO 40
   43 CD = FFD*CD
      IF (TWIST)44,95,44
   44 IF (CMA(9,1)-VM) 45,45,46
   45 CM = CMA(9,2)
      GO TO 50
   46 I=2
   47 DIFF = VM-CMA(I,1)
      IF (DIFF) 48,48,49
   48 CM = CMA(I,2)+DIFF*(CMA(I,2)-CMA(I-1,2))/(CMA(I,1)-CMA(I-1,1))
      GO TO 50
   49 I=I+1
      GO TO 47
   50 CM = FFM*CM
      SG = SGC*(GNU**2)*PMASS/(RHO*CM)
      IF (SG-1.0) 51,51,53
   51 PRINT 52, SG
   52 FORMAT (F10.3,10H  UNSTABLE)
   53 YR =(YRC*PMASS*GNU/(RHO*CM*V**2)) * COSF (THETA)
      CD = CD + CDD2*YR**2
   95 GACC = -32.17*SINF(THETA)
      DRAG = RHO05*RHO*(V**2)*S*CD
      ACC = GACC + (THST-DRAG)/PMASS
```

```
      DT = DTL/(ACC*ACC)**DTE
      IF (DT-DTM) 60,60,59
   59 DT = DTM
   60 IF (SENSE SWITCH 1) 57,55
   55 PINTT = PINTT-1.0
      IF (PINTT) 57,57,56
   56 IF (THT*THETA) 70,70,58
   70 ZF = ZT
   57 PRINT 6,TIME,X,DIST,V,CD,CM,RHO,PMASS
      PRINT 6, THETA,Z,THST,DRAG,YR,VM,GNU,SG,DT
      PINTT = PINT
      IF (SENSE SWITCH 2)54,58
   54 ACCEPT 6,DTL,DTM
   58 IF (TIME-SBT) 62,61,61
   61 IF (THST)64,64,63
   63 THST = 0.0
      PMASS = WTB/32.17
      GO TO 57
   62 IF (TIME+DT-SBT) 69,68,68
   68 DT = DTM/4.0
   69 PMASS=PMASS-DMASS*DT
   64 DRAG = DRAG*(1.0+2.0*ACC*DT/V)
      ACCT = GACC + (THST-DRAG)/PMASS
      VBAR = V + (ACC+ACCT)*DT/4.0
      DS = VBAR*DT
      V = 2.0*VBAR - V
      DIST = DIST + DS
      TIME = TIME + DT
      THT = THETA
      THBAR = THETA - 16.09*COSF(THETA)*DT/VBAR
      X = X + DS*COSF(THBAR)
      Z = Z + DS*SINF(THBAR)
      THETA = THETA - 32.17*COSF(THBAR)*DT/VBAR
      GNU = GNU*(1.0 +((DRAG*CLP/(PMASS*CD*RGA**2))-ACCT)*DT/V)
C     TEST FOR END OF TRAJECTORY
      IF (Z-ZF) 67,67,31
   67 DS = (ZT-Z)/SINF(THETA)
      TIME = TIME + DS/V
      X =(X + DS*COSF(THETA))/3.281
      THETA = THETA/.01745329
      READ 1
      PRINT 1
      PRINT 6, TIME, X, V, THETA, GNU, SG
      PAUSE
      IF (SENSE SWITCH 4) 20,100
      END
```

SW 1 ONFOR SYMBOL TABLE

FFD	Ratio of drag coefficient curve to typical curve in memory
FFM	Ratio of static moment coefficient curve to typical curve in memory
TYPE	Identification of typical drag and moment curves in memory
RGA	Axial radius of gyration, calibers
RGT	Transverse radius of gyration, calibers
D	Maximum body diameter, ft

WTO	Projectile weight at launch, lb
VO	Projectile velocity at launch, fps
SPIS	Specific impulse of rocket fuel, sec
SRT	Rocket motor burning time, sec
TWIST	Twist of rifling, calibers per turn
QE	Quadrant elevation, deg
WTB	Projectile weight at rocket burnout, lb
ZO	Elevation of launcher, ft
ZT	Elevation of target, ft
TEMP	Air temperature at launcher, °F
CDD2	Yaw-drag coefficient, per rad^2
CLP	Roll damping moment coefficient
DTL	Numerator of expression used to compute time intervals
DTE	Exponent in expression used to compute time intervals
DTH	Maximum length of time interval permitted
PINT	Number of time intervals between automatic print-outs
CDO(1,1)	Element of mach no. column in drag coefficient table
CDO(1,2)	Element of drag coeff. column in drag coefficient table
CMA(1,1)	Element of mach no. column in moment coefficient table
CMA(1,2)	Element of static moment coeff. column in moment coeff. table
THST	Rocket thrust, lb
DMASS	Rate of change of projectile mass, slugs/sec
TEMPR	Ratio of std. absolute temp.to absolute temp.of air at launcher
VAO	Sea level (Z=0) vel. of sound in air at temp.of air at launcher
RHOO5	One-half air density at sea level at air temp.at launch, slugs/ft^3
X	Horizontal distance from launcher in range direction, ft
DIST	Arc distance along trajectory, from launcher, ft
THT	Variable carrying sign of traj.angle at beginning of time interval
S	Frontal area of projectile, ft^2
PMASS	Projectile mass, slugs
THBAR	Trajectory angle at middle of time interval, radians
THETA	Trajectory angle at end of time interval, radians
V	Projectile velocity, fps
SGC	Constant in computation of gyroscopic stability factor
GNU	Spin of projectile, rad/cal
YRC	Constant in computation of yaw of repose, ft^2/ slug . sec^2
Z	Altitude of projectile, measured from sea level, ft
RHO	Ratio of air density at altitude to density at sea level
VM	Mach number
CD	Drag coefficient
DIFF	Mach no.difference from tabular value, for interpolation in table
CM	Static moment coefficient, per radian
SG	Gyroscopic stability factor
YR	Yaw of repose, radians
PINTT	Counter for automatic print-out
TIME	Elapsed time since launch, sec
GACC	Projectile acceleration along trajectory, due to gravity, ft/sec^2
DRAG	Drag, lb
ACC	Proj.acceleration along traj.at beginning of time interval, ft/sec^2
ACCT	Proj.acceleration along traj.at end of interval, ft/sec^2
DT	Length of time interval, sec
VBAR	Average velocity over time interval, fps
DS	Arc distance traveled during time interval, ft

(129) 30 Blank

REFERENCES

General

1. R. H. Fowler, E. G. Gallop, C. N. H. Lock and H. W. Richmond, "The Aerodynamics of a Spinning Shell," Phil. Trans. Roy. Soc. (London) (A), 221, 295-387 (1920).
2. H. P. Gay, *Notes on the Weights of Guns, Mortars, Recoilless Weapons and Their Ammunition*, BRL Memorandum Report 1360, Aberdeen Proving Ground, Md., 1961.
3. H. P. Gay and A. S. Elder, *The Lateral Motion of a Tank Gun and Its Effect on the Accuracy of Fire*, BRL Report 1070, Aberdeen Proving Ground, Md., 1959.
4. J. L. Kelley and E. J. McShane, *On the Motion of a Projectile With Small or Slowly Changing Yaw*, BRL Report 446, Aberdeen Proving Ground, Md., 1944.
5. R. H. Kent and E. J. McShane, *An Elementary Treatment of the Motion of a Spinning Projectile About Its Center of Gravity*, BRL Report 459, Aberdeen Proving Ground, Md., 1944.
6. C. G. Maple and J. L. Synge, "Aerodynamic Symmetry of Projectiles," *Quart. App. Mech.*, Vol. VI, No. 4 (1949).
7. E. J. McShane, J. L. Kelley and F. Reno, *Exterior Ballistics*, University of Denver Press, Denver, Colo., 1953.
8. J. von Neumann and O. Morgenstern, *Theory of Games and Economic Behavior*, Princeton University Press, Princeton, N. J., 1953.
9. J. D. Nicolaides and L. C. MacAllister, "A Review of Aeroballistic Range Research on Winged and/or Finned Missiles," *3rd Navy Symposium on Aeroballistics*, Applied Physics Laboratory, Silver Spring, Md., NAVORD Report 5338, 1954.
10. *Ordnance Technical Terminology*. June 1962. Special Text ST 9-152, U.S. Army Ordnance School, Aberdeen Proving Ground, Md. Also available from Clearinghouse for Federal Scientific and Technical Information, Springfield, Va. as PB 181465.
11. R. W. Pohl, *Physical Principles of Mechanics and Acoustics*. Translated by W. M. Deans, Blackie & Son Ltd., London, 1932.
12. a. C. H. Murphy, *The Free Flight Motion of Symmetric Missiles*, BRL Report 1216, Aberdeen Proving Ground, Md., 1963.
    b. R. H. Kreiger, *Address Delivered Before the Committee on Fin-Stabilized Ammunition at Picatinny Arsenal on 15 September 1954*, BRL Technical Note 962, Aberdeen Proving Ground, Md., 1954.

Estimation and Measurement of Aerodynamic Coefficients

13. E. Bluestone, *Flexible Nozzle Tunnel No. 3, Model Design Criteria and Tunnel Operating Conditions (BRL Supersonic Wind Tunnel)*, BRL Memorandum Report 711, Aberdeen Proving Ground, Md., 1953.
14. W. E. Buford and S. Shatmoff, *The Effects of Fineness Ratio and Mach number on the Normal Force and Center of Pressure of Conical and Ogival Head Bodies*, BRL Memorandum Report 760, Aberdeen Proving Ground, Md., 1954.
15. W. H. Dorrance, "Non-steady Supersonic Flow

(131)

REFERENCES (cont'd)

About Pointed Bodies of Revolution," J. Aeronaut. Sci. 18, 505 (1951).

16. H. R. Kelley, *The Estimation of Normal Force and Pitching Moment Coefficients for Blunt Base Bodies of Revolution at Large Angles of Attack*, Naval Ordnance Test Station Technical Memorandum 998, China Lake, California, 1953.
17. J. C. McMullen, *Wind Tunnel Testing Facilities at the Ballistic Research Laboratories*, BRL Memorandum Report 1292, Aberdeen Proving Ground, Md., 1960.
18. C. H. Murphy, *The Measurement of Nonlinear Forces and Moments by Means of Free Flight Tests*, BRL Report 974, Aberdeen Proving Ground, Md., 1956.
19. W. K. Rogers, Jr., *The Transonic Free Flight Range*, BRL Report 1044, Aberdeen Proving Ground, Md., 1958.
20. N. Simmons, *Simplified Methods for Estimating Static Stability of Air and Underwater Projectiles*, A.D.E. Project Note 21, Fort Halstead, 1952. *See also:* A.D.E. Technical Report 3-54, 1954.
21. R. M. Wood, *Quick Methods for Estimating the Static Aerodynamic Coefficients of Shell*, BRL Memorandum Report 854, Aberdeen Proving Ground, Md., 1954.

Drag

22. A. C. Charters and R. H. Kent, *The Relation Between The Skin Friction Drag and the Spin Reducing Torque*, BRL Report 287, Aberdeen Proving Ground, Md., 1942.
23. A. C. Charters and R. A. Turetsky, *Determination of Base Pressure from Free-Flight Data*, BRL Report 653, Aberdeen Proving Ground, Md., 1948.
24. E. R. Dickinson, *Some Aerodynamic Effects of Head Shape Variation at Mach Number 2.44*, BRL Memorandum Report 838, Aberdeen Proving Ground, Md., 1954.
25. E. R. Dickinson, *The Effect of Boattailing on the Drag Coefficient of Cone-Cylinder Projectiles at Supersonic Velocities*, BRL Memorandum Report 842, Aberdeen Proving Ground, Md., 1954.
26. T. Hailperin, *Comparison of Boat-tail and Square Base: Part I*, BRL Memorandum Report 347, Aberdeen Proving Ground, Md., 1945.
27. S. F. Hoerner, *Fluid-Dynamic Drag*, Published by the author, 48 Busteed Dr., Midland Park, N.J., 1958.
28. L. C. MacAllister, *The Drag of a 1/5 Scale Model of the 3000-lb. Bomb M118 from a Mach Number of 0.7 to 1.2 as Obtained from Free Flight Firings*, BRL Report 927, Aberdeen Proving Ground, Md., 1955.
29. C. T. Odom, *A Drag Coefficient of HE Shell for the New Series of Field Artillery Weapons*, BRL Memorandum Report 1013, Aberdeen Proving Ground, Md., 1956.
30. G. I. Taylor and J. W. Maccoll, "The Air Pressure on a Cone Moving at High Speeds," Proc. Roy. Soc. (London) 139, 278 (1933).
31. N. Tetervin, *Approximate Analysis of Effect on Drag of Truncating the Conical Nose of a Body of Revolution in Supersonic Flow*, NOL Technical Report 62-111, Naval Ordnance Laboratory, White Oak, Md., 1962.
32. R. N. Thomas, *Some Comments on the Form of the Drag Coefficient at Supersonic Velocity*, BRL Report 542, Aberdeen Proving Ground, Md., 1942.

Dual Flow

33. B. G. Karpov and M. J. Piddington, *Effect on Drag of Two Stable Flow Configurations Over the Nose Spike of the 90-mm T316 Projectile*, BRL Technical Note 955, Aberdeen Proving Ground, Md., 1954.
34. A. S. Platou, *Body Nose Shapes for Obtaining High Static Stability*, BRL Memorandum Report 592, Aberdeen Proving Ground, Md., 1952.
35. a. C. P. Sabin, *The Aerodynamic Properties of a Spike-Nosed Shell at Transonic Velocities*, BRL Memorandum Report 1112, Aberdeen Proving Ground, Md., 1957.
    b. R. H. Krieger, paper presented at the Fin-

REFERENCES (cont'd)

Stabilized Ammunition Symposium, Picatinny Arsenal, 19-20 October 1955.

Magnus Force and Moment

36. E. R. Benton, "Supersonic Magnus Effects on a Finned Missile," *AIAA Journal*, January 1964.
37. E. D. Boyer, *Free Flight Range Tests of a 10-caliber Cone Cylinder*, BRL Memorandum Report 1258, Aberdeen Proving Ground, Md., 1960.
38. W. E. Buford, *Magnus Effects in the Case of Rotating Cylinders and Shell*, BRL Memorandum Report 821, Aberdeen Proving Ground, Md., 1954.
39. H. R. Kelley, *An Analytical Method for Predicting the Magnus Forces and Moments on Spinning Projectiles*, Naval Ordnance Test Station Technical Memorandum 1634, China Lake, California, 1954.
40. J. C. Martin, *On Magnus Effects Caused by the Boundary Layer Displacement Thickness on Bodies of Revolution at Small Angels of Attack*, BRL Report 870 (Revised), Aberdeen Proving Ground, Md., 1955.
41. R. Pizialli and L. C. MacAllister, *Effect of Magnus Torque on the Yaw Damping of the 90-mm T108E45 Shell*, BRL Memorandum Report 1076, Aberdeen Proving Ground, Md., 1957.
42. A. S. Platou and J. Sternberg, *The Magnus Characteristics of a 30-mm Aircraft Bullet*, BRL Report 994, Aberdeen Proving Ground, Md., 1956.
43. A. S. Platou, *The Magnus Force on a Short Body at Supersonic Speeds*, BRL Report 1062, Aberdeen Proving Ground, Md., 1959.
44. A. S. Platou, *The Magnus Force on a Rotating Cylinder in Transonic Cross Flows*, BRL Report 1150, Aberdeen Proving Ground, Md., 1961.
45. A. S. Platou, *The Magnus Force on a Finned Body*, BRL Report 1193, Aberdeen Proving Ground, Md., 1963.

Dynamic Stability

46. R. E. Bolz and J. D. Nicolaides, *A Method of Determining Some Aerodynamic Coefficients from Supersonic Free Flight Tests of a Rolling Missile*, BRL Report 711, Aberdeen Proving Ground, Md., 1949.
47. a. B. G. Karpov, *Aerodynamic and Flight Characteristics of the 90-mm Fin-Stabilized Shell, HEAT, T108*, BRL Memorandum Report 696, Aberdeen Proving Ground, Md., 1953.
    b. B. G. Karpov, S. Krial and B. Hull, *Aerodynamic Characteristics of the 175-mm T203 Shell and the 175-mm Square-Base Shell With Fuze M51A5*, BRL Memorandum Report 956, Aberdeen Proving Ground, Md., 1955.
48. C. H. Murphy, *On Stability Criteria of the Kelley-McShane Linearized Theory of Yawing Motion*, BRL Report 853, Aberdeen Proving Ground, Md., 1953.
49. C. H. Murphy and L. E. Schmidt, *The Effect of Length on the Aerodynamic Characteristics of Bodies of Revolution in Supersonic Flight*, BRL Report 876, Aberdeen Proving Ground, Md., 1953.
50. J. D. Nicolaides and T. F. Griffin, *On a Fluid Mechanism for Roll Lock-in and Rolling Speed-up Due to Angle of Attack of Cruciform Configurations*, Navy BuOrd Technical Note 16, Washington, D.C., 1955.
51. J. A. M. Schmidt, *A Study of the Resonating Yawing Motion of Asymmetrical Missiles By Means of Analog Computer Simulation*, BRL Report 922, Aberdeen Proving Ground, Md., 1954.
52. L. E. Schmidt, *The Dynamic Properties of Pure Cones and Cone Cylinders*, BRL Memorandum Report 759, Aberdeen Proving Ground, Md., 1954.
53. L. E. Schmidt and C. H. Murphy, *The Aerodynamic Properties of the 7-caliber Army-Navy Spinner Rocket in Transonic Flight*, BRL Memorandum Report 775, Aberdeen Proving Ground, Md., 1954.
54. W. E. Scott, *The Effect of a Rotating Band Upon Some Aerodynamic Coefficients of the 7-caliber Army-Navy Spinner Rocket at Mach*

REFERENCES (cont'd)

1.8, BRL Memorandum Report 1302, Aberdeen Proving Ground, Md., 1960.

55. R. A. Turetsky, *Dynamic Stability of Spinner Rocket Models Fired in the Free Flight Aerodynamic Range*, BRL Memorandum Report 526, Aberdeen Proving Ground, Md., 1950.

Aerodynamic Jump

56. J. G. Darpas, *Transverse Forces on Projectiles Which Rotate in the Barrel*, translated by H. P. Hitchcock, BRL Memorandum Report 1208, Aberdeen Proving Ground, Md., 1959.
57. C. H. Murphey, *Comments on Projectile Jump*, BRL Memorandum Report 1071, Aberdeen Proving Ground, Md., 1957.
58. C. H. Murphey and J. W. Bradley, *Jump Due to Aerodynamic Asymmetry of a Missile With Varying Roll Rate*, BRL Report 1077, Aberdeen Proving Ground, Md., 1959.
59. W. E. Simon, *Investigation of the Causes of High Dispersion of the Production 90-mm Fin-Stabilized Shell, HEAT, T108E40*, BRL Memorandum Report 987, Aberdeen Proving Ground, Md., 1956.
60. S. J. Zaroodny, *On Jump Due to Muzzle Disturbances*, BRL Report 703, Aberdeen Proving Ground, Md., 1949.

Arrow Projectiles

61. W. H. Allan, "Sabots Used at the Thompson Aeroballistics Laboratory," *Proceedings of the Aerodynamic Range Symposium, January 1957*, BRL Report 1005, Part I, Aberdeen Proving Ground, Md., 1957.
62. L. C. MacAllister, *Drag Properties and Gun Launching Long Arrow Projectiles*, BRL Memorandum Report 600, Aberdeen Proving Ground, Md., 1952.
63. L. C. MacAllister and E. J. Roschke, *The Drag Properties of Several Winged and Finned Cone-Cylinder Models*, BRL Memorandum Report 849, Aberdeen Proving Ground, Md., 1954.
64. S. T. Marks, L. C. MacAllister, J. W. Gehring, H. D. Vitagliano and B. T. Bentley, *Feasibility Test of an Upper Atmosphere Gun Probe System*, BRL Memorandum Report 1368, Aberdeen Proving Ground, Md., 1961.
65. G. Taylor, *Sabot-Launching Systems for Experimental Penetrators*, BRL Memorandum Report 1505, Aberdeen Proving Ground, Md., 1963.

Rocket-Assisted Projectiles

66. L. Davis, J. W. Follin and L. Blitzer, *The Exterior Ballistics of Rockets*, D. Van Nostrand N. Y., 1958.
67. C. H. Murphey, *Advances in the Dynamic Analysis of Range Data*, BRL Memorandum Report 1270, Aberdeen Proving Ground, Md., 1960.
68. S. J. Zaroodny, *On the Scaling of Rockets*, BRL Memorandum Report 1421, Aberdeen Proving Ground, Md., 1962.
69. R. C. Bullock and W. J. Harrington, *Summary Report on Study of the Gun-Boosted Rocket System*, PSR-9/8, North Carolina State College, Raleigh, N. C., 1962.
70. S. J. Zaroodny, *Accuracy of Unguided Finned Rockets*, BRL Report 1232, Aberdeen Proving Ground, Md., 1964.

Liquid-Filled Projectiles

71. B. G. Karpov, *Experimental Observations of the Dynamic Behavior of Liquid-Filled Shell*, BRL Report 1171, Aberdeen Proving Ground, Md., 1962.
72. B. G. Karpov, *Dynamics of Liquid-Filled Shell, Aids for Designers: a) Milner's Graph, b) Stewartson's Tables*, BRL Memorandum Report 1477, Aberdeen Proving Ground, Md., 1963.
73. K. Stewartson, "On the Stability of a Spinning Top Containing Liquid," J. Fluid Mech. 5, Part 4 (1959).

Prototype Testing

74. E. R. Dickinson, *Physical Measurements of Projectiles*, BRL Technical Note 874, Aberdeen Proving Ground, Md., 1954.

REFERENCES (cont'd)

75. AMCP 706-110, Engineering Design Handbook, *Experimental Statistics, Section 1, Basic Concepts and Analysis of Measurement Data.*
76. AMCP 706-112, Engineering Design Handbook, *Experimental Statistics, Section 3, Planning and Analysis of Comparative Experiments.*
77. *Test and Evaluation Command Materiel Test Procedures*, TECP 700-700, Aberdeen Proving Ground, Md.

Aerodynamic Data-Spinners

78. E. D. Boyer, *Aerodynamic Characteristics of 20-mm Shell, HEI, T282E1*, BRL Memorandum Report 813, Aberdeen Proving Ground, Md., 195-.
79. E. D. Boyer, *Aerodynamic Properties of the 90-mm HE M71 Shell*, BRL Memorandum Report 1475, Aberdeen Proving Ground, Md., 1963.
80. E. R. Dickinson, *The Effects of Annular Rings and Grooves, and of Body Undercuts on the Aerodynamic Properties of a Cone-Cylinder Projectile at M = 1.72*, BRL Memorandum Report 1284, Aberdeen Proving Ground, Md., 1960.
81. H. P. Hitchcock, *Aerodynamic Data for Spinning Projectiles*, BRL Report 620 (1947), with Errata Sheet (1952), Aberdeen Proving Ground, Md.
82. H. R. Kelly, *The Subsonic Aerodynamic Characteristics of Several Spin-Stabilized Rocket Models, I. Static Coefficients*. Naval Ordnance Test Station Technical Memorandum 375, China Lake, California, 1953. *II. Magnus Coefficients*, Naval Ordnance Test Station Technical Memorandum 376, China Lake, California, 1953.
83. L. C. MacAllister, *The Aerodynamic Properties and Related Dispersion Characteristics of a Hemispherical-Base Shell, 90-mm, HE, T91, With and Without Tracer Element*, BRL Memorandum Report 990, Aberdeen Proving Ground, Md., 1956.
84. L. C. MacAllister, *Comments on the Effect of Punched and Plain Fuze Covers on the Aerodynamic Properties of the 90-mm T91E1 Shell at M = 1.2*, BRL Technical Note 1119, Aberdeen Proving Ground, Md., 1957.
85. E. T. Roecker, *The Aerodynamic Properties of the 105-mm HE Shell, M1, in Subsonic and Transonic Flight*, BRL Memorandum Report 929, Aberdeen Proving Ground, Md., 1955.
86. L. E. Schmidt and C. H. Murphey, *Effect of Spin on Aerodynamic Properties of Bodies of Revolution*, BRL Memorandum Report 715, Aberdeen Proving Ground, Md., 1953.

Aerodynamic Data-Finners

87. E. D. Boyer, *Aerodynamic Properties of 60-mm Mortar Shell, T24*, BRL Memorandum Report 1020, Aberdeen Proving Ground, Md., 1956.
88. R. H. Krieger and J. M. Hughes, *Wind Tunnel Tests on the Budd Company T153, 120-mm HEAT Spike Nose, Folding Fin Projectile*, BRL Memorandum Report 738, Aberdeen Proving Ground, Md., 1953.
89. L. C. MacAllister, *The Aerodynamic Properties of a Simple Non-Rolling Finned Cone-Cylinder Configuration Between Mach Numbers 1.0 and 2.5*, BRL Report 934, Aberdeen Proving Ground, Md., 1955.
90. L. C. MacAllister and E. T. Roecker, *Aerodynamic Properties, Spin, and Launching Characteristics of 105-mm Mortar Shell T53E1 With Two Types of Fins*, BRL Memorandum Report 618, Aberdeen Proving Ground, Md., 1952.
91. M. J. Piddington, *Some Aerodynamic Properties of a Typical Fin-Stabilized Ordnance Shell*, BRL Memorandum Report 1215, Aberdeen Proving Ground, Md., 1959.
92. A. S. Platou, *The Effect of High Stability Noses on Finned Configurations*, BRL Technical Note 707, Aberdeen Proving Ground, Md., 1952.
93. L. J. Rose and R. H. Krieger, *Wind Tunnel Tests of the T106, 90-mm HEAT Projectile at Mach Number 1.72*, BRL Memorandum Report 763, Aberdeen Proving Ground, Md., 1954.

REFERENCES (cont'd)

Projectile Geometry

94. *Tables for the Design of Missiles, Staff*, Computation Laboratory, Harvard University, Cambridge, Mass., 1948.
95. *Mechanical Integration for Solids of Revolution*, Development Engineering Division, Artillery Ammunition Department, Frankford Arsenal, Philadelphia, Pa.
96. AMCP 706-247, Engineering Design Handbook, Ammunition Series, *Section 4, Design for Projection*.
97. AMCP 706-140, Engineering Design Handbook, Ballistics Series, *Trajectories, Differential Effects, and Data for Projectiles*.
98. Jay L. Politzer, *"Shell" A Computer Program for Determining the Physical Properties of Artillery Shell and Related Items*, Technical Memorandum Report No. ORDBB-DR1-14 (SAAS No. 36), Picatinny Arsenal, Dover, N.J., 1962.

BIBLIOGRAPHY

General

1. H. J. Coon, *Evaluation of Shell, HE, 81-mm, M362, Modified*, BRL Technical Note 1288, Aberdeen Proving Ground, Md., 1959. (Confidential)
2. E. R. Dickinson, *Design of a Ductile Cast Iron Shell for the 155-mm Howitzer*, BRL Technical Note 1196, Aberdeen Proving Ground, Md., 1958. (Confidential)
3. B. G. Karpov and J. W. Bradley, *A Study of Causes of Short Ranges of the 8-inch T317 Shell*, BRL Report 1049, Aberdeen Proving Ground, Md., 1958. (Secret-Restricted Data)
4. L. C. MacAllister, *Comparative Firings of 105-mm Shell T131E31 and 105-mm Shell M1 from Unmodified and Counterbored M2A1 Howitzer Tubes*, BRL Technical Note 739, Aberdeen Proving Ground, Md., 1952. (Confidential)
5. L. C. MacAllister, "Some Problems Associated with the Determination, from Range Firings, of Dynamic Stability of Ballistic Missile Re-entry Shapes," *Proceedings of the Aerodynamic Range Symposium, January 1957*, BRL Report 1005, Part II, Aberdeen Proving Ground, Md., 1957. (Confidential)
6. R. Sedney, *Aerodynamic Heating of the Projectile 20-mm, HEI, M56A1, Fuze M505*, BRL Memorandum Report 1037, Aberdeen Proving Ground, Md., 1956.
7. R. Sedney, *Aerodynamic Heating Problems in Shell Design*, BRL Report 1043, Aberdeen Proving Ground, Md., 1958.

Estimation and Measurement of Aerodynamic Coefficients

8. F. DeMeritte and A. May, "A Comparison of Aerodynamic Data from Wind Tunnels and Free Flight Ranges," *3rd Navy Symposium on Aeroballistics*, Applied Physics Laboratory, Silver Spring, Md., NAVORD Report 5338, Paper 22, 1954.
9. G. E. Hanson, *A Method for Estimating Forces, Moments and Drag Due to Lift Acting on Slender Bodies and Fin-Stabilized Bodies at Supersonic Speeds* (Includes IBM 1620 program.) Report No. RS-TR-63-2, U.S. Army Missile Command, Redstone Arsenal, Ala., 1963. DDC No. AD 335484. (Confidential)
10. R. H. Krieger, *The Aerodynamic Design of Fin-Stabilized Ammunition*, BRL Memorandum Report 971, Aberdeen Proving Ground, Md., 1956. (Confidential)
11. A. S. Platou, *Body Nose Shapes for Obtaining High Static Stability*, BRL Memorandum Report 592, Aberdeen Proving Ground, Md., 1952.
12. W. E. Scott, *Some Aerodynamic Properties of a 105-mm Model of the 155-mm T358 Shell*. BRL Memorandum Report 1369, Aberdeen Proving Ground, Md., 1961.
13. a. R. H. Whyte and H. E. Hudgins, *Effects of Nose Shape and Boattail Angle on Static Aerodynamic Characteristics of a 105-mm Shell at Mach 4.0, 4.5 and 5.0*, Picatinny Arsenal Technical Memorandum 1248, Dover, N.J. 1964.
    b. Elizabeth R. Dickinson, *Some Aerodynamic Effects of Varying the Body Length and Head Length of a Spinning Projectile*, BRL Memorandum Report 1664, Aberdeen Proving Ground, Md., 1965.

Arrow Projectiles

14. R. C. Huyett, "Aerodynamic Characteristics of Fin-Boattail Combinations at M = 2.00,"

BIBLIOGRAPHY (cont'd)

3rd Navy Symposium on Aeroballistics, Applied Physics Laboratory, Silver Spring, Md., NAVORD Report 5338, Paper 14, 1954. (Confidential)

15. F. G. King and R. H. Kent, *Kill Probability of the 127/60 Gun for Two Drag Estimates, and Comparison with the Loki Rocket*, BRL Memorandum 721, Aberdeen Proving Ground, Md., 1954. (Confidential)
16. A. R. Krenkel and J. F. Mello, "High Angle of Attack Aerodynamic Rolling Moments and Stability Phenomena for Cruciform Wing-Body Combinations," *3rd Navy Symposium on Aeroballistics*, Applied Physics Laboratory, Silver Spring, Md., NAVORD Report 5338, Paper 13, 1954. (Confidential)
17. M. J. Piddington, *Retardation and Velocity Histories of an 8-grain Flechette*, BRL Memorandum Report 1140, Aberdeen Proving Ground, Md., 1958. (Confidential)
18. M. J. Piddington, *The Drag Characteristics of a 10.2-grain Flechette (XM110)*, BRL Memorandum Report 1501, Aberdeen Proving Ground, Md., 1963. (Confidential)
19. M. A. Sylvester, *Wind Tunnel Tests of Hypervelocity Cone Cylinder Finned Projectiles at Mach Numbers 4.00, 4.53 and 4.89*, BRL Memorandum Report 1166, Aberdeen Proving Ground, Md., 1958.

Drag

20. E. R. Dickinson, *Design Data for a Series of HE Projectile Shapes at Mach Number 3.0*, BRL Memorandum Report 920, Aberdeen Proving Ground, Md., 1955.
21. E. R. Dickinson, *The Effectiveness of Base-Bleed in Reducing Drag of Boattailed Bodies at Supersonic Velocities*, BRL Memorandum Report 1244, Aberdeen Proving Ground, Md., 1960.
22. G. D. Kahl, *Supersonic Drag and Base Pressure of a 70° Cone Cylinder*, BRL Memorandum Report 1178, Aberdeen Proving Ground, Md., 1958.
23. M. J. Piddington, *Some Brief Comments on the Drag and Stability of the 37-mm Spotting Projectile*, BRL Technical Note 1416, Aberdeen Proving Ground, Md., 1961. (Confidential)
24. E. J. Roschke and M. J. Piddington, *Drag and Dispersion of Banded Spheres With and Without Strings*, BRL Memorandum Report 995, Aberdeen Proving Ground, Md., 1956.
25. M. A. Sylvester and R. H. Krieger, *Wind Tunnel Tests of the T340E11, 90-mm HE Projectile With Varying Spike Nose and Spool-Type-Body Parameters*, BRL Memorandum Report 1146, Aberdeen Proving Ground, Md., 1958.

Dual Flow

26. E. D. Boyer, *Drag and Stability Properties of the AVCO 52 Nose Cone Model*, BRL Technical Note 1145, Aberdeen Proving Ground, Md., 1957. (Confidential)
27. E. D. Boyer, *Drag and Stability Properties of the AVCO 13 Nose Cone Model*, BRL Technical Note 1147, Aberdeen Proving Ground, Md., 1957. (Confidential)
28. H. H. Album, *Spiked Blunt Bodies in Supersonic Flow*, Air Force Office of Scientific Research Report 307, Washington, D. C., 1961.

Dynamic Stability

29. B. G. Karpov and S. Krial, *Aerodynamic Characteristics of the 110-mm HE, T194 Shell and Its Modifications, with Fuze M51A5*, BRL Memorandum Report 1057, Aberdeen Proving Ground, Md., 1957. (Confidential)
30. L. C. MacAllister, *Some Instability Problems With Re-entry Shapes*, BRL Memorandum Report 1224, Aberdeen Proving Ground, Md., 1959. (Confidential)
31. M. J. Piddington, *The Effects of Spin and Magnus Torque on a Spike-Nose, Fin-Stabilized, HEAT Projectile, 76-mm T180E23*, BRL Memorandum Report 1310, Aberdeen Proving Ground, Md., 1960. (Confidential)

Folding Fin Characteristics

32. R. H. Krieger, *Wind Tunnel Tests of the T84 75-mm HEAT Projectile*, BRL Memorandum

BIBLIOGRAPHY (cont'd)

Report 518, Aberdeen Proving Ground, Md., 1950. (Confidential)

33. R. H. Krieger and J. M. Hughes, *Wind Tunnel Tests of the Chamberlain Corporation 76-mm T319 Folding-Fin HEAT Projectile*, BRL Memorandum Report 790, Aberdeen Proving Ground, Md., 1954. (Confidential)
34. R. H. Krieger, *Wind Tunnel Tests of a 76-mm HEAT Projectile With Thin Folding Fins*, BRL Memorandum Report 836, Aberdeen Proving Ground, Md., 1954. (Confidential)

Liquid-Filled Projectiles

35. a. G. Sokol, *Some Experiments With the Liquid-Filled, Impulsively Started, Spinning Cylinder*, BRL Technical Note 1473, Aberdeen Proving Ground, Md., 1962.
    b. B. G. Karpov, *Dynamics of a Liquid-Filled Shell: Instability During Spin-up*, BRL Memorandum Report 1629, Aberdeen Proving Ground, Md., 1965.
36. H. M. Stoller, *Apparatus for Study of Fluid Motion in a Spinning Cylinder*, BRL Technical Note 1355, Aberdeen Proving Ground, Md., 1960.
37. E. H. Wedemeyer, *The Unsteady Flow Within a Spinning Cylinder*, BRL Report 1225, Aberdeen Proving Ground, Md., 1963.

Magnus Force and Moment

38. S. Fagin, "Magnus Characteristics of Typical Projectile Configurations (12.75-inch AS Rocket; Called 'Weapon A' and 7-caliber *A-N Spinner Rocket*)," *3rd Navy Symposium on Aeroballistics*, Applied Physics Laboratory, Spring, Md., NAVORD Report 5338, Paper 2. 1954. (Confidential)
39. H. R. Kelly and G. R. Thacker, *The Effect of High Spin on the Magnus Force on a Cylinder at Small Angles of Attack*, NAVORD Report 5036, 1956.
40. W. Luchuck and W. Sparks, *Wind Tunnel Magnus Characteristics of the 7-caliber A-N Spinner Rocket*, NAVORD Report 3813, 1954.

Rocket-Assisted Projectiles

41. E. D. Boyer, *Comparison of Aerodynamic Characteristics of Live and Inert 70-mm T231 Gun-Boosted Rockets*, BRL Memorandum Report 1086, Aberdeen Proving Ground, Md., 1957.
42. S. J. Harnet and S. Wasserman, *Second Status Report, Research and Development of Boosted Artillery Projectiles*, Picatinny Arsenal Technical Memorandum Report 1183, Dover, N.J., 1963. DDC No. AD 339982. (Confidential)
43. F. H. McIntosh, *The Theory and the Calculations of the Behavior of Self-Aligning Rockets*, BRL Report 1228, Aberdeen Proving Ground, Md., 1963.
44. G. J. Pietrangeli, I. Faro and W. Amos, "Ramjet Engine Design Optimization and the Comparative Performance Evaluation of Supersonic Diffusers for Long Range Triton Missile," *3rd Navy Symposium on Aeroballistics*, Applied Physics Laboratory, Silver Spring, Md., NAVORD Report 5338, Paper 7, 1954.
45. *Design Studies on a 105-mm Gun-Boosted Rocket*. Final Report, A. D. Little, Inc., Cambridge, Mass., prepared for Picatinny Arsenal, Dover, N.J., 25 January 1963. DDC No. AD 336539. (Confidential)
46. *5-inch 38-caliber Rocket Sustained Projectiles*, The Budd Company, Philadelphia, Pa., prepared for Bureau of Naval Weapons, Study Project RM-2061, November 1961. (Confidential)

Spin of Fin-Stabilized Projectiles

47. E. D. Boyer, and M. R. Yeager, *Aerodynamic Properties of 90-mm, HE-T, T340 Shell*, BRL Technical Note 1094, Aberdeen Proving Ground, Md., 1956. (Confidential)
48. J. W. Bradley, *A Comparison of Measured Spin Histories of 105-mm Mortar Shell T53E1 With Solutions of Linearized Roll Equation*, BRL Memorandum Report 1074, Aberdeen Proving Ground, Md., 1957.
49. J. W. Bradley, *A Comparison of Measured*

BIBLIOGRAPHY (cont'd)

Spin Histories of 81-mm Mortar Shell T28E6 With Solutions of Linearized Roll Equation, BRL Technical Note 1234, Aberdeen Proving Ground, Md., 1958. (Confidential)

50. B. G. Karpov and W. E. Simon, *Effectiveness of Several Simple Methods of Aerodynamic Control of Spin of the 90-mm, HEAT, T108E40 Shell*, BRL Memorandum Report 879, Aberdeen Proving Ground, Md., 1955.

51. M. J. Piddington, *Some Aerodynamic Properties of Two 90-mm Spited-Nose Shell, T300E53 and T316E6*, BRL Memorandum Report 1082, Aberdeen Proving Ground, Md., 1957. (Confidential)

52. A. S. Platou, *Roll Characteristics of Off-axis Fin Configuration*, BRL Memorandum Report 936, Aberdeen Proving Ground, Md., 1955. (Confidential)

ENGINEERING DESIGN HANDBOOK SERIES

Listed below are the Handbooks which have been published or are currently being printed. Handbooks with publication dates prior to 1 August 1962 were published as 20-series Ordnance Corps pamphlets. AMC Circular 310-38, 19 July 1963, redesignated those publications as 706-series AMC pamphlets (i.e., ORDP 20-138 was redesignated AMCP 706-138). All new, reprinted, or revised Handbooks are being published as 706-series AMC pamphlets.

General and Miscellaneous Subjects

No.	Title
106	Elements of Armament Engineering, Part One, Sources of Energy
107	Elements of Armament Engineering, Part Two, Ballistics
108	Elements of Armament Engineering, Part Three, Weapon Systems and Components
110	Experimental Statistics, Section 1, Basic Concepts and Analysis of Measurement Data
111	Experimental Statistics, Section 2, Analysis of Enumeration and Classificatory Data
112	Experimental Statistics, Section 3, Planning and Analysis of Comparative Experiments
113	Experimental Statistics, Section 4, Special Topics
114	Experimental Statistics, Section 5, Tables
121	Packaging and Pack Engineering
134	Maintainability Guide for Design
135	Inventions, Patents, and Related Matters (Revised)
136	Servomechanisms, Section 1, Theory
137	Servomechanisms, Section 2, Measurement and Signal Converters
138	Servomechanisms, Section 3, Amplification
139	Servomechanisms, Section 4, Power Elements and System Design
170(C)	Armor and Its Application to Vehicles (U)
270	Propellant Actuated Devices
290(C)	Warheads--General (U)
331	Compensating Elements (Fire Control Series)

Ammunition and Explosives Series

175	Solid Propellants, Part One
176(C)	Solid Propellants, Part Two (U)
177	Properties of Explosives of Military Interest, Section 1
178(C)	Properties of Explosives of Military Interest, Section 2 (U)
179	Explosive Trains
210	Fuzes, General and Mechanical
211(C)	Fuzes, Proximity, Electrical, Part One (U)
212(S)	Fuzes, Proximity, Electrical, Part Two (U)
213(S)	Fuzes, Proximity, Electrical, Part Three (U)
214(S)	Fuzes, Proximity, Electrical, Part Four (U)
215(C)	Fuzes, Proximity, Electrical, Part Five (U)
242	Design for Control of Projectile Flight Characteristics
244	Section 1, Artillery Ammunition--General, with Table of Contents, Glossary and Index for Series
245(C)	Section 2, Design for Terminal Effects (U)
246	Section 3, Design for Control of Flight Characteristics (out of print)
247	Section 4, Design for Projection
248	Section 5, Inspection Aspects of Artillery Ammunition Design
249	Section 6, Manufacture of Metallic Components of Artillery Ammunition

Automotive Series

	The Automotive Assembly
366	Automotive Suspensions

Ballistic Missile Series

281(S-RD)	Weapon System Effectiveness (U)
282	Propulsion and Propellants

Ballistic Missile Series (continued)

No.	Title
283	Aerodynamics
284(C)	Trajectories (U)
286	Structures

Ballistics Series

140	Trajectories, Differential Effects, and Data for Projectiles
150	Interior Ballistics of Guns
160(S)	Elements of Terminal Ballistics, Part One, Introduction, Kill Mechanisms, and Vulnerability (U)
161(S)	Elements of Terminal Ballistics, Part Two, Collection and Analysis of Data Concerning Targets (U)
162(S-RD)	Elements of Terminal Ballistics, Part Three, Application to Missile and Space Targets (U)

Carriages and Mounts Series

340	Carriages and Mounts--General
341	Cradles
342	Recoil Systems
343	Top Carriages
344	Bottom Carriages
345	Equilibrators
346	Elevating Mechanisms
347	Traversing Mechanisms

Gun Series

250	Guns--General
252	Gun Tubes

Military Pyrotechnics Series

186	Part Two, Safety, Procedures and Glossary
187	Part Three, Properties of Materials Used in Pyrotechnic Compositions
189	Part Five, Bibliography

Surface-to-Air Missile Series

291	Part One, System Integration
292	Part Two, Weapon Control
293	Part Three, Computers
294(S)	Part Four, Missile Armament (U)
295(S)	Part Five, Countermeasures (U)
296	Part Six, Structures and Power Sources
297(S)	Part Seven, Sample Problem (U)

*Materials Series**

149	Rubber and Rubber-Like Materials
212	Gasket Materials (Nonmetallic)
691	Adhesives
692	Guide to Selection of Rubber O-Rings
693	Magnesium and Magnesium Alloys
694	Aluminum and Aluminum Alloys
697	Titanium and Titanium Alloys
698	Copper and Copper Alloys
699	Guide to Specifications for Flexible Rubber Products
700	Plastics
721	Corrosion and Corrosion Protection of Metals
722	Glass

*The Materials Series is being published as Military Handbooks (MIL-HDBK-) which are available to Department of Defense Agencies from the Naval Supply Depot, 5801 Tabor Avenue, Philadelphia, Pennsylvania 19120.

☆ U.S. GOVERNMENT PRINTING OFFICE: [illegible]